MONASH University

Anoxic metabolism in permeable sediments

Michael Francis Bourke
BA/BSc(Hons)

Water Studies Centre
School of Chemistry
Monash University
September 2017

A thesis submitted to the Faculty of Science, Monash University, Clayton in the fulfilment of the requirements for the degree of *Doctor of Philosophy*.

Copyright notice

Table of contents

Abstract

Microorganisms within permeable sediments perform an integral role in organic carbon fixation and mineralization. Despite this, anoxic metabolism in permeable sediments remains poorly understood, with no systematic studies performed in the context of anoxic permeable sediments. A common assumption in biogeochemistry is that bacterial communities will utilise the most energetically favoured electron acceptor. Under anoxic conditions, this would normally be expected to be denitrification. Previous studies and preliminary experiments have, however, showed that even in the presence of large concentrations of nitrate, denitrification only accounted for <5% of total dissolved inorganic carbon (DIC) production. The large majority of DIC production under such conditions could not be assigned to a known process and the investigation of which became the primary focus of this research.

In chapter 2, this phenomenon was consistently observed in flow through reactor (FTR) experiments, with denitrification, sulfate and iron reduction accounting for <7% of mean anoxic DIC production. These FTR experiments were also used to investigate possible sources of anoxic DIC production including calcium carbonate dissolution, dissimilatory nitrate reduction to ammonium (DNRA) via stored nitrate, and respiration by meiofauna. Each of these possible sources were found to contribute a negligible quantity of DIC relative to measured productions rates and were therefore excluded as possible sources.

In chapter 3, fermentation was investigated as a possible major source of anoxic DIC production by quantifying common fermentative products, such as C1-3 alcohols and volatile fatty acids, in FTR effluent. Acetate and ethanol were detected, however, these accounted for between 2.1 and 4.7% of anoxic DIC production. Broad spectrum antibiotic treatments in FTR experiments revealed that DIC production remained relatively constant, whilst bacterial processes were inhibited. This suggested that eukaryotic microorganisms were very likely dominating anoxic DIC production in permeable sediments.

In chapter 4, large dissolved hydrogen production rates and accumulation of lipids were found to accompany DIC production, indicating eukaryotic fermentation was occurring. The production of DIC and hydrogen persisted despite the administration of broad spectrum bactericidal antibiotics, but ceased following treatment with metronidazole. Metronidazole serves to inhibit the ferredoxin/hydrogenase pathway of fermentative eukaryotic hydrogen production, confirming that the observed hydrogen production occurred via eukaryotic dark fermentation.

In research chapter 5, hydrogen production was observed in axenic cultures of five distinct diatoms (*Fragilariopsis* sp.) and a chlorophyte (*Pyramimonas*) under dark anoxic conditions. The existence of a hydrogen consumption mechanism was indicated as the hydrogen concentration would peak within 24 hours of incubation, then gradually decline. These findings confirm that eukaryotic microalgae found in permeable sediments are capable of hydrogen production.

In chapter 6, heterotrophic metabolism in permeable carbonate sediment from Heron Island was found to account for <12% of mean anoxic dissolved inorganic carbon (DIC) production. Metabolomic analyses revealed very large increases in the relative quantity of C18-23 lipids, including wax monoesters and unsaturated fatty acids, after short term (<24 hrs) exposure to anoxic conditions. Following further anoxic incubation, high rates of dissolved hydrogen production were observed and accompanied by further accumulation of these lipid compounds. These observations indicate that fermentation is likely a major process in anoxic carbonate sediments.

Declaration

This thesis contains no material which has been accepted for the award of any other degree or diploma at any university or equivalent institution and that, to the best of my knowledge and belief, this thesis contains no material previously published or written by another person, except where due reference is made in the text of the thesis.

Signature: …….　▮▮▮▮▮▮▮▮　……………
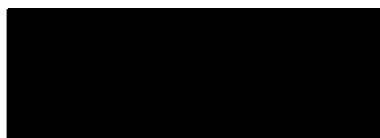
Print Name: …Michael Bourke……………….

Date: …31/08/2017……………………….

Thesis including published works declaration

I hereby declare that this thesis contains no material that has been accepted for the award of any other degree or diploma at any university or equivalent institution and that, to the best of my knowledge and belief, this thesis contains no material previously published or written by another person, except where due reference is made in the text of the thesis.
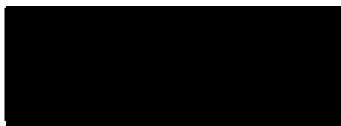
Material presented in chapters 2, 3, 4 and 5 of this thesis has been published in a peer reviewed journal. This thesis contains no submitted publications. The core theme of the thesis is investigating anoxic dissolved inorganic carbon production in permeable sediments. The ideas, development and writing up of all the papers in the thesis were the principal responsibility of myself, the student, working within the Water Studies Centre under the supervision of Assoc. Prof. Perran Cook.

I have not renumbered sections of submitted or published papers in order to generate a consistent presentation within the thesis.

For the material from chapters 2, 3, 4 and 5 that was published, my contribution to the work involved the following:

Thesis Chapters	Publication Title	Status	Nature and % of student contribution	Co-author name(s) Nature and % of Co-author's contribution	Co-author(s), Monash student Y/N
2, 3, 4 and 5.	Metabolism in anoxic permeable sediments is dominated by eukaryotic dark fermentation.	Published	Performed all experiments, analyzed samples and wrote draft of research paper. 70%.	1) Assoc. Prof. Perran L.M. Cook, major input with respect to direction of research, assisted in editing manuscript.15% 2) Prof. Ronnie N. Glud, input with respect to direction of research, assisted in editing manuscript. 5% 3) Prof. Phillip Marriott, assisted in editing manuscript.2% 4) Dr. Harald Hasler-Sheetal., performed metabolomics analyses (Ch. 4)assisted in editing manuscript. 2% 5) Dr. Manoj Kamalanathan, major assistance in the growth of cultures (Ch. 5), assisted in editing manuscript.2% 6) Prof. John Beardall, contributed to the direction of research and assisted in editing manuscript. 2%, 7) Dr. Chris Greening, assisted in editing manuscript. 2%	No, for all co-authors.

Student signature: ████████████ **Date:** **31/08/2017**

The undersigned hereby certify that the above declaration correctly reflects the nature and extent of the student's and co-authors' contributions to this work. In instances where I am not the responsible author I have consulted with the responsible author to agree on the respective contributions of the authors.

Main Supervisor signature: ████████████ **Date:** **31/08/2017**

Acknowledgements

This research was, in no small part, made possible by the support and advice from some key people in my life.

My primary supervisor, Perran Cook, has been a tremendous resource throughout my candidature and was strongly committed to helping me be successful. His passion for biogeochemistry is a major reason why working with him continues to be such an appealing prospect and it shines the brightest when discussing new frontiers of research. Perran, I'm very proud of the research we've undertaken together and I'm very grateful for all of your hard work over the years.

I'd like to acknowledge Mike Grace and Kellie Vanderkruk, who have constantly made themselves available to me for advice and support.

I'd also like to warmly thank Adam Kessler. Whether it was joining me for field trips, dropping everything to answer questions or offering guidance with my research, Adam has always been happy to help and exceedingly generous with his time, almost to a fault. Adam, thank you for your friendship and all the help.

I'm also very appreciative of the other members of the Water Studies Centre, for their friendship and assistance. In particular, Doug Russell, Nick Young (honorary WSC member), Peter Fabre, Keryn Roberts, Keralee Browne, Vera Eate, Wei Wen Wong (W^3), Erinn Richmond, Todd Scicluna, Ryan Woodland, Caitlyn McNaughton, Victor Evrard, Jesse Pottage, Dale Christensen, Stephanie Robson, David Brehm, Cami Plum and Sharlynn Koh. My PhD journey was a challenging and rewarding experience and each of you added a bit of joy along the way.

Lastly, I want to acknowledge the support of my family and my wife, Bec. Bec, thank you for your unending encouragement, love and understanding. I couldn't have asked for a more loving respite from the rigours of research than you and the dogs. To the rest of my family, thank you all for your love and support. Without it, this research would not have been possible.

List of Figures

List of Tables

Chapter 1: Introduction

1.1 Permeable sediment type and solute transport

Despite permeable sediments comprising a majority of the continental shelf [1], most research

into organic carbon metabolism has been within the context of cohesive sediments[2,3].

Sediment types are distinguished by their grain size and subsequent permeability. Cohesive

(muddy) sediments are made up of very small, tightly packed grains whilst permeable (sandy)

sediments have comparatively larger grains (> 100 μm^4). Due to the low permeability of

cohesive sediments, solutes are transported only via molecular diffusion, down concentration

gradients [5]. Permeable sediments, however, transport solutes via both diffusion and advective

pore water flow, i.e. bulk flow through the sediment[6]. Wave action results in the formation of

sediment ripples (Figure 1.1). Oxic water is advected through sediment ripple troughs[7], whilst

sediment porewater is expelled at ripple crests[8].
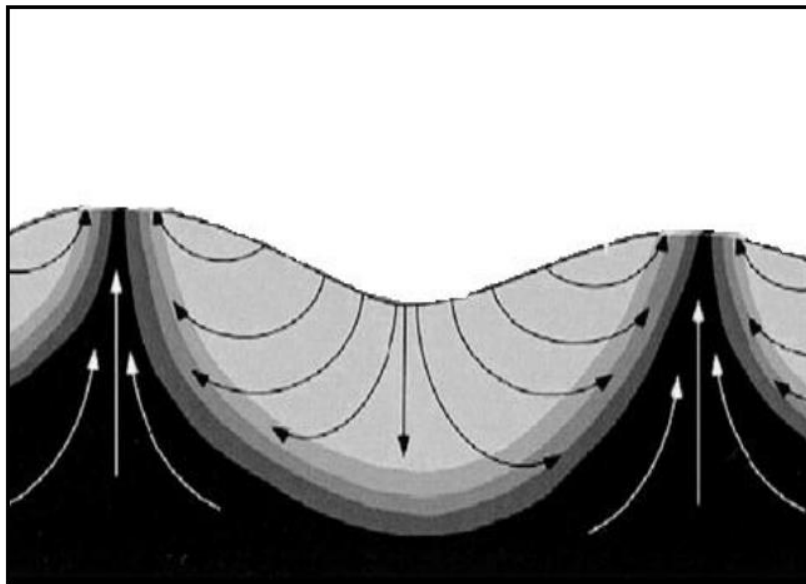
Figure 1.1: Conceptual diagram of a typical advective flow profile through a permeable sediment ripple. Arrows represent the path of advection [9]. Relative dissolved oxygen concentration is represented by light and dark shading corresponding to high and low dissolved oxygen concentrations, respectively.

Rates of advective transport are caused by water pressure gradients from wave action interacting with sediment ripple topography [10,11], resulting in dynamic sediment conditions that can shift between oxic and anoxic on an hourly-daily-weekly timescale[12]. Research focusing on how metabolism in permeable sediments change in response to rapid shifts in oxygen concentration is scarce and to the author's knowledge, the research presented in this thesis is the first to do so.

1.2 Flow through reactors (FTRs) and the challenge of replicating flow conditions

Nutrient fluxes in cohesive sediments may be readily studied by employing benthic chambers that enclose a portion of sediment and enable solutes to be easily sampled and fluxes calculated[13]. However, enclosing permeable sediments in the same manner will disrupt the overlying hydrodynamic pressure gradients from interacting with sediment topography, altering conditions so that they may not be representative of natural conditions[14]. Another means to estimate nutrient fluxes in permeable sediments is with flume tanks[15]. Flume tanks reproduce wave action over sculpted sediment ripples and allow for measurement of nutrient fluxes by sampling overlying water and direct sampling of porewater via silicon ports. Flume experiments have allowed for excellent estimations of the spatial distribution of dissolved oxygen[12] and nitrogen[16] in permeable sediments.

Flow through reactors (FTRs) (Figures 1.2 and 1.3), however, use idealized, non-representative advective plug flow[17,18] and have been widely used to determine volumetric biogeochemical rates at fixed solute concentrations[19-21].
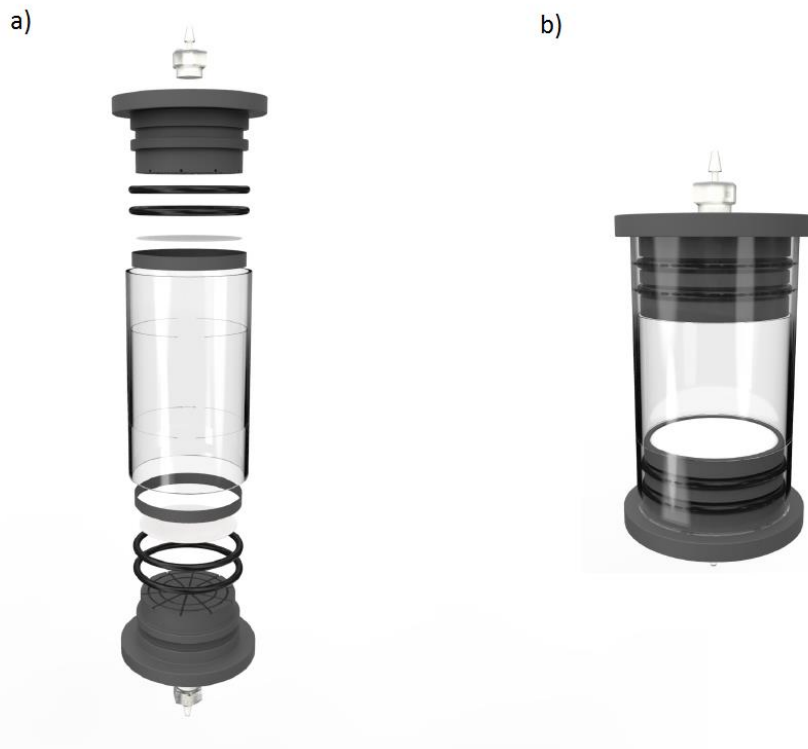
Figure 1.2: Rendering of a flow through reactor in exploded (a) and collapsed (b) perspectives. FTRs are comprised of an acrylic cylinder with a diameter of 4.6 cm and a length of 8.5cm to allow for a sediment height of 4.5 cm. PVC caps at either ends are machined with groves converging on a central outlet port overlaid with a 0.1 mm nylon mesh to allow even plug flow through the column. Plug flow within these columns has been verified during breakthrough curve experiments performed by Evrard *et al*[18] and Bourke *et al*[17].

FTRs are a convenient means of determining potential rates under a wide variety of conditions. Factors that influence porewater conditions, such as nutrient concentration, flow velocity and temperature are easily manipulated. FTR experiments (Figure 1.3) can be rapidly assembled within hours of collecting sample sediment and seawater. Reaction rates are calculated based on the difference between the relevant solute concentration in the reservoir and the outlet of the FTRs. Potential biochemical rates, measured in FTR experiments have also been instrumental in constraining computational reactive transport models[16,22,23].
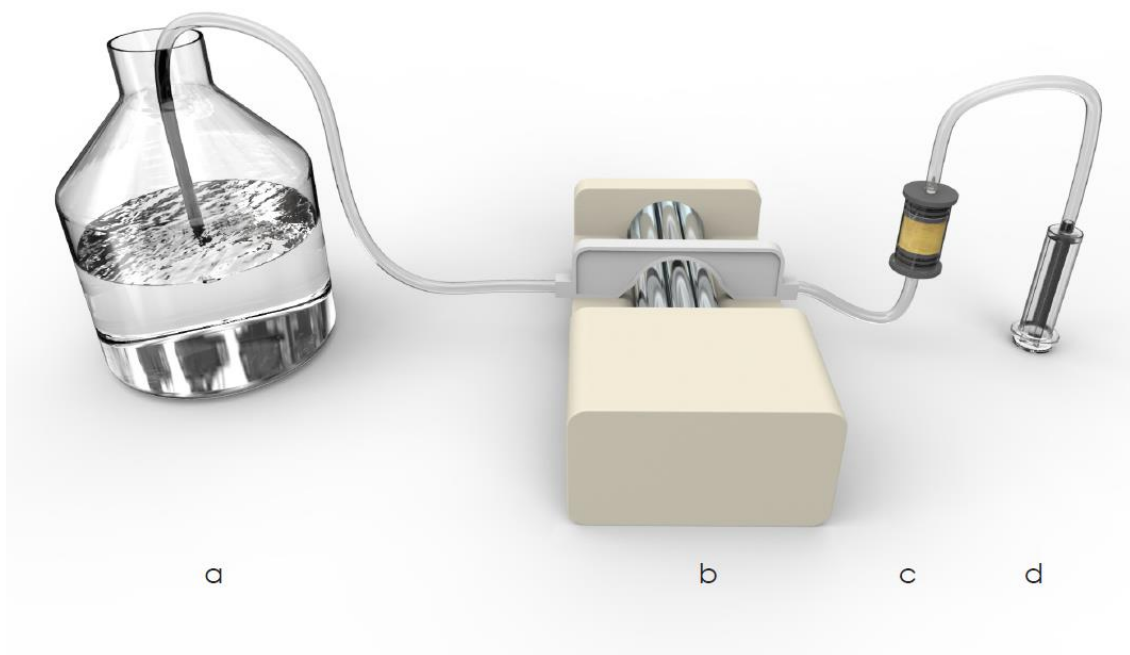
Figure 1.3: Rendering of a FTR experimental setup. Seawater is pumped from a reservoir (a) using a peristaltic pump (b) up through a FTR, packed with permeable sediment (c) and effluent is collected using a glass syringe (d).

1.3 Anaerobic heterotrophic metabolism

Groups of microorganisms can be broadly categorized by how they obtain organic carbon, necessary for adenosine triphosphate (ATP) generation and cell function. Photoautotrophs fix their own organic carbon using photosynthesis, while heterotrophs do not photosynthesize and instead source their carbon extracellularly, usually from decaying matter or exuded from photoautotrophs. Although there are several other methods of carbon fixation, e.g. chemoautotrophs, lithotrophs etc., coastal permeable sediments are typically dominated by autotrophic and heterotrophic microorganisms[27] and therefore other forms of carbon fixation have little relevance. For this reason, only autotrophic and heterotrophic microorganisms will be discussed in further detail.

Large particulate organic polymers are gradually mineralized via a series of hydrolytic and fermentative reactions by a mutualistic consortia of heterotrophic microorganisms[24].

Prokaryotes are only able to transport molecules smaller than 600 Da across their cell membranes[25], and must therefore perform hydrolytic reactions extracellularly, relying upon either enzymes embedded to the external surface of their cells (ectoenzymes) or enzymes excreted from the cell (exoenzymes). The smaller organic molecules produced may then be transported across cell membranes and undergo fermentation reactions. Fermentation reactions are a diverse group of microbially-mediated pathways that involve organic carbon simultaneously undergoing oxidation and reduction, serving as both the electron acceptor and electron donor[26]. Common products of fermentation reactions in anaerobic carbon mineralization include volatile fatty acids, short chain alcohols, dissolved H_2 and CO_2 (reactions i-iv)[27].

i) Glucose fermentation to ethanol:

$C_6H_{12}O_6 \longrightarrow 2CH_3CH_2OH + 2CO_2$ $\Delta G^0 = -244.1$ kJ mol^{-1}

ii) Ethanol fermentation to acetate:

$CH_3CH_2OH + H_2O \longrightarrow CH_3COOH + 2H_2$ $\Delta G^0 = +34.8$ kJ mol^{-1}

iii) Lactate fermentation to acetate:

$CH_3CHOHCOOH + H_2O \longrightarrow CH_3COOH + CO_2 + 2H_2$ $\Delta G^0 = +23.9$ kJ mol^{-1}

iv) Propionate fermentation to acetate:

$CH_3CH_2COOH + 2H_2O \longrightarrow CH_3COOH + CO_2 + 3H_2$ $\Delta G^0 = +105.1$ kJ mol^{-1}
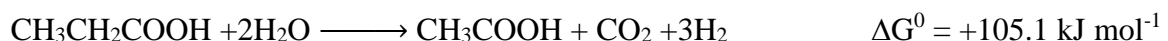
The products of these fermentative reactions generally do not accumulate in sediments, as these reactions are considered to be closely coupled to terminal heterotrophic reactions (reactions v-viii)[27], which involve electrons being donated from small organic molecules to an inorganic electron acceptor. These processes occur in the inner membrane of cell mitochondria and utilize several redox steps to ultimately generate ATP at varying

efficiencies depending upon the electron acceptor used. The hydrolysis of the terminal phosphate on ATP is a high energy yield reaction (ΔG= -32 kJ mol^{-1}) that enables otherwise unfavourable reactions necessary for cell function.

v) Aerobic respiration:
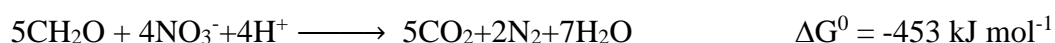
$$CH_2O + O_2 \longrightarrow CO_2 + H_2O \qquad\qquad \Delta G^0 = -501 \text{ kJ mol}^{-1}$$

vi) Denitrification:

$$5CH_2O + 4NO_3^- + 4H^+ \longrightarrow 5CO_2 + 2N_2 + 7H_2O \qquad\qquad \Delta G^0 = -453 \text{ kJ mol}^{-1}$$

vii) Iron reduction:

$$CH_2O + 4FeOOH + 8H^+ \longrightarrow CO_2 + 4Fe^{2+} + 7H_2O \qquad\qquad \Delta G^0 = -114 \text{ kJ mol}^{-1}$$

viii) Sulfate reduction:

$$2CH_2O + SO_4^{\,2-} + H^+ \longrightarrow 2CO_2 + HS^- + H_2O \qquad\qquad \Delta G^0 = -77 \text{ kJ mol}^{-1}$$

Microbial selectivity for electron acceptors is primarily based upon the magnitude of their energetic yield and their availability. Once the most energetically favourable electron acceptor has been depleted, the next most favourable will be utilised, resulting in a gradual cascade of progressively less favourable electron acceptors with increasing depth[28]. The research presented throughout this thesis, represents the first systematic study of electron acceptor utilization in freshly collected permeable sediments.

1.4 The discrepancy between rates of dissolved inorganic carbon (DIC) production and rates of heterotrophic metabolism

According to the redox cascade, under anoxic conditions in the presence of nitrate, denitrification (reaction vi) is expected to be the dominant metabolic pathway utilized. The stoichiometric ratio of denitrification (reaction vi) indicates that for every 4 moles of NO_3^- consumed, 5 moles of CO_2 should be produced. However, preliminary flow through reactor (FTR) experiments revealed a large discrepancy between the measured dissolved inorganic carbon (DIC) production rates and the expected DIC production rate (Figure 1.4). This expected DIC production rate was calculated using the measured denitrification rate and accompanying stoichiometric ratio between of NO_3^- consumption and CO_2 production. In fact, across five days of sampling, denitrification only accounted for between 2-5% of the total DIC production, leaving a great deal of DIC without a known mechanism for production. This phenomenon has also been observed in Kessler, et al. [16] and Evrard, et al. [29] and the investigation of which, is the primary focus of this research.
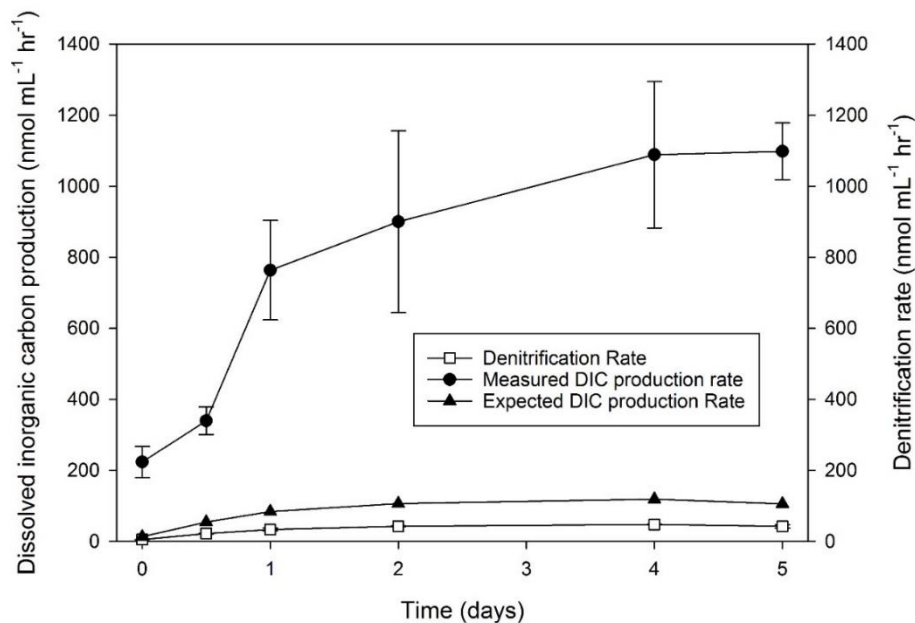
Figure 1.4. Large gap between measured DIC production rate and expected DIC production rate, based on denitrification rates (nmol ml^{-1} h^{-1}) against time (days) from preliminary FTR experiments in Kertimende, Denmark, performed by Assoc. Prof. Perran L.M Cook.

1.5 Possible sources of large quantities of DIC under anoxic conditions

1.5.1 Aerobic respiration

One possibly substantial source of DIC may be that FTRs were not gas tight, allowing leakage of oxygen into the sediment, and aerobic respiration to occur at high rates.

1.5.2 Anoxic respiration by benthic meiofauna

Another possible source of DIC that will be investigated is respiration by meiofauna. Meiofauna are a group of invertebrates that are small enough to pass through a 1 mm sieve, but will be retained by a 42 μm mesh[30]. It includes representatives from 23 different phyla[31], however, nematodes, copepods and turbellarians typically comprise >95% of the total meiofaunal community in sediments[31]. While select species of meiofauna are capable of facultative anaerobic respiration, such as the *foraminifera Ammonia spp.*[32], the large majority are not. Copepods and turbellarians are generally considered to be highly sensitive to low oxygen concentrations, with incubation experiments revealing almost all such organisms perished within 24 hours of anoxia[32,33]. Nematodes are considered to be more tolerant to anoxic conditions, however, this is highly species dependent[34,35]. For example, during an anoxic incubation experiment performed on marine permeable sediments, whole populations of nematodes, belonging to three dominant species, perished within an 8 day incubation period. The populations of 3 other dominant species did not diminish, despite a 14 day period of extended anoxic incubation[35]. In this experiment the total nematode community decreased to one third of its original number over the 14 day period[35].

While species of nematodes may exhibit adaptations to allow for survival of hypoxic conditions, such as an increase in the surface area to volume ratio of their morphology[36] and

decreasing oxygen demand by reducing rates of metabolism[37], adaptations enabling the survival of extended anoxic conditions have not been well studied. Due to the varying degrees of success by which nematode species survive extended anoxic conditions[35], several different strategies or adaptions may be being employed. One such strategy could be analogous to that observed in the free-living terrestrial nematode species *Caenorhabditis elegans*. This organism enters a state of recoverable suspended animation whereby energy requiring processes are arrested upon exposure to anoxic conditions, including movement, developmental progression and cell division[38]. These processes are resumed upon the return to oxic sediment conditions and allow for the organism to survive extended periods of anoxia. DIC production from meiofaunal respiration can therefore be expected to decrease substantially after 24 hours of anoxic FTR conditions, as the majority of meiofauna will likely perish. Thereafter, rates of DIC production by meiofauna would be expected to gradually decline as a relatively small proportion of foraminifera may respire via facultative anaerobic respiration and anoxic-tolerant nematodes survive to varying degrees of success. Given this, it is unlikely that meiofauna are responsible for the majority of the anoxic DIC production in permeable sediments, however, the size of their contribution may be substantial and will be quantified during this research.

1.5.3 DNRA via intracellular nitrate pool

Dissimilatory nitrate reduction to ammonium (DNRA) (reaction ix) is a heterotrophic metabolic process in which nitrate is reduced via the oxidation of organic carbon[39]. As nitrate is reduced to nitrite and then to ammonium, bioavailable nitrogen is recycled within the system[40]. As DNRA is far less energetically favourable compared to aerobic respiration, it is exclusively an anaerobic process[41,42].

ix) Dissimilatory nitrate reduction to ammonium (DNRA):

$$NO_3^- \longrightarrow NO_2^- \longrightarrow NH_4^+$$

DNRA may be performed by a wide range of microorganisms including large sulphur

bacteria[43,44] and eukaryotic microorganisms such as benthic and pelagic diatoms[45,46]. Large

pools of intracellular nitrate have been observed to accumulate in excess of 100 mmol L^{-1} in

the vacuoles of both prokaryotic[47,48] and eukaryotic microorganisms[49,50]. As diatoms

dominate intertidal sediments[51], DNRA via intracellularly stored nitrate may be an

overlooked process and a substantial source of anoxic DIC production. Although rates of

DNRA in permeable sediments have not been observed to occur at rates comparable to

anoxic DIC production, recent reports of high concentrations of intracellularly stored nitrate[46]

in both prokaryotic and eukaryotic microorganisms suggests that DNRA may be an

alternative catabolic pathway for diatoms once oxygen is depleted.

1.5.4 Calcium carbonate dissolution

Calcium carbonate is the primary component of shells of marine organisms and has a

relatively low degree of solubility. Since seawater is oversaturated with respect to $CaCO_3$ and

precipitation is inhibited by high magnesium concentrations[27], the deposition of this mineral

in natural settings is almost exclusively biologically mediated. Carbonate dissolution

(reaction x) can be promoted by the acidity produced during H_2S oxidation[52] and aerobic

carbon mineralization[53].

x) Calcium Carbonate Dissolution
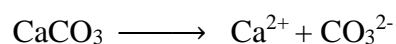
$$CaCO_3 \longrightarrow Ca^{2+} + CO_3^{2-}$$

Since the large majority of oxic DIC production can typically be ascribed to aerobic

respiration, rates of $CaCO_3$ dissolution would need to begin immediately following the

transition from oxic to anoxic conditions for this process to be responsible for the observed large quantities of anoxic DIC production.

1.5.5 Fermentation uncoupled to heterotrophic metabolism

Another potential source of anoxic DIC production is fermentation, uncoupled to heterotrophic metabolism. As previously mentioned, in sediments, fermentation reactions may be utilized during organic carbon mineralization, via reactions i-iv, and the small organic molecules produced are thought to be consumed rapidly by the closely coupled terminal heterotrophic metabolic processes[28] (reactions v-viii). However, should rates of fermentation exceed rates of heterotrophic metabolism, the contribution of anoxic DIC may be being underestimated. Quantifying the rate of fermentation poses a challenge as the consumption of an electron acceptor (like oxygen or nitrate) cannot be employed. It is further complicated as there are a wide variety of reactants, products and stoichiometries that are often used in combination with one another[54,55].

In prokaryotes, culture studies have revealed that the degree to which different fermentative pathways are utilized is largely dependent upon what organic carbon source is metabolized[26]. For example, *E. Coli* has been observed to produce ethanol when provided with sorbitol, but when given glucuronic acid, no ethanol production was observed, and instead acetate was the dominant product[56,57]. Bacterial fermentation of low molecular weight organic carbon molecules commonly produces dissolved hydrogen, carbon dioxide (DIC), lactate, succinate, ethanol, formate and acetate[56,58,59].

Fermentation may also be performed by autotrophic eukaryotic microorganisms as a means of sustaining cell function in periods where sediment resuspension has resulted in cells being buried at depths where no light or oxygen is available[45]. Eukaryotic fermentation includes a wide variety of pathways and reaction stoichiometries that vary with species, substrate and

environmental factors[60-62]. For example, *C Reinhardtii* has been observed to produce formate, acetate and ethanol in a 2:2:1 ratio under dark conditions[63]. Whilst, *C.moewusii* produced no formate under dark conditions, with acetate, glycerol and ethanol being the major products[64]. Amongst marine eukaryotic microalgae, common products that arise from the fermentation of starch have included acetate, ethanol, formate, glycerol, lactate, H_2 and CO_2[63,65,66].

Some microalgae do not excrete fermentative products and instead accumulate them intracellularly[67]. *Euglena gracilis* has been found to store large concentrations of wax esters when incubated anoxically[68] and has been found to accumulate them to such an extent that they have made up 65% of the algae's dry weight[69]. Upon returning to oxic conditions, these wax esters are oxidized to generate ATP.

If fermentation by prokaryotic or eukaryotic microorganisms is occurring at rates exceeding heterotrophic metabolism, the aforementioned fermentative products should be present in high concentrations in sediment porewater, or be accumulating intracellularly. Quantification of these products will determine whether fermentation may be dominating anoxic metabolism in permeable sediments.

1.6 Project aims and thesis structure

The primary aim of this research was to investigate metabolic pathways in permeable sediments under anoxic conditions.

This was achieved by addressing 4 key research questions:

1. Can anaerobic DIC production be attributed to an abiotic source, such as calcium carbonate dissolution?

2. Can anaerobic DIC production be attributed to a biotic source and if so, via what process?

3. What group of organisms are responsible?

4. How widespread is this phenomenon and can it be observed in other permeable sediments such as tropical carbonate sediments?

1.7 References

1   Emery, K. O. Relict sediments on continental shelves of the world. *American Association of Petroleum Geologists Bulletin* 52, 445-464, (1968).

2   Lohse, L., Kloosterhuis, H. T., vanRaaphorst, W. & Helder, W. Denitrification rates as measured by the isotope pairing method and by the acetylene inhibition technique in continental shelf sediments of the North Sea. *Mar. Ecol. Prog. Ser.* 132, 169-179, (1996).

3   Vance-Harris, C. & Ingall, E. Denitrification pathways and rates in the sandy sediments of the Georgia continental shelf, USA. *Geochemical Transactions* 6, 12-18, (2005).

4   Huettel, M. & Rusch, A. Transport and degradation of phytoplankton in permeable sediment. *Limnol. Oceanogr.* 45, 534-549, (2000).

5   Burdige, D. J. Geochemistry of Marine Sediments. *1 ed. Princeton University Press*, (2006).

6   Huettel, M., Roy, H., Precht, E. & Ehrenhauss, S. Hydrodynamical impact on biogeochemical processes in aquatic sediments. *Hydrobiologia* 494, 231-236, (2003).

7   Janssen, F., Huettel, M. & Witte, U. Pore-water advection and solute fluxes in permeable marine sediments (II): Benthic respiration at three sandy sites with different permeabilities. *Limnol. Oceanogr.* 50, 779-792, (2005).

8   Shum, K. T. Wave induced advective transport below a rippled water sediment interface. *Journal of Geophysical Research-Oceans* 97, 789-808, (1992).

9   Precht, E., Franke, U., Polerecky, L. & Huettel, M. Oxygen dynamics in permeable sediments with wave-driven pore water exchange. *Limnology and Oceanography* 49, 693-705, (2004).

10   Webb, J. E. & Theodor, J. Irrigation of submerged marine sands through wave action. *Nature* 220, 682-&, (1968).

11   Santos, I. R., Cook, P. L. M., Rogers, L., de Weys, J. & Eyre, B. D. The "salt wedge pump": Convection-driven pore-water exchange as a source of dissolved organic and inorganic carbon and nitrogen to an estuary. *Limnol. Oceanogr.* 57, 1415-1426, (2012).

12   Precht, E., Franke, U., Polerecky, L. & Huettel, M. Oxygen dynamics in permeable sediments with wave-driven porewater exchange. *Limnol. Oceanogr.* 49, 693-705, (2004).

13   Glud, R. N., Gundersen, J. K., Revsbech, N. P., Jorgensen, B. B. & Huttel, M. Calibration and performance of the stirred flux chamber from the benthic lander Elinor. . *Deep-Sea Research Part I-Oceanographic Research Papers* 42, 1029-1042, (1995).

14   Cook, P. L. M. *et al.* Quantification of denitrification in permeable sediments: Insights from a two-dimensional simulation analysis and experimental data. *Limnology and Oceanography-Methods* 4, 294-307, (2006).

15   Huettel, M., Ziebis, W., Forster, S. & Luther, G. W. Advective transport affecting metal and nutrient distributions and interfacial fluxes in permeable sediments. *Geochim. Cosmochim. Acta* 62, 613-631, (1998).

16   Kessler, A. J. *et al.* Quantifying denitrification in rippled permeable sands through combined flume experiments and modeling. *Limnol. Oceanogr.* 57, 1217-1232, (2012).

17   Bourke, M., Kessler, A. & Cook, P. Influence of buried Ulva lactuca on denitrification in permeable sediments. *Mar. Ecol. Prog. Ser.* 498, 85-94, (2014).

18   Evrard, V., Glud, R. N. & Cook, P. L. M. The kinetics of denitrification in permeable sediments. *Biogeochemistry* 113, 563-572, (2012).

19   Rao, A. M. F., McCarthy, M. J., Gardner, W. S. & Jahnke, R. A. Respiration and denitrification in permeable continental shelf deposits on the South Atlantic Bight: Rates of carbon and nitrogen cycling from sediment column experiments. *Cont. Shelf Res.* 27, 1801-1819, (2007).

20   Roychoudhury, A. N., Viollier, E. & Van Cappellen, P. A plug flow-through reactor for studying biogeochemical reactions in undisturbed aquatic sediments. *Appl. Geochem.* 13, 269-280, (1998).

21   Gao, H. *et al.* Aerobic denitrification in permeable Wadden Sea sediments. *Isme Journal* 4, 417-426, (2010).

22   Meysman, F. J. R. *et al.* Quantifying biologically and physically induced flow and tracer dynamics in permeable sediments. *Biogeosciences* 4, 627-646, (2007).

23   Cardenas, M. B., Cook, P. L. M., Jiang, H. & Traykovski, P. Constraining denitrification in permeable wave-influenced marine sediment using linked hydrodynamic and biogeochemical modeling. *Earth and Planetary Science Letters* 275, 127-137, (2008).

24   Holmer, M. & Kristensen, E. Organic matter mineralization in an organic rich sediment. Experimental stimulation of sulfate reduction by fish food pellets. *FEMS Microbiol. Ecol.* 14, 33-44, (1994).

25   Weiss, M. S. *et al.* Molecular architecture and electrostatic properties of a bacterial porin. *Science* 254, 1627-1630, (1991).

26   Catalanotti, C., Yang, W., Posewitz, M. C. & Grossman, A. R. Fermentation metabolism and its evolution in algae. *Front. Plant. Sci.* 4, 150, (2013).

27   Canfield, D. E., Kristensen, E. & Thamdrup, B. in *Aquatic Geomicrobiology* Vol. 48 *Advances in Marine Biology* Ch. 10, 383-414 (Academic Press Ltd-Elsevier Science Ltd, 2005).

28   Canfield, D. E., Thamdrup, B. & Hansen, J. W. The anaerobic degradation of organic matter in danish coastal sediments- iron reduction, manganese reduction and sulfate reduction. *Geochim. Cosmochim. Acta* 57, 3867-3883, (1993).

29   Evrard, V., Glud, R. N. & Cook, P. L. M. The kinetics of denitrification in permeable sediments. *Biogeochemistry* 113, 563-572, (2013).

30   Mare, M. F. A study of a marine benthic community with special reference to the micro-organisms. *Jour Marine Biol Assoc* 25, 517-554, (1942).

31   Vincx, M. in *Methods for the examination of organismal diversity in soils and sediments.*   Ch. 15, 187-195 (CAB, 1996).

32   Moodley, L. & Hess, C. Tolerance of infaunal benthic foraminefera for low and high oxygen concentrations. *Biological Bulletin* 183, 94-98, (1992).

33   Moodley, L., vanderZwaan, G. J., Herman, P. M. J., Kempers, L. & vanBreugel, P. Differential response of benthic meiofauna to anoxia with special reference to Foraminifera (Protista: Sarcodina). *Mar. Ecol. Prog. Ser.* 158, 151-163, (1997).

34   Soetaert, K., Muthumbi, A. & Heip, C. Size and shape of ocean margin nematodes: morphological diversity and depth-related patterns. *Mar. Ecol. Prog. Ser.* 242, 179-193, (2002).

35   Steyaert, M. *et al.* Responses of intertidal nematodes to short-term anoxic events. *J. Exp. Mar. Biol. Ecol.* 345, 175-184, (2007).

36   Braeckman, U., Vanaverbeke, J., Vincx, M., van Oevelen, D. & Soetaert, K. Meiofauna Metabolism in Suboxic Sediments: Currently Overestimated. *Plos One* 8, (2013).

37   Taheri, M., Braeckman, U., Vincx, M. & Vanaverbeke, J. Effect of short-term hypoxia on marine nematode community structure and vertical distribution pattern in three different sediment types of the North Sea. *Mar. Environ. Res.* 99, 149-159, (2014).

38   Padilla, P. A., Nystul, T. G., Zager, R. A., Johnson, A. C. M. & Roth, M. B. Dephosphorylation of cell cycle-regulated proteins correlates with anoxia-induced suspended animation in Caenorhabditis elegans. *Molecular Biology of the Cell* 13, 1473-1483, (2002).

39   Fewson, C. A. & Nicholas, D. J. NITRIC OXIDE REDUCTASE FROM PSEUDOMONAS AERUGINOSA. *Biochem. J.* 78, P09-&, (1961).

40   An, S. M. & Gardner, W. S. Dissimilatory nitrate reduction to ammonium (DNRA) as a nitrogen link, versus denitrification as a sink in a shallow estuary (Laguna Madre/Baffin Bay, Texas). *Mar. Ecol. Prog. Ser.* 237, 41-50, (2002).

41   Strohm, T. O., Griffin, B., Zumft, W. G. & Schink, B. Growth yields in bacterial denitrification and nitrate ammonification. *Appl. Environ. Microbiol.* 73, 1420-1424, (2007).

42   Kraft, B., Strous, M. & Tegetmeyer, H. E. Microbial nitrate respiration - Genes, enzymes and environmental distribution. *J. Biotechnol.* 155, 104-117, (2011).

43   Otte, S. *et al.* Nitrogen, carbon, and sulfur metabolism in natural Thioploca samples. *Appl. Environ. Microbiol.* 65, 3148-3157, (1999).

44   Preisler, A. *et al.* Biological and chemical sulfide oxidation in a Beggiatoa inhabited marine sediment. *Isme Journal* 1, 341-353, (2007).

45   Kamp, A., de Beer, D., Nitsch, J. L., Lavik, G. & Stief, P. Diatoms respire nitrate to survive dark and anoxic conditions. *Proc. Nat. Acad. Sci. USA* 108, 5649-5654, (2011).

46   Stief, P., Kamp, A. & de Beer, D. Role of Diatoms in the Spatial-Temporal Distribution of Intracellular Nitrate in Intertidal Sediment. *Plos One* 8, (2013).

47   McHatton, S. C., Barry, J. P., Jannasch, H. W. & Nelson, D. C. High nitrate concentrations in vacuolate, autotrophic marine Beggiatoa spp. *Appl. Environ. Microbiol.* 62, 954-958, (1996).

48   Mussmann, M. *et al.* Phylogeny and distribution of nitrate-storing Beggiatoa spp. in coastal marine sediments. *Environ. Microbiol.* 5, 523-533, (2003).

49   Risgaard-Petersen, N. *et al.* Evidence for complete denitrification in a benthic foraminifer. *Nature* 443, 93-96, (2006).

50   Hogslund, S., Revsbech, N. P., Cedhagen, T., Nielsen, L. P. & Gallardo, V. A. Denitrification, nitrate turnover, and aerobic respiration by benthic foraminiferans in the oxygen minimum zone off Chile. *J. Exp. Mar. Biol. Ecol.* 359, 85-91, (2008).

51   Barranguet, C., Herman, P. M. J. & Sinke, J. J. Microphytobenthos biomass and community composition studied by pigment biomarkers: importance and fate in the carbon cycle of a tidal flat. *J. Sea Res.* 38, 59-70, (1997).

52   Aller, R. C. Carbonate dissolution in nearshore terrigenous muds. The role of physical and biological reworking. *Journal of Geology* 90, 79-95, (1982).

53   Walter, L. M. & Burton, E. A. Dissolution of recent platform carbonate sediments in marine pore fluids. *Am. J. Sci.* 290, 601-643, (1990).

54   Revsbech, N. P., Trampe, E., Lichtenberg, M., Ward, D. M. & Kuhl, M. In Situ Hydrogen Dynamics in a Hot Spring Microbial Mat during a Diel Cycle. *Appl. Environ. Microbiol.* 82, 4209-4217, (2016).

55   Hoehler, T. M., Alperin, M. J., Albert, D. B. & Martens, C. S. Thermodynamic control on hydrogen concentrations in anoxic sediments. *Geochim. Cosmochim. Acta* 62, 1745-1756, (1998).

56   Wolfe, A. J. The acetate switch. *Microbiol. Mol. Biol. Rev.* 69, 12-+, (2005).

57   Alam, K. Y. & Clark, D. P. Anaerobic fermentation balance of escherichia coli as observed by invivo nuclear magnetic resonance spectroscopy. *J. Bacteriol.* 171, 6213-6217, (1989).

58   Gottschalk, G. *Bacterial Metabolism*. 2nd Edition edn, (Springer-Verlag, 1985).

59   Dien, B. S., Cotta, M. A. & Jeffries, T. W. Bacteria engineered for fuel ethanol production: current status. *Appl. Microbiol. Biotechnol.* 63, 258-266, (2003).

60   Kreuzberg, K. Starch fermentation via a formate producing pathway in chlamydomonas reinhardii, chlorogonium elongatum and chlorella fusca. *Physiol. Plant.* 61, 87-94, (1984).

61   Ohta, S., Miyamoto, K. & Miura, Y. Hydrogen evolution as a consumption mode of reducing equivalents in green algal fermentation. *Plant Physiol.* 83, 1022-1026, (1987).

62   Atteia, A., van Lis, R., Tielens, A. G. M. & Martin, W. F. Anaerobic energy metabolism in unicellular photosynthetic eukaryotes. *Biochimica Et Biophysica Acta-Bioenergetics* 1827, 210-223, (2013).

63   Mus, F., Dubini, A., Seibert, M., Posewitz, M. C. & Grossman, A. R. Anaerobic acclimation in Chlamydomonas reinhardtii - Anoxic gene expression, hydrogenase induction, and metabolic pathways. *J. Biol. Chem.* 282, 25475-25486, (2007).

64   Meuser, J. E. *et al.* Phenotypic diversity of hydrogen production in chlorophycean algae reflects distinct anaerobic metabolisms. *J. Biotechnol.* 142, 21-30, (2009).

65   Gaffron, H. & Rubin, J. Fermentative and photochemical production of hydrogen in algae. *The Journal of general physiology* 26, 219-240, (1942).

66   Klein, U. & Betz, A. Fermentative metabolism of hydrogen evolving chlamydomonas moewusii. *Plant Physiol.* 61, 953-956, (1978).

67   Valdemarsen, T. & Kristensen, E. Degradation of dissolved organic monomers and short-chain fatty acids in sandy marine sediment by fermentation and sulfate reduction. *Geochim. Cosmochim. Acta* 74, 1593-1605, (2010).

68   Inui, H., Miyatake, K., Nakano, Y. & Kitaoka, S. Wax ester fermentation in euglena gracilis. *FEBS Lett.* 150, 89-93, (1982).

69   Tucci, S., Vacula, R., Krajcovic, J., Proksch, P. & Martin, W. Variability of Wax Ester Fermentation in Natural and Bleached Euglena gracilis Strains in Response to Oxygen and the Elongase Inhibitor Flufenacet. *J. Eukaryot. Microbiol.* 57, 63-69, (2010).

Chapter 2: Investigation of pathways of dissolved inorganic carbon production in anoxic permeable sediments

2.1 Abstract:

Heterotrophic metabolism using terminal inorganic electron acceptors has long been thought to dominate respiration in anoxic permeable sediments. However, recent measurements indicate that the contribution of these processes to total anoxic dissolved inorganic carbon production may be smaller than previously assumed. During this research, experiments using flow through reactors (FTRs) revealed that in anoxic permeable sediments, there exists a large proportion (93-98%) of dissolved inorganic carbon production that cannot be attributed to the consumption of well-known terminal electron acceptors. This phenomenon was observed in all FTR experiments performed, indicating a highly reproducible phenomenon. Dissimilatory nitrate reduction to ammonium (DNRA) via pools of intracellularly stored nitrate, was investigated as a possible source of anoxic DIC, but was discounted after intracellular nitrate pools were found to be negligible compared to rates of DIC production. Calcium carbonate ($CaCO_3$) dissolution was discounted as a possible major source of anoxic DIC production after alkalinity production rates were determined to be negative following the change from oxic to anoxic conditions and there was no net increase in the ratio of dissolved Ca^{2+} to Na^+ ions throughout the FTR experiment. Gas leakage into the FTRs was negligible, which discounted the possibility of aerobic respiration substantially contributing towards anoxic DIC production. Isotopic analysis of DIC from FTR effluent gave a $^{13}C/^{12}C$ enrichment endpoint revealing the breakdown of organic material, produced by phytoplankton and microphytobenthos, as the source of anoxic DIC production (as opposed to carbonate dissolution). Meiofaunal respiration was also investigated as a contributing source of anoxic DIC, but was estimated to be negligible after the expected gradual decline of anoxic DIC production typical of meiofaunal anoxic survival was not observed.

2.2 Introduction

In permeable sediments, solutes are transported via both molecular diffusion and advective pore water flow [1], i.e. bulk flow through the sediment [2]. Rates of advective transport are determined by water pressure gradients from wave action interacting with sediment ripple topography [3,4], resulting in a dynamic nature where sediment conditions can shift between oxic and anoxic on an hourly-daily-weekly timescale[5]. This makes replicating environmentally relevant flow conditions difficult[6]. However, flow through reactors (FTRs) offer a convenient means of studying biogeochemical processes and measuring volumetric rates accurately.

Microorganisms within permeable sediments derive energy by facilitating the breakdown of organic carbon. Photoautotrophs catabolize photosynthetically derived organic polymers, whilst heterotrophic microorganisms utilize organic carbon typically sourced from decaying matter or exuded from photoautotrophs[7]. Particulate organic polymers are gradually mineralized via a series of hydrolysis and fermentation reactions by a mutualistic consortia of heterotrophic microorganisms[8]. The final stages of which, involve the donation of electrons from small organic molecules (<600 Da[9]) to an appropriate inorganic electron acceptor[10]. These processes (reactions i-iv) occur in the inner membrane of cell mitochondria and utilize several redox steps to ultimately produce adenosine triphosphate (ATP). The hydrolysis of the terminal phosphate on ATP is a high energy yield reaction (ΔG= -32 kJ mol^{-1}) that enables otherwise unfavourable reactions necessary for cell function.

Microbial selectivity for electron acceptors is primarily based upon their availability and the magnitude of their energetic yield (reactions i-iv). Once the most energetically favourable electron acceptor has been depleted, the next most favourable will be utilised, resulting in a gradual cascade of progressively less favourable electron acceptors with increasing depth.

However, these reactions are not altogether mutually exclusive, as iron reduction and sulfate reduction have been observed to occur concurrently[11].

i) Aerobic respiration:

$$CH_2O + O_2 \longrightarrow CO_2 + H_2O \qquad\qquad \Delta G^0 = -501 \text{ kJ mol}^{-1}$$

ii) Denitrification:

$$5CH_2O + 4NO_3^- + 4H^+ \longrightarrow 5CO_2 + 2N_2 + 7H_2O \qquad\qquad \Delta G^0 = -453 \text{ kJ mol}^{-1}$$

iii) Iron reduction:

$$CH_2O + 4FeOOH + 8H^+ \longrightarrow CO_2 + 4Fe^{2+} + 7H_2O \qquad\qquad \Delta G^0 = -114 \text{ kJ mol}^{-1}$$

iv) Sulfate reduction:

$$2CH_2O + SO_4^{2-} + H^+ \longrightarrow 2CO_2 + HS^- + H_2O \qquad\qquad \Delta G^0 = -77 \text{ kJ mol}^{-1}$$
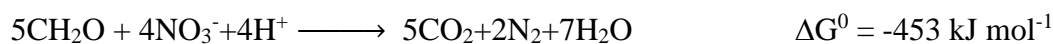
According to the stoichiometric ratio of denitrification (reaction ii), for every 4 moles of NO_3^- consumed, 5 moles of CO_2 should be produced. However, preliminary flow through reactor experiments (discussed in chapter 1) revealed a large discrepancy between the measured and predicted denitrification rates. In fact, across five days of sampling, denitrification only accounted for 2-5% of the total CO_2 production, leaving a great deal of dissolved inorganic carbon without a known mechanism for production. This phenomenon has also been observed in Kessler, et al. [12] and Evrard, et al. [13].

Throughout this chapter, this phenomenon was investigated by analysing FTR effluent for all reduced products of heterotrophic metabolism (reactions i-iv). Other possible sources were also investigated, including aerobic respiration brought about by oxygen leakage into FTRs, abiotic DIC production from $CaCO_3$ dissolution, respiration by meiofauna and DIC production via dissimilatory nitrate reduction to ammonia (DNRA). Furthermore, isotopic analysis of DIC produced during FTR experiments was also used to identify the source(s) responsible.

$CaCO_3$ is the primary component of shells of marine organisms and has a relatively low degree of solubility[14]. Since seawater is oversaturated with respect to $CaCO_3$ and precipitation is inhibited by high magnesium concentrations[15], the deposition of this mineral in natural settings is almost exclusively biologically mediated.

<div align="center">v) Calcium Carbonate Dissolution</div>
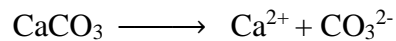
$$CaCO_3 \longrightarrow Ca^{2+} + CO_3^{2-}$$

Since the large majority of oxic DIC production can typically be ascribed to aerobic respiration[15,16], rates of $CaCO_3$ dissolution would need to begin immediately following the transition from oxic to anoxic conditions for this process to be responsible for the observed large quantities of anoxic DIC production. An increase in the alkalinity production rates proportional to twice the observed DIC production rates would be expected, due to the large quantities of carbonate being released.

Another means of determining whether $CaCO_3$ dissolution or a biotic process like organic carbon mineralization is responsible for the majority of anoxic DIC production in permeable sediments is by determining its isotopic signature ($\delta^{13}C$). In chemical and physical processes, the small difference in mass between ^{13}C and ^{12}C isotopes, leads to a preferential usage of one isotope over the other[17]. This results in a degree of isotopic enrichment characteristic of the carbon source[18]. The isotopic signature can then be determined by comparing the ratio of ^{13}C and ^{12}C isotopes to the Pee Dee Belemnite standard. For example, the DIC produced by the dissolution of calcium carbonate would have an isotopic signature of approximately -7.8‰[19]. Whereas, DIC produced during the metabolism of organic carbon produced by microphytobenthos and phytoplankton will typically have $\delta^{13}C$ values of between -15 to -16 ‰[20] and -21.1‰[21], respectively.

However, the high background concentration of DIC in seawater means that the isotopic signature of anoxic DIC production cannot be measured directly. Instead, a linear relationship

between the sample DIC $\delta^{13}C$ values and the inverse DIC concentration, also known as a Keeling plot, must be used[22]. The y intercept of this relationship is known as the $\delta^{13}C$ end member, which can then be used to identify the carbon source.

Dissimilatory nitrate reduction to ammonium (DNRA) is a heterotrophic metabolic process in which nitrate is reduced via the oxidation of organic carbon[23]. As nitrate is reduced to nitrite and then to ammonium, bioavailable nitrogen is recycled within the system, rather than being removed[24]. As DNRA is far less energetically favourable compared to aerobic respiration, it is considered to be exclusively anaerobic process[25,26].

vi) Dissimilatory nitrate reduction to ammonium (DNRA):

$$NO_3^- \longrightarrow NO_2^- \longrightarrow NH_4^+$$

DNRA may be performed by a wide range of microorganisms including large sulphur bacteria[27,28] and eukaryotic microorganisms such as benthic and pelagic diatoms[29,30]. Large pools of intracellular nitrate have been observed to accumulate in excess of 100 mmol L^{-1} in the vacuoles of both prokaryotic[31,32] and eukaryotic microorganisms[33,34]. As diatoms dominate intertidal sediments[35], DNRA via intracellularly stored nitrate may be an overlooked process and a substantial source of anoxic DIC production. Although DNRA rates in permeable sediments have not been observed to occur at rates comparable to anoxic DIC production, recent reports of high concentrations of intracellularly stored nitrate[30] in both prokaryotic and eukaryotic microorganisms suggests that DNRA may be an alternative catabolic pathway for diatoms once oxygen is depleted. Quantification of the intracellular nitrate pool will allow for a conclusive determination of whether DNRA could be a possible source of anoxically produced DIC.

Another possible source of DIC that will be investigated is respiration by meiofauna. Meiofauna are a group of invertebrates that are small enough to pass through a 1 mm sieve, but will be retained by a 42 μm mesh[36]. It includes representatives from 23 different phyla[37],

however, nematodes, copepods and turbellarians typically comprise >95% of the total meiofaunal community in sediments[37]. While select species of meiofauna are capable of facultative anaerobic respiration, such as the *foraminifera Ammonia spp.*[38], the large majority are not. Copepods and turbellarians are generally considered to be highly sensitive to low oxygen concentrations, with incubation experiments revealing almost all such organisms perished within 24 hours of anoxia[38,39]. Nematodes are considered to be more tolerant to anoxic conditions, however, this is highly species dependent[40,41]. For example, during an anoxic incubation experiment performed on marine permeable sediments, whole populations of nematodes, belonging to three dominant species, perished within an 8 day incubation period. The populations of 3 other dominant species did not diminish, despite a 14 day period of extended anoxic incubation[41]. In this experiment the total nematode community decreased to one third of its original number over the 14 day period[41].

While species of nematodes may exhibit adaptations to allow for survival of hypoxic conditions, such as an increase in the surface area to volume ratio of their morphology[42] and decreasing oxygen demand by reducing rates of metabolism[43], adaptations enabling the survival of extended anoxic conditions have not been well studied. Due to the varying degrees of success by which nematode species survive extended anoxic conditions[41], several different strategies or adaptions may be being employed. One such strategy could be analogous to that observed in the free-living terrestrial nematode species *Caenorhabditis elegans*. This organism enters a state of recoverable suspended animation whereby energy requiring processes are arrested upon exposure to anoxic conditions, including movement, developmental progression and cell division[44]. These processes are resumed upon the return to oxic sediment conditions and allow the organism to survive extended periods of anoxia, on a timescale of weeks to months.

DIC production from meiofaunal respiration can therefore be expected to decrease substantially after 24 hours of anoxic sediment conditions, as the majority of meiofauna will likely perish. Thereafter, rates of DIC production by meiofauna would be expected to gradually decline as a relatively small proportion of foraminifera may respire via facultative anaerobic respiration and anoxic-tolerant nematodes survive to varying degrees of success. Given this, it is unlikely that meiofauna are responsible for the majority of the anoxic DIC production in permeable sediments, however, the size of their contribution may be substantial and will be quantified during this research.

The key research questions addressed in this chapter will be:

1) What proportion of anoxic DIC production can be attributed to heterotrophic metabolic processes (reactions i-iv)?

2) Does gas leakage in anoxic FTRs result in meaningful rates of aerobic respiration, contributing to measured anoxic DIC production?

3) Does $CaCO_3$ dissolution substantially contribute to anoxic DIC production and can the source of anoxic DIC production be identified using isotopic analysis of FTR effluent?

4) To what extent does DNRA via an intracellularly stored nitrate pool contribute to anoxic DIC production?

5) Does meiofaunal respiration contribute substantially to anoxic DIC production?

2.3 Method

2.3.1 Sample collection

Seawater and sediment used in intracellular nitrate pool experiments were collected from 5 sites around Port Phillip Bay (PPB), Victoria (Table 2.1). Sea seawater and sediment used in FTR experiments were collected from Elwood Beach in Port Phillip Bay, Victoria (Table 2.1). Sediment from Elwood beach has been characterized in related flow through reactor studies[13,45] and reportedly has sediment permeability in the range of between to 8.3×10^{-12} and 3.1×10^{-11} m^2 and has a porosity of between 0.39 to 0.53. Sediment was collected from the top 5 cm of sediment ripples approximately 5 meters from the shoreline, at low tide. Sea water was collected using rinsed plastic carboys. Within 90 minutes of collection, sample sediment was transported to Monash University and stored under oxic conditions using an aquarium aerator.

Table 2.1: Sites and site coordinates where sample sediment and seawater were collected for intracellular nitrate pool experiments.

Site	Coordinates
Hobsons Bay	37°50'23.253"S, 144°55'12.173"E
Albert park	37°50'53.967"S, 144°56'53.328"E
Elwood	37°53'23.156"S, 144°59'1.869"E
Hampton	37°56'10.965"S, 144°59'45.996"E
Beaumaris	37°58'59.369"S, 145°1'17.766"E

2.3.2 Flow through reactors and experimental design

Flow through reactors (FTRs), used in FTR experiments 1-4, consisted of acrylic cylinders with a diameter of 4.6 cm and a length of 3 cm sediment. PVC caps were placed at either end of the cylinder, and were machined with grooves converging to a central inlet/outlet port overlaid with 0.1 mm nylon mesh to allow even plug flow through the FTRs and to prevent sediment grain transport. Plug flow within these FTRs has been verified during breakthrough

curve experiments performed by Evrard, et al. [13] and Bourke, et al. [45]. Freshly collected site

water was pumped through the FTRs using a peristaltic pump located upstream of the FTRs.

Reservoirs were maintained in oxic/anoxic states by continuous purging with air or Ar,

respectively. Appropriate filtration, preservation and storage of samples were implemented

and are summarized in Table 2.2.

Table 2.2: Summary of sample filtration, preservation and storage methods. Approximate temperatures of sample fridges and freezers were 4°C and -20 °C, respectively.*For DIC samples intended for isotopic analysis, 12.5 mL of sample was collected with 200 μL of HgCl$_2$ preservative added. Methods of preservation and storage remained the same.

Target Analyte	Volume sampled (mL)	Method of filtration	Preservation	Storage
N$_2$	12.5	-	100 μL of 50 % (m/m) ZnCl$_2$	-
Dissolved inorganic carbon (DIC)	3*		100 μL of 6% HgCl$_2$ *	-
Fe^{2+}	2	MicroAnalytix 0.2 μm Cellulose-Acetate Filters	0.5 mL of Ferrozine added per mL of sample	Dark Cupboard
S^{2-}	2		100 μL of 48 mmol L^{-1} Zn Acetate per mL of sample	Refrigerator
Alkalinity	10		100 μL of 6% HgCl$_2$	Refrigerator
Ca^{2+} and Na$^+$	2		-	Frozen
Ammonium, Filterable Reactive Phosphorus, Nitrite	5		-	Frozen

Sample sediment was sieved using a 2mm mesh to remove large debris, such as shell grit,

rocks and macroalgae, which can interfere with FTR plug flow. Four FTR experiments of

varying length, experimental conditions and sampling regimes were performed and are

summarized below (Table 2.3).

Table 2.3. Summary of the flow through reactor (FTR) experiments performed.

FTR experiment	Date performed	Purpose	Sampling	Experimental summary
1	23.04.13	To determine what proportion of anoxic DIC production can be attributed to heterotrophic metabolic processes.	DO, DIC, N_2, Fe^{2+}, S^{2-}	Sampling occurred over an 8 hour period with oxic conditions maintained for the first 3.5 hours, then changed to anoxic for the remainder of the experiment. 5 FTRs were used. Reservoir was spiked with 50 μmol L^{-1} of $^{15}NO_3^-$. Flow velocity was maintained at 1.1 mL min^{-1}.
2	11.09.13	To determine whether $CaCO_3$ dissolution contributes substantially to anoxic DIC production.	DO, DIC, N_2, Na^+ and Ca^{2+} and Alkalinity.	Sampling occurred over a 12 hour period with oxic conditions maintained for the first 4.5 hours, then changed to anoxic for the remainder of the experiment. 3 FTRs were used. Flow velocity was maintained at 1.1 mL min^{-1}. Reservoir contained seawater spiked with 50 μmol L^{-1} $^{15}NO_3^-$.
3	16.09.14	To identify the source of anoxic DIC production using isotopic analysis, as well as to further investigate the contribution of DNRA and $CaCO_3$ dissolution to anoxic DIC production.	DO, N_2, DIC, $\delta^{13}C$-DIC, APN, Alkalinity	Sampling occurred over a 55 hour period with oxic conditions maintained for the first 11 hours, then changed to anoxic for the remainder of the experiment. 5 FTRs were employed. Flow velocity was maintained at 1.0 mL min^{-1}. Reservoir contained seawater spiked with 50 μmol L^{-1} $^{15}NO_3^-$. At t=16 hrs, Reservoir was changed to regular anoxic seawater.
4	15.07.15	To determine whether meiofauna contribute substantially to anoxic DIC production.	DO, DIC, N_2 and S^{2-}	Sampling occurred over a 245 hour period, during which, anoxic sediment conditions were maintained. 4 FTRs were employed. Reservoir contained 50 μmol L^{-1} of $^{15}NO_3^-$. Flow velocity was maintained at 0.74 mL min^{-1}.

2.3.3 Intracellular nitrate pool experiment

Intracellular nitrate pools within sediment microorganisms were investigated by examining three experimental treatments (Table 2.4), each with two subsamples: a and b. Preparation of these subsamples involved placing 10mL of wet sediment into 50 mL falcon tubes along with 20 mL of deionised water. The falcon tubes were then shaken thoroughly and the sample either: had its supernatant immediately filtered and frozen (subsample a), or was subjected to three cycles of freezing and heating and then had its supernatant filtered and frozen (subsample b). This freezing and heating cycle has been demonstrated to reliably rupture cell walls[30,46], thereby releasing any pools of intracellularly stored nitrate.

Treatment 1 involved no sample pre-treatment and therefore represented intracellular nitrate pools in in situ conditions. The sediment used in treatment 2 however, had been exposed to spiked 50 μM NO_3^- seawater for one hour, then washed three times with sample seawater from appropriate field sites. Treatment 3 involved the incubation of 10 mL of saturated sediment within a 12.5 mL gas-tight exetainer in the dark, for a period of 3 days to induce consumption of any intracellular nitrate pools.

Table 2.4: List of experimental treatments for determining intracellular nitrate pools under varying conditions.

Treatment	Purpose
1	Determine nitrate pool under environmental conditions
2	Determine nitrate pool following recent exposure to high nitrate concentrations.
3	Determine nitrate pool following extended anoxic incubation

The concentration of nitrate within sample supernatant was analysed and the quantity of intracellularly stored nitrate was determined by comparing nitrate concentrations between subsamples a and b. Freezing and heating cycles were achieved using a freezer reaching -20°C and a hotplate programmed to approximately 80°C. All treatments were performed in triplicate and on five separate samples of sediment collected from different sample sites

around Port Phillip Bay (Table 2.1). All supernatant samples were filtered using a 0.2 µm cellulose-acetate filter.

2.3.4 Dissolved oxygen gas leakage method validation experiment

The gas leakage rate into the FTRs was determined by undertaking an experiment, during which, three FTRs were assembled without sediment and had anoxic deionized water pumped through them. Flow through dissolved oxygen sensors were fitted to the inlet and outlet ports allowing for a highly representative determination of the dissolved oxygen concentrations.

2.3.5 Sample Analysis

2.3.5.1 Denitrification Rates

Concentrations of ^{15}N-N$_2$ in FTR effluent were determined using headspace analysis on a Gas Chromatograph (He carrier) coupled to isotope ratio mass spectrometer (Sercon 20-22). The rates of denitrification reported throughout this chapter are total denitrification ($D_{14}+D_{15}$) and were calculated using the isotope pairing technique [47]. No QC was used for this analysis, therefore accuracy could not be determined.

2.3.5.2 Analysis of nutrients (Nitrite, Filterable reactive phosphorus and Ammonium)

Concentrations of ammonium, filterable reactive phosphorus and nitrite were determined spectrophotometrically using a Lachat Quick-Chem 8500 Flow injection Analyser (FIA). Nitrite concentrations were determined via a reaction with sulphanilamide and N-(1-napthyl) ethylene diamine dihydrochloride that formed a purple azo dye (absorbance maxima at 520 nm). Ammonium concentrations were determined by reacting the sample with a dilute solution of hypochlorite, forming monochloroamine, which, when reacted with phenol and nitroprusside, forms indophenol blue (absorbance maxima at 630 nm). Filterable reactive phosphorus concentrations were determined by exposing FTR effluent samples to ammonium molybdate and antimony potassium tartrate to form phosphomolybdic acid, which may then be reduced by ascorbic acid, producing a complex with a strong blue colour (absorbance

maxima at 880 nm). No QC was used for this analysis, therefore accuracy could not be determined.

2.3.5.3 Dissolved inorganic carbon

The concentration of dissolved inorganic carbon was evaluated using flow injection analysis, fitted with a photometric detector. This method involved acidifying FTR sample effluent so that any carbonate species would be converted to carbon dioxide, which, diffused across a microporous membrane (Accurel® PP Q3/2 tubular membrane, ID 0.6 mm)[48]. The resulting change in pH caused the Bromothymol Blue indicator solution to produce a measurable colour change proportional to the quantity of diffused carbon dioxide. The accuracy of this analysis, measured as % relative error, was found to be 1.6% and was determined using a 2016.5 μmol L^{-1} QC.

2.3.5.4 Isotopic analysis of dissolved inorganic carbon.

Effluent samples stored in 12 mL gas tight exetainers had 4 mL of sample substituted with a He headspace and 0.1 mL of 1 mol L^{-1} H_3PO_4 added. DIC present within headspace was analysed using a Sercon 20-22 Isotope-Ratio Mass Spectrometer and isotopic ratios were expressed in delta notation, relative to the Pee Dee Belemnite standard.

2.3.5.5 Dissolved oxygen

Dissolved oxygen was monitored at the inlet and outlet of the FTR using Pyroscience Firesting flow through dissolved oxygen sensors.

2.3.5.6 Dissolved Ca^{2+} and Na^+

The concentration of dissolved Ca^{2+} and Na^+ ions was performed using a Dionex 2100 Ion Chromatography system fitted with a CS12A cation exchange column and CG12A guard column. Mobile phase was generated using 20 mmol L^{-1} methanesulfonic acid. Analytical precision was determined to be <1% RSD. Na^+ ions were quantified so as to serve as a conservative ion to compare with Ca^{2+} ion concentrations which would allow for the

exclusion of any errors introduced via possible sample evaporation. A ratio between the concentrations of Ca^{2+} and Na^+ ions was calculated and the difference between this ratio in FTR inlet and effluent samples was used as a metric for Ca^{2+} production via $CaCO_3$ dissolution, expressed as 'measured $\Delta[Ca^{2+}/Na^+]$'. The $\Delta[Ca^{2+}/Na^+]$ required for $CaCO_3$ dissolution to be responsible for the anoxic DIC production observed in FTR experiment 2 was calculated and expressed as '$CaCO_{3\ Diss}\ \Delta[Ca^{2+}/Na^+]$'. This value was calculated based on the flow velocity and the stoichiometry of reaction v. No QC was used for this analysis, therefore accuracy could not be determined.

2.3.5.7 Alkalinity

Alkalinity production was quantified using a modified Gran titration[49]. Following the addition of 100 μL aliquots of 0.01 mol L^{-1} HCl, changes in pH were recorded using an NBS buffer calibrated pH electrode attached to a portable HACH HQ40d meter. Acid was standardised during a separate titration using 1 mmol L^{-1} Na_2CO_3. Analytical precision was < 1% RSD. No QC was used for this analysis, therefore accuracy could not be determined.

2.3.5.8 Iron and Sulfide Analysis

The concentration of iron was determined using the Ferrozine method described in Stookey [50]. A GBC UV Visible Spectrophotometer was used to measure the resulting absorbance at 632 nm following the addition of Ferrozine [51,52]. Sulphide was also analysed using a GBC UV Visible Spectrophotometer, however, samples were treated with a sulfide colour reagent comprised of an acidified $FeCl_3$ solution mixed with N,N'- dimethyl-1,4-phenylenediamine sulfate. The resulting blue complex (methylene blue) exhibits an absorbance maxima at 670 nm[53]. Analytical precision in iron and sulfide analyses was <1% RSD. No QC was used for the sulfide analysis, therefore accuracy could not be determined. The accuracy of the iron analysis, measured as % relative error, was found to be 1.3% and was determined using a 0.5 mg L^{-1} QC.

2.4 Results

2.4.1 Intracellular nitrate lysing experiment

Mean concentrations of intracellular nitrate pools were determined for treatments 1-3 (Table 2.5) for 5 sediment sampling sites around Port Phillip Bay (Table 2.1). Intracellular nitrate pools across all treatments were found to be extremely low, falling below 2 nmol mL^{-1} in each treatment. The intracellular nitrate pool was the highest in the second treatment (T2), where sediment had been exposed to high concentrations of nitrate. However, the datasets from T1 and T2 were found not to be significantly different ($p > 0.05$). The intracellular nitrate pool of treatment 3 (T3) was considerably lower than T1 and T2.

Table 2.5: Mean quantities of intracellular nitrate pools per mL of sediment from treatments 1-3.

In situ pool (T1) (nmol/mL)	Spiked sediment pool (T2) (nmol/mL)	In situ pool after anoxic incubation (T3) (nmol/mL)
1.4 ± 0.4	1.5 ± 1.1	0.1 ± 0.8

2.4.2 Rates of DIC production and heterotrophic metabolism.

Mean aerobic DIC production approximately matched the mean dissolved oxygen consumption rates during oxic sampling rounds in FTR experiments 1, 2 and 3. Single factor ANOVA analyses revealed that these datasets were not significantly different (Table 2.6). Oxic DIC production in FTR experiments 1, 2 and 3 was also found to have no significant difference from DIC production under anoxic conditions.

Table 2.6: Comparing rates of dissolved oxygen consumption under oxic conditions, DIC production under oxic conditions and DIC production under anoxic conditions in FTR experiments using single factor ANOVA statistical analyses.

FTR Expt	Dissolved oxygen consumption rate (nmol mL^{-1} hr^{-1})	Oxic DIC production (nmol mL^{-1} hr^{-1})	Anoxic DIC production (nmol mL^{-1} hr^{-1})	p values DO and oxic DIC	p values Oxic DIC and Anoxic DIC
1	126 ± 17	135 ± 43	161 ± 49	0.65	0.08
2	178 ± 25	149 ± 27	134 ± 78	0.053	0.56
3	174 ± 15	210 ± 85	186 ± 97	0.23	0.47

Predicted denitrification rates were calculated using anoxic DIC production rates and the NO_3^- :CO_2 stoichiometry of 0.8 (reaction ii). Measured denitrification rates did not approach predicted denitrification rates ($p < 0.05$) at any point throughout FTR experiments 1, 2 or 3 (Figure 2.1a-c). Combined mean rates of nitrate, iron and sulfate reduction were measured during FTR experiment 1 and amounted to less than 1% of mean anoxic DIC production.
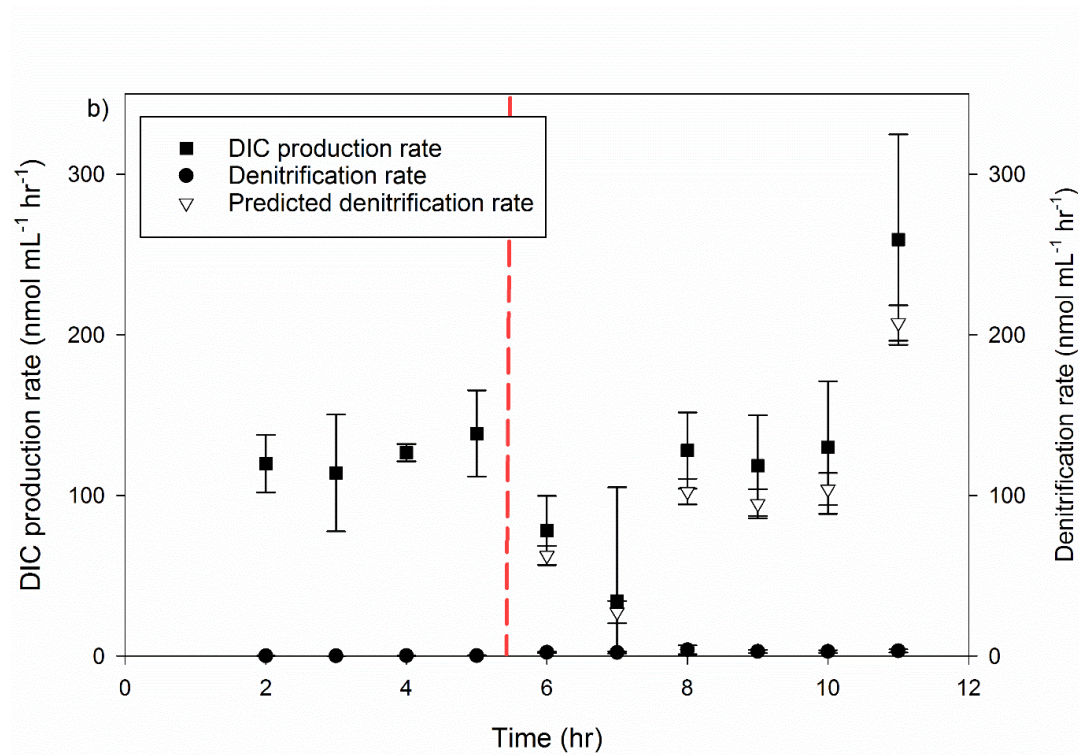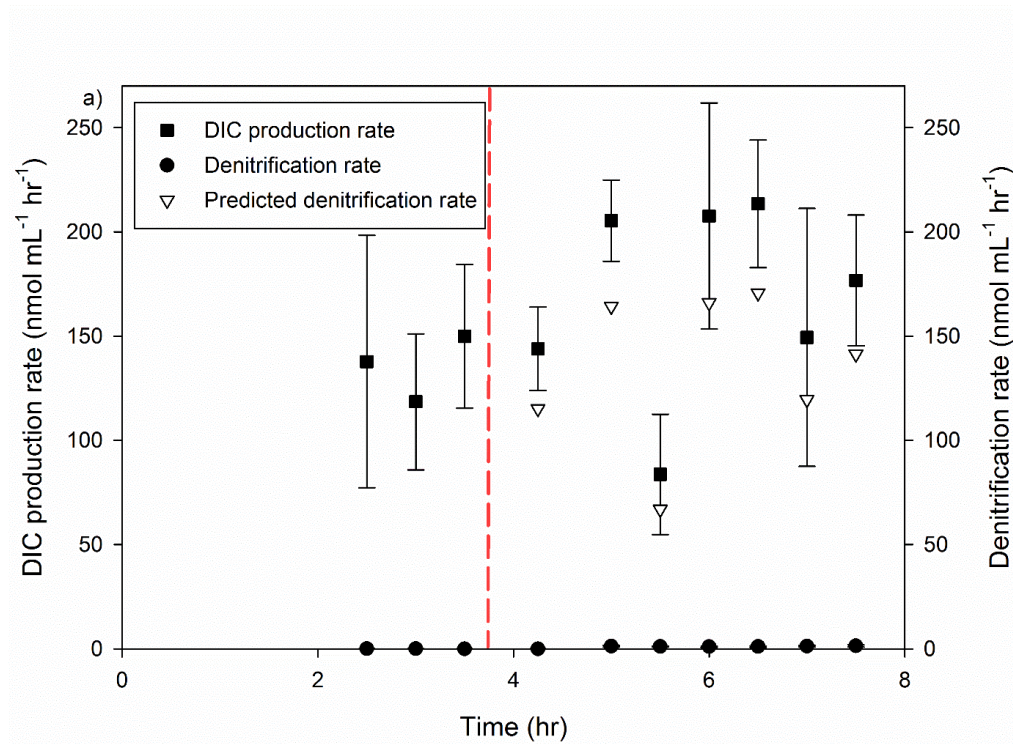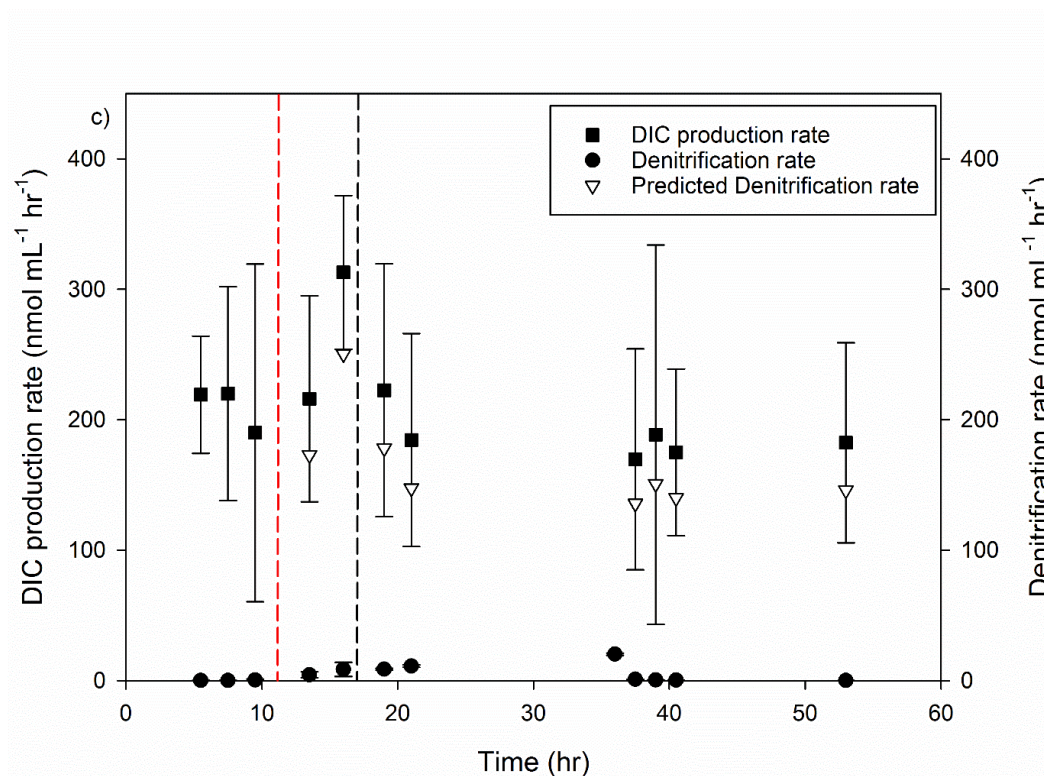
Figure 2.1 (a-c): Rates of DIC production, denitrification and predicted denitrification in FTR experiments 1 (a), 2 (b) and 3 (c) over time. Red dashed line represents when conditions were changed from oxic to anoxic. n=5, 3 and 5, respectively. FTR reservoirs in experiments 1 and 2 had been spiked with 50 μmol L^{-1} $^{15}NO_3^-$. Black dashed line in Figure 2.1c represents when reservoir was changed from 50 μmol L^{-1} $^{15}NO_3^-$ seawater to regular seawater. Error bars represent standard deviation in all instances.

2.4.3 Alkalinity production and dissolved Ca^{2+} and Na$^+$ ratios.

During FTR experiment 2, mean alkalinity production during oxic sampling rounds was 37 ± 31 nmol mL^{-1} hr^{-1} (Figure 2.2a). Following the change from oxic to anoxic conditions, mean alkalinity production dropped to -118 ±61 nmol mL^{-1} hr^{-1}. The same trend was observed in FTR experiment 3 (Figure 2.2b). Mean oxic alkalinity production was 26 ±36 nmol mL^{-1} hr^{-1} and under anoxic conditions, alkalinity production dropped to a mean production rate of -36 ±24 nmol mL^{-1} hr^{-1}.
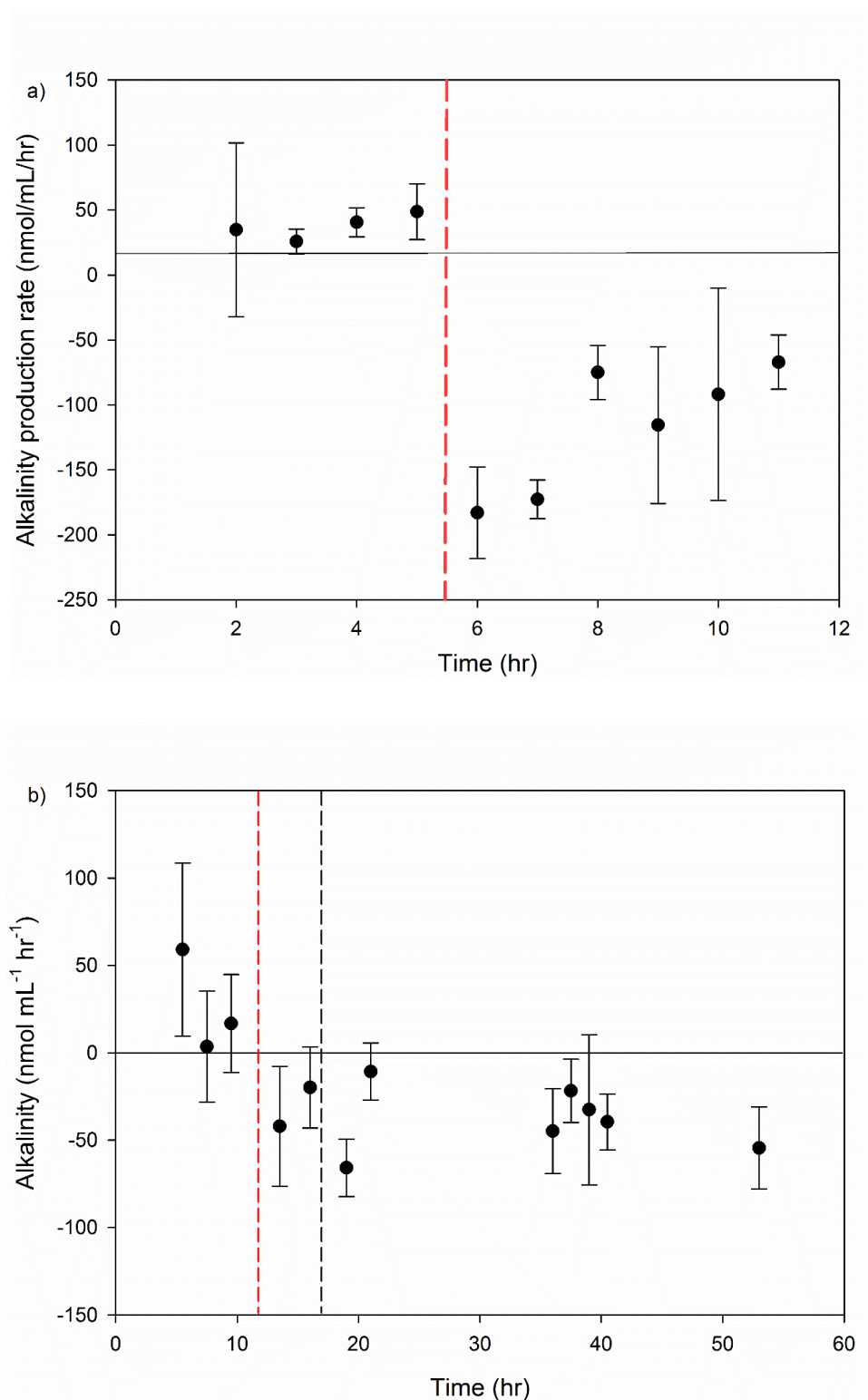
Figure 2.2 (a and b): Rates of alkalinity production over time in FTR experiment 2 and 3. Red dashed line represents when conditions were changed from oxic to anoxic. Black dashed line represents when reservoir was changed from 50 μmol L^{-1} ^{15}NO$_3$$^-$ seawater to regular seawater. n=3 and 5, respectively. All error bars represent standard deviation.

Measured $\Delta[Ca^{2+}/Na^+]$ varied very little throughout FTR experiment 2 (Figure 2.3). Mean

values for measured $\Delta[Ca^{2+}/Na^+]$ under oxic conditions were found not to have any

significant difference between mean values of measured $\Delta[Ca^{2+}/Na^+]$ under anoxic conditions

($p > .05$). At no point during the FTR experiment 2 did the measured $\Delta[Ca^{2+}/Na^+]$ approach

$CaCO_{3\ Diss}\ \Delta[Ca^{2+}/Na^+]$.

Figure 2.3: The change in the ratio between dissolved Ca^{2+} and Na^+ ions ($\Delta[Ca^{2+}/Na^+]$) over time in FTR experiment 2. 'Measured $\Delta[Ca^{2+}/Na^+]$' represent the difference in this ratio between FTR effluent samples relative to the inlet reservoir. 'CaCO_{3\ Diss} $\Delta[Ca^{2+}/Na^+]$' represents the $\Delta[Ca^{2+}/Na^+]$ required for $CaCO_3$ dissolution to be responsible for the anoxic DIC production observed in FTR experiment 2. Red dashed line represents when conditions were changed from oxic to anoxic. n=3. All error bars represent standard deviation.

2.4.4 Ammonium, phosphorus and nitrite production.

Under oxic conditions, mean rates of ammonium, phosphate and nitrite production were

relatively negligible, <1 nmol mL^{-1} hr^{-1} in each instance (Figure 2.4). Following the change to

anoxic conditions, ammonium production decreased so that mean production rates were -1.2

$\pm$ 0.6 nmol mL^{-1} hr^{-1}. Production rates of phosphate were inconsistent under anoxic

conditions, as rates of production increased to a maximum of 1.8 $\pm$ 0.4 nmol mL^{-1} hr^{-1} at t= 15

hr, then gradually declined to a minimum of -0.5 $\pm$ 0.2 nmol mL^{-1} hr^{-1}, at t= 39 hr. Nitrite

production rates were also inconsistent as production rates fluctuated between 6 and -6 nmol

mL^{-1} hr^{-1} in the first 10 hours of anoxia. Production rates of nitrite began to stabilize at near

zero production rates (<0.1 nmol mL^{-1} hr^{-1}) from t=35 hr onwards. Mean anoxic nitrite

production rates contributed <0.3% of mean anoxic DIC production rates during FTR

experiment 3.

Figure 2.4: Rates of production of ammonium, phosphate and nitrite in FTR experiment 3. Red dashed line represents when conditions were changed from oxic to anoxic (n=5). All error bars represent standard deviation. Black dashed line represents when reservoir was changed from 50 μmol L^{-1} ^{15}NO$_3$$^-$ seawater to regular seawater.
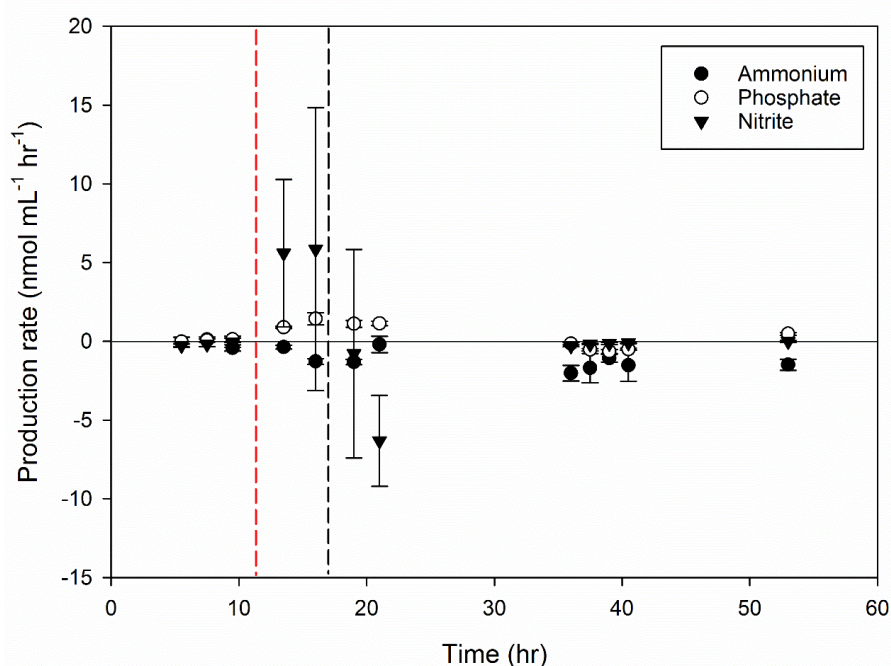
2.4.5 Dissolved oxygen leakage rate experiment

The mean difference in dissolved oxygen concentration between inlet and outlet ports across

the three FTRs was 1.8 $\pm$ 2.5 μmol L^{-1}. This value represented <1% of dissolved oxygen

saturation under the conditions specified.

2.4.6 Determining the source DIC isotope signatures

Plotting the $\delta^{13}C$ isotopic enrichment values against the inverse concentration of FTR effluent

DIC experiment 3 revealed a y intercept end member value of 20.471± 2.434 (Figure 2.5).
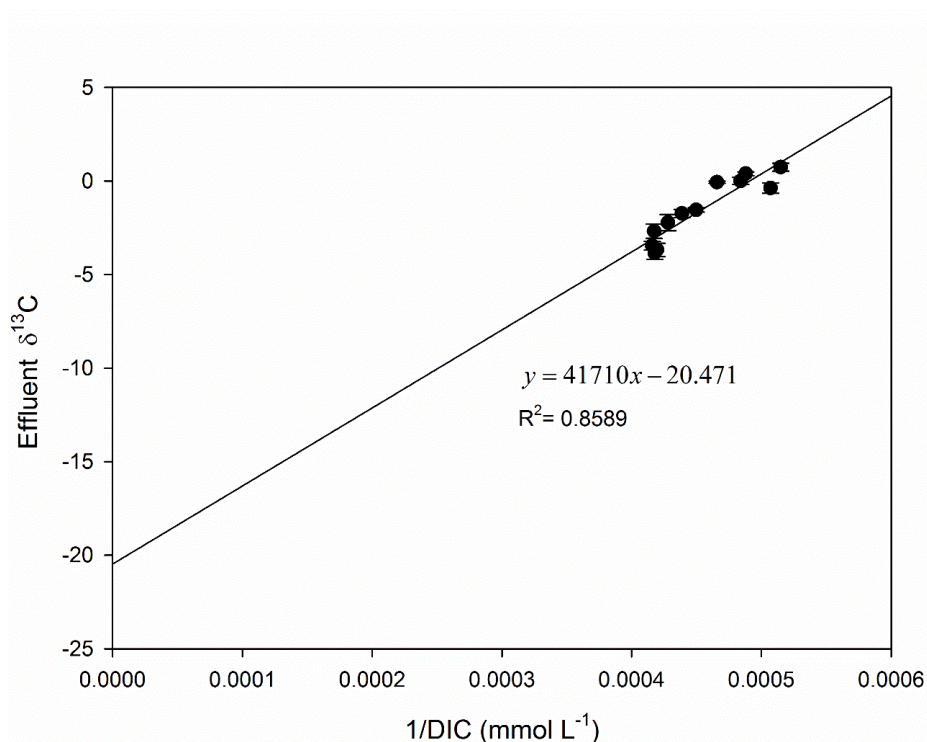
Figure 2.5: Keeling plot showing the inverse DIC concentration plotted against the isotopic $\delta^{13}C$ enrichment values of effluent samples in FTR experiment 3. High background concentrations of DIC in seawater means that the isotopic signature of anoxic DIC production cannot be measured directly. Instead, the y intercept of this linear regression equation (known as the $\delta^{13}C$ end member), can be used to identify the carbon source. All error bars are standard deviation.

2.4.7 Extended anoxic conditions in FTR experiment 4

The mean oxygen consumption rate was determined to be 158 ± 3 nmol mL^{-1} hr^{-1}, and

approximately matched the mean anoxic DIC production rate of 166 ± 36 nmol mL^{-1} hr^{-1}. A

single factor ANOVA analysis revealed that these datasets were not significantly different

($p>0.05$). Anoxic DIC production remained relatively constant throughout this experiment

(Figure 2.6) as the DIC production during the first sixty hours of FTR experiment 4 was

found to not have any statistical difference compared to the DIC production of the final sixty

hours (p>0.05). Denitrification rates reached a maximum of 15 ± 1 nmol mL^{-1} hr^{-1} at t = 173 hr, while sulfide production reached a maximum of 28 ± 1 nmol mL^{-1} hr^{-1} at t=218. Mean denitrification rate was 7 ± 5 nmol mL^{-1} hr^{-1} sulfide production was 5 ± 9 nmol mL^{-1} hr^{-1}. Combined mean rates of denitrification and sulfide production was 12 ± 7 nmol mL^{-1} hr^{-1} and accounted for <8% of the mean anoxic DIC production rate.
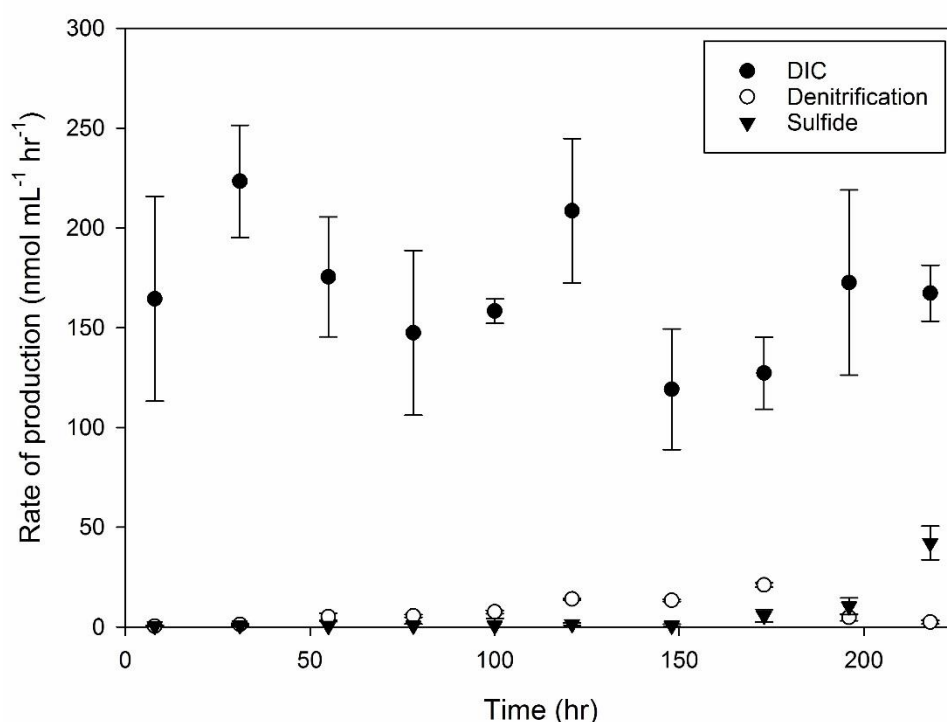
Figure 2.6: Rates of production of DIC, denitrification and sulfide in FTR experiment 4. n=4. FTR reservoir was spiked with 50 μmol L^{-1} ^{15}NO$_3^{-}$. Error bars represent standard deviation in all instances.

2.5 Discussion

2.5.1 DIC production and metabolism in FTR experiments.

In FTR experiments 1, 2 and 3, there was no statistical difference between rates of dissolved oxygen consumption and oxic DIC production ($p < 0.05$), indicating that aerobic respiration was very likely dominating DIC production under oxic conditions (Table 2.6). Despite denitrification being the next most energetically favourable process following aerobic respiration (reactions ii and i, respectively), at no point during FTR experiments 1, 2 or 3, did the measured denitrification rate approach the predicted denitrification rate (Figure 1a-c). In fact, the mean measured denitrification rate comprised <2% of mean anoxic DIC production across FTR experiments 1-3. Approximately 98% of anoxic DIC production, therefore, could not be assigned to the most energetically favourable process.

Combined rates of nitrate, iron and sulfide reduction, measured during FTR experiment 1, were determined to have a negligible contribution, accounting for <1% of mean anoxic DIC production. Nitrite production measured during FTR experiment 3 also revealed that there were negligible rates of incomplete denitrification occurring and accounted for <0.2% of anoxic DIC production (Figure 2.4). Similarly, in FTR experiment 4, combined mean rates of denitrification and sulfide production could only account for <7% of anoxic DIC production, leaving the large majority of anoxic DIC production unassigned to a known process. The excellent agreement of these FTR experiments with the preliminary observations made in Kertimende (see chapter 1) suggests that this could be a highly reproducible phenomenon. This phenomenon appears to continue regardless of the presence or absence of nitrate within the FTR reservoir. During FTR experiment 3, DIC production remained relatively constant despite reservoir conditions being changed from high nitrate concentrations to very low nitrate concentrations (Figure 1c).

2.5.2 Intracellular nitrate pools and dissimilatory nitrate reduction to ammonium.

Intracellular nitrate pool lysing treatments T1, T2 and T3 allowed for the quantification of intracellular pools under three sets of conditions. These conditions corresponded to in situ conditions (T1), recent exposure to high nitrate concentrations (T2) and sediment that had undergone extended anoxic incubation (T3). The intracellular nitrate pool determined for in situ conditions (T1) across the five sampling sites around Port Phillip Bay was found to have a mean nitrate pool of 1.4 ± 0.4 nmol mL^{-1}. This value was negligible compared to mean anoxic DIC production rates observed in FTR experiments 1-4. In fact, if this entire nitrate pool was converted to ammonium via DNRA, the DIC produced would account for <1% of the anoxic DIC produced in a single hour for each of the FTR experiments 1-4. The in situ nitrate pool determined in this research (T1) was far lower compared to the 11.7 nmol mL^{-1} pool found in sediments from the German Wadden Sea[54] and approximately 200 nmol L^{-1} pool found in sediments from the Aarhus Bight in Denmark[46].

The experimental design included using sediment collected from five sites around Port Phillip Bay, as it was anticipated that point nutrient runoff sources could lead to locally high nitrate concentrations. However, the low degree of variability observed indicated that any point source runoff did not substantially impact intracellular nitrate pools. As Port Phillip Bay is a nitrate limited oligotrophic system, it is likely that any nitrate present in point source runoff was rapidly assimilated.

Even after sediment microorganisms were subjected to 50 μmol L^{-1} nitrate concentrations for one hour (T2), mean nitrate pools did not significantly increase. The higher degree of variability observed in this treatment could indicate that the ability to accumulate nitrate varies across the microbial community. The general inability to accumulate nitrate within one hour was likely due to the scarcity of nitrate in the Port Phillip Bay system, resulting in the community being poorly adapted to nitrate accumulation.

The extended anoxic incubation treatment (T3) resulted in a decrease in the intracellular nitrate pool to 0.1 ± 0.8 nmol mL^{-1} (Table 2.5). The decrease in the nitrate pool indicated that there was some degree of consumption. However, the sizeable difference in magnitude between the in situ intracellular pool and the anoxic DIC production rate observed in FTR experiment 1-4 indicates that microbes are not using DNRA via intracellularly stored nitrate to sustain cell function during anoxic conditions.

The negligible production rate of ammonium observed in FTR experiment 3 compared to the anoxic DIC production rate (Table 2.6) further supports the notion that DNRA is not being utilized at meaningful rates in anoxic permeable sediments. DNRA via a pool of intracellularly stored nitrate can therefore be reasonably dismissed as a possible major source of anoxic DIC production.

2.5.3 Aerobic respiration arising from FTR gas leakage

The degree of gas leakage into anoxic FTRs was determined to be <1% of dissolved oxygen saturation. This indicates that rates of aerobic respiration brought about by oxygen leakage into the FTRs are relatively negligible and would not contribute substantially towards measured anoxic DIC production.

2.5.4 CaCO$_3$ Dissolution

Approximately all oxic DIC production can be assigned to aerobic respiration under anoxic conditions, whilst under anoxic conditions, in FTR experiments 1-4, between 93-98% of anoxic DIC could not be attributed to a known process. For this reason, if CaCO$_3$ dissolution was substantially contributing to anoxic DIC production, rates of dissolution must sharply increase following the shift from oxic to anoxic conditions. A large increase in alkalinity production would necessarily accompany this increase in CaCO$_3$ dissolution and would be proportional to twice the anoxic DIC production rate. However, following the change to anoxic conditions in FTR experiments 2 and 3, alkalinity dropped sharply in both instances

(Figures 2.2a and 2.2b). This is strong evidence that $CaCO_3$ dissolution could not possibly be responsible for the large quantities of unassigned anoxic DIC production.

Large scale $CaCO_3$ dissolution would also result in a noticeable increase in the ratio of dissolved Ca^{2+} to Na^+ ions ($\Delta[Ca^{2+}/Na^+]$) in FTR effluent. The $\Delta[Ca^{2+}/Na^+]$ required for $CaCO_3$ dissolution to be responsible for large quantities of anoxic DIC production was defined as '$CaCO_{3\ Diss} \Delta[Ca^{2+}/Na^+]$' and plotted against the measured $\Delta[Ca^{2+}/Na^+]$ (Figure 2.3). However, measured $\Delta[Ca^{2+}/Na^+]$ remained relatively constant throughout FTR experiment 2 and at no point did the measured $\Delta[Ca^{2+}/Na^+]$ approach '$CaCO_{3\ Diss} \Delta[Ca^{2+}/Na^+]$'. This is further evidence supporting the dismissal of $CaCO_3$ dissolution as a possible major anoxic source of DIC in permeable sediments.

2.5.5 Identifying the source of anoxic DIC production using isotopic analysis.

A plot of the effluent DIC isotopic signature against the inverse concentration revealed an end member value of 20.5‰ (Figure 2.5). This value is very close to the characteristic value of marine phytoplankton (-21.1‰) [21] and close to the characteristic value of microphytobenthos (-15 to -16‰)[20] . This result indicates that the mineralisation of algal derived material is responsible for the vast majority of DIC under anoxic conditions. This finding confirms that the major contributor of this unassigned DIC is in fact, biotic in nature and reinforces the dismissal of abiotic explanations such as $CaCO_3$ dissolution, which would have had an end member value of -7.8‰[19] .

2.5.6 Meiofaunal respiration

Due to the sensitivity of copepods and turbellarians to anoxic conditions, and the prevalence of these phyla in the meiofaunal community, any DIC arising from meiofaunal respiration under anoxic conditions would be expected to sharply fall within 24 hours of anoxic incubation. Species dependent nematode tolerance to anoxic conditions would allow aerobic respiration to continue under anoxic conditions, albeit at a far lower rate. However, as anoxic

DIC production remained relatively constant throughout FTR experiment 4 (Figure 2.6), with no statistical difference between DIC production occurring during the first sixty hours of the experiment compared to the final sixty hours, it appears that any decline in meiofauna respiration was too small to observe within the variability of the DIC data. It is therefore highly unlikely that meiofaunal respiration was contributing substantially to anoxic DIC production, and the source of the majority of anoxic DIC production remains unidentified.

2.6 Conclusion

In agreement with previous observations, all FTR experiments performed here, showed a large proportion (93-98%) of dissolved inorganic carbon production that could not be attributed to the consumption on common electron acceptors. Given how consistently this has been observed, it is highly likely that this is a common phenomenon. $CaCO_3$ dissolution, DNRA via a stored intracellular nitrate pool and meiofauna respiration were each investigated as possible sources for large quantities of anoxic DIC production, but were each found to contribute negligible quantities. The process by which the majority of anoxic DIC production in permeable sediments occurs has not yet been identified, however, the isotopic analysis has revealed that the source is likely a biochemical process with marine phytoplankton and/or microphytobenthos as the carbon source.

2.7 References

1   Shum, K. T. Wave induced advective transport below a rippled water sediment interface. *Journal of Geophysical Research-Oceans* **97**, 789-808, (1992).

2   Huettel, M., Roy, H., Precht, E. & Ehrenhauss, S. Hydrodynamical impact on biogeochemical processes in aquatic sediments. *Hydrobiologia* **494**, 231-236, (2003).

3   Webb, J. E. & Theodor, J. Irrigation of submerged marine sands through wave action. *Nature* **220**, 682-&, (1968).

4   Santos, I. R., Cook, P. L. M., Rogers, L., de Weys, J. & Eyre, B. D. The "salt wedge pump": Convection-driven pore-water exchange as a source of dissolved organic and inorganic carbon and nitrogen to an estuary. *Limnol. Oceanogr.* **57**, 1415-1426, (2012).

5   Precht, E., Franke, U., Polerecky, L. & Huettel, M. Oxygen dynamics in permeable sediments with wave-driven porewater exchange. *Limnol. Oceanogr.* **49**, 693-705, (2004).

6   Cook, P. L. M. *et al.* Quantification of denitrification in permeable sediments: Insights from a two-dimensional simulation analysis and experimental data. *Limnology and Oceanography-Methods* **4**, 294-307, (2006).

7   Rossello-Mora, R., Thamdrup, B., Schafer, H., Weller, R. & Amann, R. The response of the microbial community of marine sediments to organic carbon input under anaerobic conditions. *Syst. Appl. Microbiol.* **22**, 237-248, (1999).

8   Holmer, M. & Kristensen, E. Organic matter mineralization in an organic rich sediment. Experimental stimulation of sulfate reduction by fish food pellets. *FEMS Microbiol. Ecol.* **14**, 33-44, (1994).

9   Weiss, M. S. *et al.* Molecular architecture and electrostatic properties of a bacterial porin. *Science* **254**, 1627-1630, (1991).

10   Canfield, D. E. *et al.* Pathways of organic carbon oxidation in 3 continental margin sediments. *Mar. Geol.* **113**, 27-40, (1993).

11   Canfield, D. E., Thamdrup, B. & Hansen, J. W. The anaerobic degredation of organic matter in danish coastal sediments- iron reduction, manganese reduction and sulfate reduction. *Geochim. Cosmochim. Acta* **57**, 3867-3883, (1993).

12   Kessler, A. J. *et al.* Quantifying denitrification in rippled permeable sands through combined flume experiments and modeling. *Limnol. Oceanogr.* **57**, 1217-1232, (2012).

13   Evrard, V., Glud, R. N. & Cook, P. L. M. The kinetics of denitrification in permeable sediments. *Biogeochemistry* **113**, 563-572, (2013).

14   Tucker, M. E. & Wright, V. P. in *Carbonate Sedimentology*   70-100 (Blackwell Publishing Ltd., 2009).

15   Canfield, D. E., Kristensen, E. & Thamdrup, B. in *Aquatic Geomicrobiology* Vol. 48 *Advances in Marine Biology* Ch. 10, 383-414 (Academic Press Ltd-Elsevier Science Ltd, 2005).

16   Bourke, M. F. *et al.* Metabolism in anoxic permeable sediments is dominated by eukaryotic dark fermentation. *Nature Geoscience* **10**, 30-35, (2017).

17   Mariotti, A. *et al.* Experimental determination of nitrogen kinetic isotope fractionation: some principles; illustration for the denitrification and nitrification processes. *Plant Soil* **62**, 413-430, (1981).

18   O'leary, M. in *Carbon isotope fractionation in plants*   Ch. 20 Phytochemistry, 553-567 (1981).

19   Skidmore, M., Sharp, M. & Tranter, M. Kinetic isotopic fractionation during carbonate dissolution in laboratory experiments: implications for detection of microbial CO2 signatures using delta C-13-DIC. *Geochim. Cosmochim. Acta* **68**, 4309-4317, (2004).

20   Middelburg, J. J. *et al.* The fate of intertidal microphytobenthos carbon: An in situ C-13-labeling study. *Limnol. Oceanogr.* **45**, 1224-1234, (2000).

21   Currin, C. A., Newell, S. Y. & Paerl, H. W. The role of standing dead spartina alterniflore and benthic microalgae in salt marsh food webs. Considerations based on multiple stable isotope analysis. *Mar. Ecol. Prog. Ser.* **121**, 99-116, (1995).

22   Keeling, C. D. The concentration and isotopic abundances of atmospheric carbon dioxide in rural areas. *Geochim. Cosmochim. Acta* **13**, 322-334, (1958).

23   Fewson, C. A. & Nicholas, D. J. Nitric oxide reductase from pseudomonas aeruginosa. *Biochem. J.* **78**, P09-&, (1961).

24   An, S. M. & Gardner, W. S. Dissimilatory nitrate reduction to ammonium (DNRA) as a nitrogen link, versus denitrification as a sink in a shallow estuary (Laguna Madre/Baffin Bay, Texas). *Mar. Ecol. Prog. Ser.* **237**, 41-50, (2002).

25   Strohm, T. O., Griffin, B., Zumft, W. G. & Schink, B. Growth yields in bacterial denitrification and nitrate ammonification. *Appl. Environ. Microbiol.* **73**, 1420-1424, (2007).

26   Kraft, B., Strous, M. & Tegetmeyer, H. E. Microbial nitrate respiration - Genes, enzymes and environmental distribution. *J. Biotechnol.* **155**, 104-117, (2011).

27   Otte, S. *et al.* Nitrogen, carbon, and sulfur metabolism in natural Thioploca samples. *Appl. Environ. Microbiol.* **65**, 3148-3157, (1999).

28   Preisler, A. *et al.* Biological and chemical sulfide oxidation in a Beggiatoa inhabited marine sediment. *Isme Journal* **1**, 341-353, (2007).

29   Kamp, A., de Beer, D., Nitsch, J. L., Lavik, G. & Stief, P. Diatoms respire nitrate to survive dark and anoxic conditions. *Proc. Nat. Acad. Sci. USA* **108**, 5649-5654, (2011).

30   Stief, P., Kamp, A. & de Beer, D. Role of Diatoms in the Spatial-Temporal Distribution of Intracellular Nitrate in Intertidal Sediment. *Plos One* **8**, (2013).

31   McHatton, S. C., Barry, J. P., Jannasch, H. W. & Nelson, D. C. High nitrate concentrations in vacuolate, autotrophic marine Beggiatoa spp. *Appl. Environ. Microbiol.* **62**, 954-958, (1996).

32   Mussmann, M. *et al.* Phylogeny and distribution of nitrate-storing Beggiatoa spp. in coastal marine sediments. *Environ. Microbiol.* **5**, 523-533, (2003).

33   Risgaard-Petersen, N. *et al.* Evidence for complete denitrification in a benthic foraminifer. *Nature* **443**, 93-96, (2006).

34   Hogslund, S., Revsbech, N. P., Cedhagen, T., Nielsen, L. P. & Gallardo, V. A. Denitrification, nitrate turnover, and aerobic respiration by benthic foraminiferans in the oxygen minimum zone off Chile. *J. Exp. Mar. Biol. Ecol.* **359**, 85-91, (2008).

35   Barranguet, C., Herman, P. M. J. & Sinke, J. J. Microphytobenthos biomass and community composition studied by pigment biomarkers: importance and fate in the carbon cycle of a tidal flat. *J. Sea Res.* **38**, 59-70, (1997).

36   Mare, M. F. A study of a marine benthic community with special reference to the micro-organisms. *Jour Marine Biol Assoc* **25**, 517-554, (1942).

37   Vincx, M. in *Methods for the examination of organismal diversity in soils and sediments.*   Ch. 15, 187-195 (CAB, 1996).

38   Moodley, L. & Hess, C. Tolerance of infaunal benthic foraminefera for low and high oxygen concentrations. *Biological Bulletin* **183**, 94-98, (1992).

39   Moodley, L., vanderZwaan, G. J., Herman, P. M. J., Kempers, L. & vanBreugel, P. Differential response of benthic meiofauna to anoxia with special reference to Foraminifera (Protista: Sarcodina). *Mar. Ecol. Prog. Ser.* **158**, 151-163, (1997).

40   Soetaert, K., Muthumbi, A. & Heip, C. Size and shape of ocean margin nematodes: morphological diversity and depth-related patterns. *Mar. Ecol. Prog. Ser.* **242**, 179-193, (2002).

41   Steyaert, M. *et al.* Responses of intertidal nematodes to short-term anoxic events. *J. Exp. Mar. Biol. Ecol.* **345**, 175-184, (2007).

42   Braeckman, U., Vanaverbeke, J., Vincx, M., van Oevelen, D. & Soetaert, K. Meiofauna Metabolism in Suboxic Sediments: Currently Overestimated. *Plos One* **8**, (2013).

43   Taheri, M., Braeckman, U., Vincx, M. & Vanaverbeke, J. Effect of short-term hypoxia on marine nematode community structure and vertical distribution pattern in three different sediment types of the North Sea. *Mar. Environ. Res.* **99**, 149-159, (2014).

44   Padilla, P. A., Nystul, T. G., Zager, R. A., Johnson, A. C. M. & Roth, M. B. Dephosphorylation of cell cycle-regulated proteins correlates with anoxia-induced

suspended animation in Caenorhabditis elegans. *Molecular Biology of the Cell* **13**, 1473-1483, (2002).

45   Bourke, M., Kessler, A. & Cook, P. Influence of buried Ulva lactuca on denitrification in permeable sediments. *Mar. Ecol. Prog. Ser.* **498**, 85-94, (2014).

46   Lomstein, E., Jensen, M. H. & Sorensen, J. Intracellular ammonium and nitrate pools associated with deposited phytoplankton in a marine sediment, Aarhus bight, Denmark. *Mar. Ecol. Prog. Ser.* **61**, 97-105, (1990).

47   Nielsen, L. P. Denitrification in sediment determined from nitrogen isotope pairing. *FEMS Microbiol. Ecol.* **86**, 357-362, (1992).

48   Oshima, M. *et al.* Highly sensitive determination method for total carbonate in water samples by flow injection analysis coupled with gas-diffusion separation. *Analyt. Sci.* **17**, 1285-1290, (2001).

49   Almgren, T., Dyrssen, D. & Fonselius, S. in *Methods of seawater analysis*   (eds K. Grasshoff, M. Ehrhardt, & K. Kremling) 99-123 (Springer-Verlag, Chemie, 1983).

50   Stookey, L. L. Ferrozine- A new spectrophotometric reagent for iron. *Anal. Chem* **42**, 779-&, (1970).

51   Viollier, E., Inglett, P. W., Hunter, K., Roychoudhury, A. N. & Van Cappellen, P. The ferrozine method revisited: Fe(II)/Fe(III) determination in natural waters. *Appl. Geochem.* **15**, 785-790, (2000).

52   Hyacinthe, C., Bonneville, S. & Van Cappellen, P. Reactive iron(III) in sediments: Chemical versus microbial extractions. *Geochim. Cosmochim. Acta* **70**, 4166-4180, (2006).

53   Fonselius, S. H. in *Methods of seawater analysis*   (ed K Grasshoff) 91-100 (Springer-Verlag Chemie, 2007).

54   Heisterkamp, I. M., Kamp, A., Schramm, A. T., de Beer, D. & Stief, P. Indirect control of the intracellular nitrate pool of intertidal sediment by the polychaete Hediste diversicolor. *Mar. Ecol. Prog. Ser.* **445**, 181-192, (2012).

Chapter 3: Investigation of fermentation as a possible source of dissolved inorganic carbon production in anoxic permeable sediments

3.1 Abstract

Approximately only 5% of dissolved inorganic carbon (DIC) production in anoxic permeable sediments can be attributed to known heterotrophic metabolic processes, such as denitrification or sulfate reduction, leaving the large majority without a known source. In this chapter, effluent from flow through reactor (FTR) experiments was analysed for the typical fermentation products, C1-3 alcohols and volatile fatty acids, to determine whether fermentation uncoupled to anoxic heterotrophic metabolism was occurring, and whether it could be a major source of anoxic DIC production. Acetate and ethanol were detected in FTR effluent, however, based on established fermentation stoichiometries, these concentrations accounted for between 2.1 and 4.7% of anoxic DIC production. FTR experiments using the broad spectrum antibiotics, amoxicillin and ciprofloxacin, revealed that rates of DIC production remained relatively constant, whilst bacterial processes, such as denitrification, were inhibited. Eukaryotic fermentation is suggested as the most likely major source of anoxic DIC production in permeable sediments, however, further research must be carried out to identify the dominant pathway(s) being utilized.

3.2 Introduction

Heterotrophic microorganisms within permeable sediments derive energy by facilitating the breakdown of organic carbon, typically sourced from decaying matter or exuded from photoautotrophs[1]. Particulate organic polymers are gradually mineralized via a series of hydrolysis and fermentation reactions by a mutualistic consortia of heterotrophic microorganisms[2]. As these microbes cannot transport molecules larger than 600 Da across their cell membranes[3], they must perform these reactions extracellularly, relying upon enzymes embedded to the external surface of their cells (ectoenzymes) or enzymes excreted from the cell (exoenzymes). The smaller organic molecules produced by these extracellular hydrolytic reactions may then be transported across cell membranes and undergo fermentation. Fermentation reactions are a broad category of microbially-mediated pathways that involve organic carbon simultaneously undergoing oxidation and reduction, serving as both the electron acceptor and electron donor[4]. Common products of fermentation reactions in anaerobic carbon mineralization include volatile fatty acids, short chain alcohols, dissolved H_2 and CO_2 (reactions i-iv)[5].

i) Glucose fermentation to ethanol:

$C_6H_{12}O_6 \longrightarrow 2CH_3CH_2OH + 2CO_2$ $\quad\quad\quad\quad$ $\Delta G^0 = -244.1$ kJ mol^{-1}

ii) Ethanol fermentation to acetate:

$CH_3CH_2OH + H_2O \longrightarrow CH_3COOH + 2H_2$ $\quad\quad\quad\quad$ $\Delta G^0 = +34.8$ kJ mol^{-1}

iii) Lactate fermentation to acetate:

$CH_3CHOHCOOH + H_2O \longrightarrow CH_3COOH + CO_2 + 2H_2$ $\quad\quad$ $\Delta G^0 = +23.9$ kJ mol^{-1}

iv) Propionate fermentation to acetate:

$CH_3CH_2COOH + 2H_2O \longrightarrow CH_3COOH + CO_2 + 3H_2$ $\quad\quad$ $\Delta G^0 = +105.1$ kJ mol^{-1}
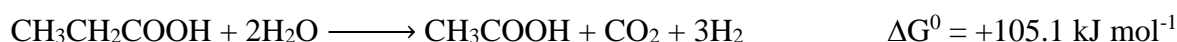
The products of these reactions are generally thought not to accumulate in sediments, as they are considered to be closely coupled to heterotrophic metabolic processes (reactions v-viii)[5]. In each of these fermentation reactions (reactions i-iv), adenosine triphosphate (ATP) is generated via substrate level phosphorylation but represents a relatively inefficient means of ATP generation compared to other respiration pathways[6]. The hydrolysis of the terminal phosphate on ATP is a high energy yield reaction (ΔG= -32 kJ mol^{-1}) that enables otherwise unfavourable reactions necessary for cell function. Only two ATP molecules are produced for each molecule of glucose fermented, whereas in aerobic respiration (reaction v), 32 ATP molecules are generated per glucose molecule oxidized[7]. Despite its poor ATP production efficiency, the key advantage fermentation presents to microorganisms is that it enables ATP production without requiring any external electron acceptor, such as in other heterotrophic metabolic pathways (reactions v-viii[8]).

<div align="center">v) Aerobic respiration:</div>

$$CH_2O + O_2 \longrightarrow CO_2 + H_2O \qquad\qquad \Delta G^0 = \text{-501 kJ mol}^{-1}$$

<div align="center">vi) Denitrification:</div>

$$5CH_2O + 4NO_3^- + 4H^+ \longrightarrow 5CO_2 + 2N_2 + 7H_2O \qquad \Delta G^0 = \text{-453 kJ mol}^{-1}$$

<div align="center">vii) Iron reduction:</div>

$$CH_2O + 4FeOOH + 8H^+ \longrightarrow CO_2 + 4Fe^{2+} + 7H_2O \qquad \Delta G^0 = \text{-114 kJ mol}^{-1}$$

<div align="center">viii) Sulfate reduction:</div>

$$2CH_2O + SO_4^{\ 2-} + H^+ \longrightarrow 2CO_2 + HS^- + H_2O \qquad \Delta G^0 = \text{-77 kJ mol}^{-1}$$
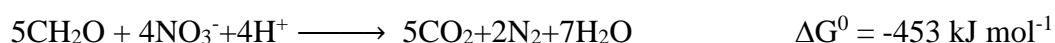
Reactions v-viii are terminal heterotrophic metabolic pathways that involve electrons being donated from organic matter to an inorganic electron acceptor. These reactions occur in the inner membrane of cell mitochondria and produce dissolved inorganic carbon (DIC) as a waste product while generating ATP at varying efficiencies dependent upon the electron

acceptor used. Microbial selectivity for electron acceptors is primarily based upon the magnitude of their energetic yield and their availability. Once the most energetically favourable electron acceptor has been depleted, the next most favourable will be used, resulting in a gradual cascade of progressively less energetically favourable electron acceptors with increasing depth[6].

However, while denitrification (reaction vi) is widely considered to be the next most favourable process following aerobic respiration[5] (reaction v), research presented in chapter 2 of this thesis revealed that a large discrepancy exists between the measured and expected DIC production rates arising from denitrification in anoxic flow through reactor (FTR) experiments. Denitrification accounted for only between 2-5% of the total anoxic DIC production, leaving a great deal without a known source. This phenomenon has also been observed in Kessler, et al. [9] and Evrard, et al. [10] and the identification of the process responsible is the overarching focus of this thesis. In chapter 2 of this thesis, meiofauna respiration, calcium carbonate dissolution and dissimilatory nitrate reduction to ammonium (DNRA) were investigated as possible sources of anoxic DIC production and were each found to have a negligible contribution.

One potential source that may be contributing to the 95-98% of currently unassigned anoxic DIC production is fermentation, uncoupled to heterotrophic metabolism. In sediments, fermentation is utilized by both prokaryotic and eukaryotic microorganisms and quantifying the rate of fermentation poses a challenge as the rate of consumption of an electron acceptor (like oxygen or nitrate) cannot be employed. It is further complicated as there are a wide variety of reactants, products and stoichiometries that are often used in combination with one another and products of some fermentation reactions will be quickly consumed by coupled terminal heterotrophic metabolic processes (reactions v-viii)[11-13]. It is therefore very difficult to estimate rates of fermentation and current rates may therefore be underestimated.

Prokaryotic and/or eukaryotic fermentation could potentially be responsible for large quantities of anoxic DIC production in permeable sediments.

In prokaryotes, culture studies have revealed that the degree to which different fermentative pathways are utilized is largely dependent upon what organic carbon source is metabolized[4]. For example, *E. Coli* has been observed to produce ethanol when provided with sorbitol, but when given glucuronic acid, no ethanol production was observed, and instead acetate was the dominant product[14,15]. Consistent with the reactions i-iv, bacterial fermentation of low molecular weight organic carbon molecules commonly produces dissolved hydrogen, carbon dioxide (DIC), lactate, succinate, ethanol, formate and acetate[14,16,17].

Fermentation may also be performed by autotrophic eukaryotic microorganisms as a means of sustaining cell function in periods where sediment resuspension has resulted in cells being buried at depths where no light or oxygen is available[18]. Eukaryotic fermentation includes a wide variety of pathways and reaction stoichiometries that vary with species, substrate and environmental factors[19-21]. For example, *C Reinhardtii* has been observed to produce formate, acetate and ethanol produced in a 2:2:1 ratio under dark conditions[22]. Whilst, *C.moewusii* produced no formate under dark conditions, with acetate, glycerol and ethanol being the major products[23]. Amongst marine eukaryotic microalgae, common products that arise from the fermentation of starch include acetate, ethanol, formate, glycerol, lactate, H_2 and CO_2[22,24,25].

Some microalgae do not excrete the products of fermentation reactions and instead accumulate them intracellularly[26]. *Euglena gracilis* has been found to store large concentrations of wax esters when incubated anoxically[27] and have been found to accumulate them to such an extent that they have made up 65% of the algae's dry weight[28]. Upon returning to oxic conditions, these wax esters are oxidized to generate ATP.

In this chapter, I used flow through reactor (FTR) experiments to determine whether fermentation could be a major source of anoxic DIC production. FTR experiments are a convenient means of determining volumetric biogeochemical rates at fixed solute concentrations[29] and effluent from these experiments will be analyzed for typical products of prokaryotic and eukaryotic fermentation including short chain alcohols (C1-3) and volatile fatty acids. If these products are accumulating in FTR effluent, fermentation could be occurring at higher than expected rates and may be a major, if not dominant process in anoxic permeable sediments.

In addition to the targeted analysis of typical fermentation products, the role of bacteria in anoxic metabolic pathways will also be investigated. This will be accomplished using FTR experiments that incorporate treatments spiked with the broad spectrum bactericidal antibiotics, amoxicillin and ciprofloxacin. Amoxicillin is a beta lactam antibiotic and functions by binding to the enzymes transpeptidase and D-alanyl-carboxypeptidase. This disrupts structural cross linking during cell wall synthesis, resulting in damaged cell walls[30]. The difference in the osmotic pressure inside and outside the cell causes the cell wall to rupture, resulting in cell death. Amoxicillin has been demonstrated to be effective against gram positive and negative bacteria and has an EC-50 concentration between 330 to 1400 nmol L^{-1} [30,31]. Eukaryotic microorganisms have a far greater tolerance towards amoxicillin, with EC-50 values of 1700 μmol L^{-1} with respect to green algae[32].

Ciprofloxacin belongs to the class of antibiotics known as a fluoroquinolones and are considered to be bactericidal to gram negative and gram positive bacteria[33]. The antibacterial mechanism of fluoroquinolones is to complex with a DNA molecule and the enzymes topoisomerase II and IV in gram negative and positive bacteria, respectively. While these interferences occur at two distinct stages of DNA polymerization for gram positive and negative bacteria, both interactions result in heavy DNA fragmentation that causes

irreversible cell death[34],[35]. Single species assays have shown ciprofloxacin to have an EC-50 value ranging between 15 and 51 nmol L^{-1} [36-38].

The key research questions addressed in this chapter will be:

6) Can key fermentative products, specifically C1-3 alcohols or volatile fatty acids be detected in FTR effluent?

7) Are any of these compounds present in large concentrations that could indicate fermentation could be a major source of anoxic DIC production?

8) Can broad spectrum antibiotic treatments reveal the degree to which prokaryotic microorganisms contribute to anoxic DIC production?

3.3 Methods

3.3.1 Flow through reactor experiments

Flow through reactors, (FTRs) were packed with sediment, using approximately the top 15 cm layer from Middle Park beach, Victoria, Australia (site coordinates are 37°51'8.73"S, 144°57'27.07"E). Within 90 minutes of collection, sample sediment was transported to Monash University and stored under oxic conditions using an aquarium aerator.

The FTRs used were acrylic cylinders with a diameter of 4.6 cm and a length of 3 cm of sediment (see Figure 1.2, Ch. 1). PVC caps were placed at either end of the cylinder, and were machined with grooves converging to a central outlet port overlaid with 0.1 mm nylon mesh to allow even plug flow through the sediment. Plug flow within these FTRs has been verified via breakthrough curve experiments performed by Evrard *et al*[39] and Bourke *et al* [40]. Freshly collected sample seawater was pumped through the FTRs using a peristaltic pump located upstream. Seawater was pumped in an upwards direction from the base of the FTR to assist in maintaining plug flow (see Figure 1.3, Ch.1). Reservoirs were maintained in oxic/anoxic states by continuous purging with air or argon, respectively.

Sample sediment was sieved using a 2mm mesh to remove large debris, such as shell grit, rocks and macroalgae, which can interfere with plug flow. The system was confirmed to have a negligible leak rate of oxygen by running deoxygenated water through the system, which was then observed to have a concentration of <1 $\mu mol\ L^{-1}$ at the outlet.

Water samples were collected by directly connecting glass syringes to the outlet, ensuring no bubbles were introduced. Reaction rates were calculated based on the difference between the relevant solute concentration in the reservoir and that present in the effluent, factoring in the FTR volume and flow rate used. Appropriate filtration, preservation and storage of samples are summarized in Table 3.1.

Table 3.1: Summary of sample filtration, preservation and storage methods. Approximate temperature of sample freezer was -20 °C.

Target Analyte	Method of filtration	Preservation and conditions of storage
N_2	-	50% $ZnCl_2$ 100 µL No refrigeration required
Dissolved inorganic carbon	-	6% $HgCl_2$ 100 µL No refrigeration required
C1-3 Alcohols and Volatile Fatty Acids	PALL Polypropylene 47 mm 0.2 µm membrane filters	Samples frozen

4 FTR experiments were performed (Table 3.2) with the overarching goal of determining whether fermentation was dominating DIC production in anoxic permeable sediments and what broad group of microorganisms were responsible. FTR experiments 1 and 2 were carried out with the purpose of quantifying the typical fermentative products, C1-3 alcohols and volatile fatty acids, present in FTR effluent. Effluent samples from FTR experiment 1 were analysed using ion chromatography to carry out a non-targeted quantification of short chain volatile fatty acids. Analysis of effluent samples collected during FTR experiment 2, however, utilized Gas Chromatography-Mass Spectrometry (GC-MS) allowing for the quantification of C1-3 alcohols and volatile fatty acids present.

FTR experiments 3 and 4 were both performed in order to identify whether prokaryotic microorganisms substantially contributed to anoxic DIC production. This was achieved by comparing rates of biogeochemical processes, such as DIC production and denitrification, from a control treatment to a treatment spiked with amoxicillin or ciprofloxacin in FTR experiments 3 and 4, respectively. Amoxicillin was replaced by ciprofloxacin in FTR experimental treatments as research progressed, as it became apparent that ciprofloxacin would affect a broader spectrum of bacteria and was commonly used to target marine bacteria[36,41].

Table 3.2: Summary of the flow through reactor experiments performed.

FTR experiment	Date performed	Purpose	Sampling	Experimental summary
1	16.05.14	To determine whether short chain volatile fatty acids were present in FTR effluent.	DO, DIC, N_2 and short chain VFAs (C1-3).	Sampling occurred over a 30 hour period with oxic conditions maintained for the first 5 hours, then changed to anoxic for the remainder of the experiment. 3 FTRs were used. Reservoir was spiked with 50 µmol L^{-1} of $^{15}NO_3^-$. Flow velocity was maintained at 0.80 mL min^{-1}.
2	16.09.14	To determine whether short chain (C1-3) alcohols or volatile fatty acids were present in FTR effluent.	Short chain alcohols and VFAs for GC-MS analysis (Other samples presented Ch. 2.)	Sampling occurred over a 55 hour period with oxic conditions maintained for the first 11 hours, then changed to anoxic for the remainder of the experiment. 5 FTRs were used. Flow velocity was maintained at 1.0 mL min^{-1}. Reservoir contained seawater spiked with 50 µmol L^{-1} $^{15}NO_3^-$. At t=16 hrs, Reservoir was changed to regular anoxic seawater
3	06.03.15	To determine whether prokaryotes substantially contribute to anoxic DIC production.	DO, DIC and N_2.	Sampling occurred over an 8 hour period, during which, anoxic sediment conditions were maintained. 5 FTRs were employed in 3 parallel experimental treatments. One included a reservoir concentration of 130 µmol L^{-1} of the broad spectrum antibiotic amoxicillin (2 FTRs), one was a control treatment (2 FTRs) and one had the reservoir spiked with 2.2 mmol L^{-1} $HgCl_2$. All reservoirs were spiked with 50 µmol L^{-1} of $^{15}NO_3^-$. Flow velocity was maintained at 0.72 mL min^{-1}.
4	22.04.15	To determine whether prokaryotes substantially contribute to anoxic DIC production, using a broader spectrum antibiotic.	DO, DIC and N_2.	Sampling occurred over an 22 hour period, during which, anoxic sediment conditions were maintained. 7 FTRs were employed in 2 parallel experimental treatments. One included a reservoir concentration of 150 µmol L^{-1} of the broad spectrum antibiotic ciprofloxacin (3 FTRs) and one was a control treatment (4 FTRs). All reservoirs were spiked with 50 µmol L^{-1} of $^{15}NO_3^-$. Flow velocity was maintained at 0.33 mL min^{-1}.

62

3.3.2 Sample analysis

3.3.2.1 Dissolved oxygen

Dissolved oxygen was continuously recorded during FTR experiments using Pyroscience Firesting flow through dissolved oxygen sensors. These flow through sensors were attached directly to the inlet and outlet ports of the FTRs.

3.3.2.2 Dissolved inorganic carbon

The concentration of dissolved inorganic carbon was evaluated using flow injection analysis apparatus (FIA), fitted with a photometric detector. This method involved acidifying FTR sample effluent so that any carbonate species would be converted to carbon dioxide, which, would then diffuse across a microporous membrane (Accurel® PP Q3/2 tubular membrane, ID 0.6 mm)[42]. The resulting change in pH causes the Bromothymol Blue indicator solution to produce a measurable colour change proportional to the quantity of diffused carbon dioxide with a precision <1%.

3.3.2.3 Denitrification rates

Concentrations of ^{15}N-N_2 in FTR effluent were determined using headspace analysis on a Gas Chromatograph (He carrier) coupled to isotope ratio mass spectrometer (Sercon 20-22). The rates of denitrification reported throughout this chapter are total denitrification (D_{14}+D_{15}) and were calculated using the isotope pairing technique[43]. Samples from FTR experiments were transferred from glass syringes into 12 mL gastight Exetainers (Labco, High Wycombe).

3.3.2.4 Volatile fatty acid analysis via ion chromatography

The analysis of volatile fatty acids was performed using a Dionex 2100 Ion Chromatography system fitted with an AS12A anion exchange column and AG12A guard column. Mobile phase was generated using a potassium hydroxide cartridge at a programmed concentration of 20mmol L^{-1}. Analytical precision was determined to be <1% RSD. Standards of formate, acetate and propionate were used to identify VFA peak retention times. A 1/50 sample

dilution step was required to prevent detector saturation by the chloride concentration present in seawater samples.

3.3.2.5 Alcohol and volatile fatty acid (C1-3) analysis via SPME-GC-MS

FTR effluent samples from FTR experiment 2 were analyszed for C1-3 volatile fatty acids and alcohols using a Solid Phase Micro Exctraction (SPME) preconcentration step combined with Gas Chromatography-Mass Spectrometry (GC-MS). Analyses were performed using a 20m Polyethyleneglycol column with a ramping oven temperature from 40 to 250°C over a period of 21 minutes. No QC was analyzed therefore, analytical accuracy could not be determined. Helium was used as the mobile phase at a flow rate of 1.5 mL/min. 10 mL of sample effluent was used during the SPME preconcentration step and a variety of factors were tested in order to optimize the method's detection limit. Such factors included selecting which SPME fibre would best adsorb the target analytes (Table 3.3), the length of time the SPME fibre was exposed to the sample effluent headspace at 50 $°C$ and whether the addition of 2g of NaCl and/or 200 uL of 0.3 mol L^{-1} HCl would improve analyte adsorption.

Table 3.3: List of SPME fibre coatings and their typical target analytes.

Fibre	Coating	Typical target analyte
PEG	Polyethylene glycol	Alcohols and polar compounds (MW 40-275)
DVB/CAR/PDMS	Divinylbenzene/Carboxen on polydimethylsiloxane	Flavor compounds: volatiles and semi-volatiles, C3-C20 (MW 40-275)
PDMS/DVB	polydimethylsiloxane and divinylbenzene	Volatiles, amines and nitro-aromatic compounds (MW 50-300)
CAR/PDMS	Carboxen/polydimethylsiloxane	Gases and low molecular weight compounds

3.4 Results

3.4.1 Comparison of DIC production and heterotrophic metabolism in FTR experiments

Mean aerobic DIC production approximately matched mean dissolved oxygen consumption rates during oxic sampling rounds in FTR experiments 1 and 2 (Table 3.6). In fact, single factor ANOVA analyses revealed that neither of these datasets were significantly different. Oxic DIC production in FTR experiments 1 and 2 were also demonstrated to have no significant difference from DIC production under anoxic conditions (Table 3.4).

Table 3.4: Mean rates of dissolved oxygen consumption, DIC production under oxic and anoxic conditions in FTR experiments 1 and 2. Single factor ANOVA statistical tests were used to evaluate statistically significant difference.

				p values	
FTR Experiment	Dissolved oxygen consumption rate (nmol mL^{-1} hr^{-1})	Oxic DIC production (nmol mL^{-1} hr^{-1})	Anoxic DIC production (nmol mL^{-1} hr^{-1})	DO and oxic DIC	Oxic DIC and Anoxic DIC
1	132 ± 12	129 ± 39	114 ± 58	0.76	0.18
2	174 ± 15	210 ± 85	186 ± 97	0.23	0.47

In FTR experiment 1, expected denitrification rates (Figure 3.1) were calculated using anoxic DIC production rates and the NO_3^- :CO_2 stoichiometry of 4:5 (reaction vi). Measured denitrification rates did not approach expected denitrification rate at any of the sampling times. The mean measured denitrification rate amounted to <5% of anoxic DIC production, leaving a large proportion of DIC without a known source.
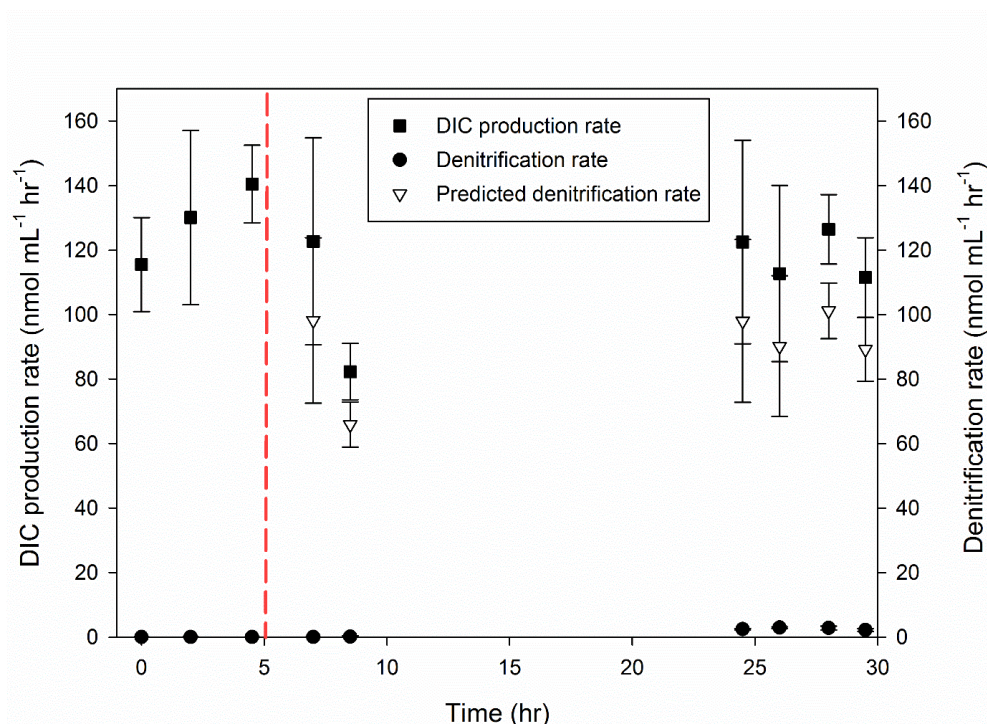
Figure 3.1: Rates of DIC production, denitrification and expected denitrification (based on denitrification stoichiometry of 4:5 with respect to NO_3^- and CO_2 (reaction vi)) from FTR experiment 1 over time. Red dashed line represents when conditions were changed from oxic to anoxic. n=3. FTR reservoir had been spiked with 50 μmol L^{-1} $^{15}NO_3^-$. Error bars represent standard deviation in all instances.

3.4.2 Volatile fatty acid analysis via ion chromatography

Effluent samples from FTR experiment 1 were analysed using ion chromatography and C1-3 VFA standards were used to identify analyte peaks. Neither formate or propionate peaks were detected in effluent samples from either oxic or anoxic sampling rounds. Acetate peaks were detected in FTR effluent samples from anoxic sampling rounds at an approximate concentration range of between 0.1 to 0.5 μmol L^{-1}. The method detection limit for acetate was 0.1 μmol L^{-1} and the limit of quantitiation was determined to be 4 μmol L^{-1}. As a 1/50 dilution step was required to prevent chloride ions from saturating the detector, the effective detection limit for acetate in FTR effluent samples was 5 μmol L^{-1} and the effective limit of quantitation was 200 μmol L^{-1}. Based on the mean anoxic DIC production rate and stoichiometry of reactions iii and iv, acetate production would need to exceed 5.3 and 213.3 nmol mL^{-1} hr^{-1}, respectively, to reach the limits of detection and quantitation, respectively.

These rates would account for 4.7 and 187% of anoxic DIC production in FTR experiment 1, respectively.

The maximum detected acetate concentration of 0.5 μmol L^{-1}, would corresponod to a FTR effluent concentration of 25 μmol L^{-1} and a maximum production rate of 27 nmol mL^{-1} hr^{-1}. Based on the mean anoxic DIC production during FTR experiment 1 and the stoichiometry of reactions iii or iv, this would account for a maximum of 23.4% of anoxic DIC production. However, the acetate peaks detected in anoxic FTR effluent samples were below the limit of quantitation and therefore cannot be reliably quantified.

3.4.3 Optimization of SPME for C1-3 volatile fatty acids and alcohols analysis via GC-MS

Using the CAR/PDMS fibre during SPME pre-treatment consistently resulted in the highest average peak area for all C1-3 alcohol and fatty acid analytes targeted (Figure 3.2a). It was therefore used in all subsequent SPME GC-MS analyses. The PEG fibre offered the next most effective adsorption of target analytes. For all fibres tested, 1-propanol and 1-propionate were most effectively adsorbed, whilst ethanol and acetate were adsorbed to a far lower degree (between 8-13 % of 1-propanol and propionate peak areas). Methanol and formate were not adsorbed effectively, with their respective peak areas comprising only between 0.3 and 0.6 % of the C3 alcohol and fatty acid peaks.

The addition of salt and/or acid to the mixed standards during SPME pre-treatment was also examined as way to further optimize this method (Figure 3.2b). Relative to the control analyses (no salt or acid added), the 'Control + salt' treatment appeared to only marginally improve the adsorption efficiency of the CAR/PDMS fibre, having a higher mean peak area of all alcohols and all VFA's with the exception of propionic acid which was 10% lower compared to its control analysis.

The addition of acid to the mixed standard resulted in a large improvement of the adsorbing efficiency for the VFA components (Figure 3.2b), with a 46-62% increase in peak area compared to the same peaks in the control treatment. The addition of acid did not appear to affect the quantity of alcohol analytes adsorbed as the peak area of all alcohol analytes remained relatively constant in the 'Control + acid' treatment compared to the control treatment. The 'Control + salt + acid' treatment exhibited a greater adsorption efficiency with largest mean peak areas for all target analytes compared to any other treatment.
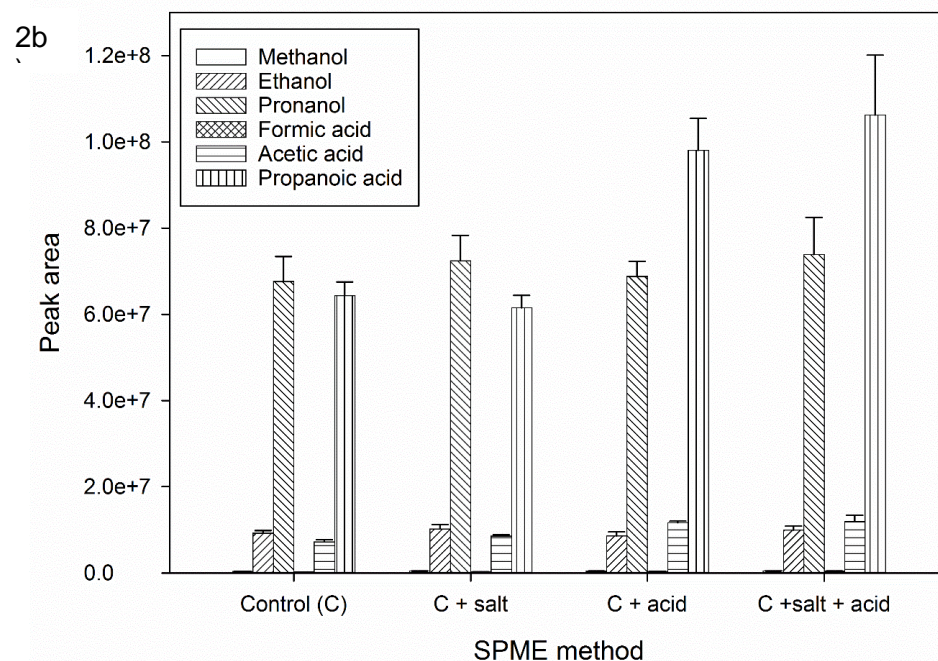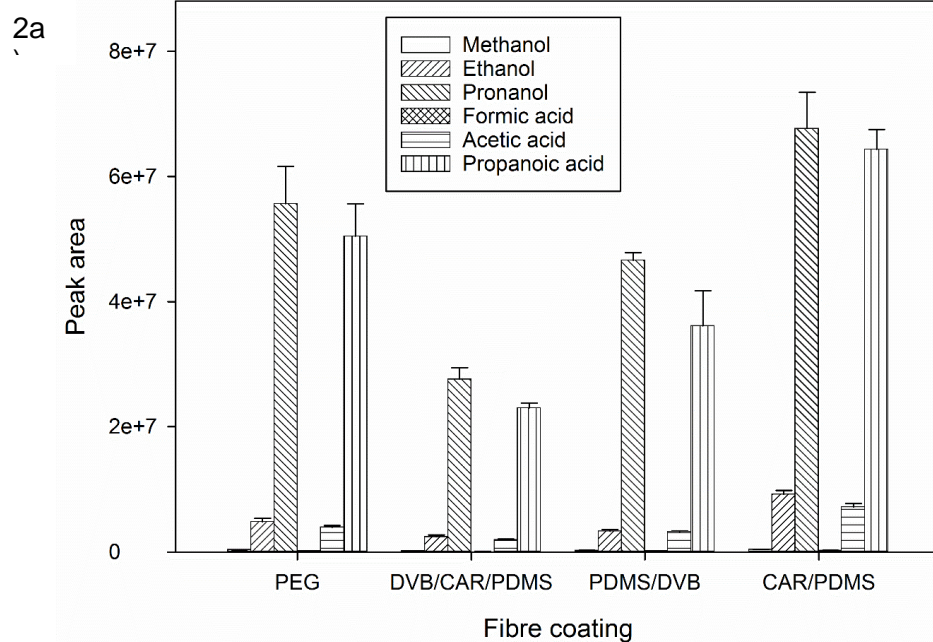
Figure 3.2a and b: Comparison of adsorption efficiency of pre-treatment methods. 3.2a) comparing different SPME fibres. 3.2b) comparing how the addition of salt and/or acid affects adsorption of target analytes. Each data point represents triplicate analysis. Error bars are standard deviation in all cases.

The final factor that was tested was the duration of time the CAR/PDMS fibre was exposed to the sample headspace during the SPME pre-treatment step. The greater length of time the fibre was exposed, the more effectively analytes were adsorbed (Figure 3.3), until approximately t= 50 min, where the quantity of analytes adsorbed began to plateau. The maximum adsorbance was observed at t= 60 min. For all subsequent sample analyses, a 60 minute fibre exposure time was used. The positive correlation between the degree of analyte adsorption and exposure time was consistent for all C1-3 alcohol and VFA analytes examined.

For all subsequent FTR effluent sample analysed via SPME GC-MS, additions of salt and acid were employed in conjunction with a 60 minute exposure time to the CAR/PDMS fibre. The limits of detection and quantitation for each analyte were also determined (Table 3.5).
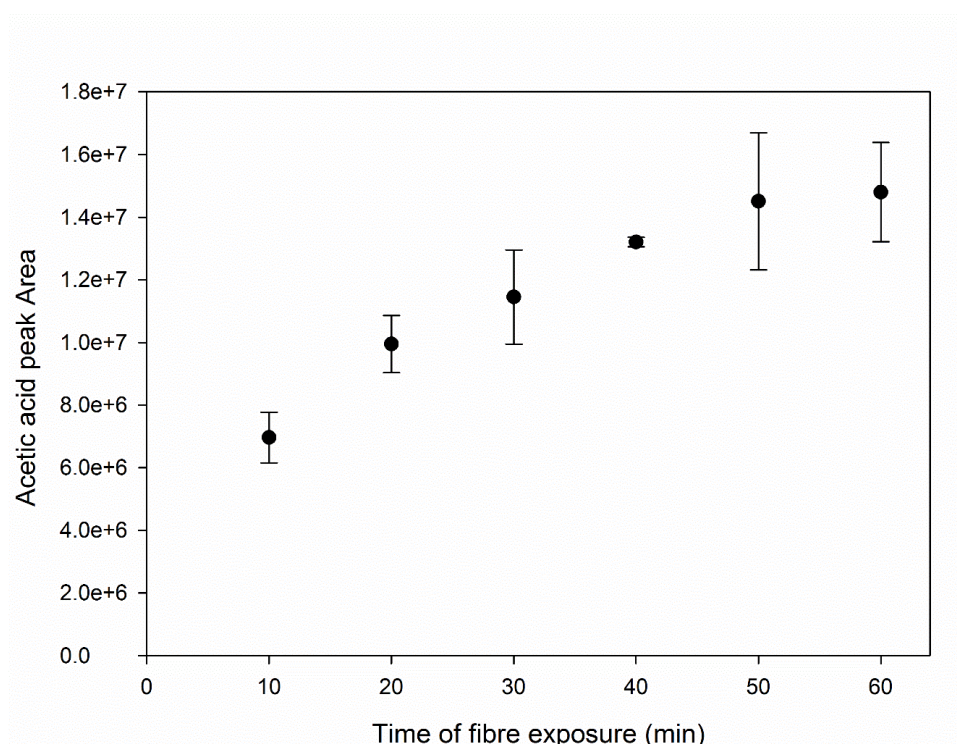
Figure 3.3: Acetic acid peak area plotted against increasing length of SPME fibre exposure time. Each data point represents triplicate analysis. Error bars are standard deviation in all instances.

Table 3.5: List of target analytes, their retention time and limits of detection and quantitation using the optimized SPME pre-treatment with GC-MS analysis.

Target analyte	Retention time (min)	Limit of detection (μmol L^{-1})	Limit of quantitation (μmol L^{-1})
Methanol	7.1	150	194
Ethanol	7.6	1	18
Propanol	8	0.04	12
Formate	14.1	150	313
Acetate	16.7	0.5	12
Propionate	17.8	0.02	12

3.4.4 FTR effluent analysis of C1-3 alcohol and volatile fatty acids via SPME GC-MS

Effluent from FTR experiment 2 was analysed and no peaks for formate, methanol, propionate or 1-propanol were detected in any of the samples analyzed. Peaks corresponding to ethanol and acetate were detected in all anoxic sampling round samples analyzed. Though in all instances, the peak area for both analytes fell below the respective limits of quantitation (Table 3.5) and could therefore not be reliably quantified. The peak areas corresponded to an approximate concentration of 1 μmol L^{-1} for both acetate and ethanol. These concentrations would correspond to production rates of approximately 1.3 nmol mL^{-1} hr^{-1}, and based on the reaction stoichiometries from reactions i, iii and iv, would account for only 0.7 and 1.4 % of anoxic DIC production for acetate and ethanol, respectively.

3.4.5 Antibiotics FTR experiments

Dissolved oxygen consumption rates approximately matched anoxic DIC production rates for all treatments, across both experiments 3 and 4 (Table 3.6). In FTR experiment 3, there was no statistical difference between control and amoxicillin treatments with respect to dissolved oxygen consumption rates ($p>0.05$) or anoxic DIC production ($p>0.05$) (single factor ANOVA analyses). In the HgCl$_2$ treatment however, rates of dissolved oxygen consumption and anoxic DIC production were both negligible compared to either the control or amoxicillin treatments.

In FTR experiment 4, there was no statistical difference between control and ciprofloxacin treatments with respect to rates of dissolved oxygen consumption ($p > 0.05$) and anoxic DIC production ($p > 0.05$) (single factor ANOVA analyses).

Denitrification rates for the control treatment in FTR experiment 3 gradually increased over time, in contrast with the amoxicillin and $HgCl_2$ treatments, which stayed constant (Figure 3.4a). The control treatment reached an experimental maximum of 6 ± 2 nmol mL^{-1} hr^{-1} and had a mean production rate of 4 ± 2 nmol mL^{-1} hr^{-1}, while amoxicillin and $HgCl_2$ treatments had mean production rates of 1.2 ± 0.4 and 0.1 nmol mL^{-1} hr^{-1}, respectively. These mean denitrification rates accounted for $< 4\%$ and $<1\%$ of the anoxic DIC production rates in the control and amoxicillin treatments, respectively.

Table 3.6: Mean rates of dissolved oxygen consumption and anoxic DIC production across the various treatment in FTR experiments 3 and 4.

FTR Experiment	Treatment	Dissolved oxygen consumption rate (nmol mL^{-1} hr^{-1})	Anoxic DIC production (nmol mL^{-1} hr^{-1})
3	Control	102 ± 2	110 ± 21
	Amoxicillin	97 ± 4	119 ± 28
	HgCl$_2$	0	3
4	Control	64 ± 5	71 ± 17
	Ciprofloxacin	68 ± 7	60 ± 23

In FTR experiment 4, denitrification rates in the ciprofloxacin treatment were far lower than the control treatment (Figure 3.4b). Mean denitrification rates were 4 ± 1 and 0.5 ± 0.4 nmol mL^{-1} hr^{-1} for control and ciprofloxacin treatments, respectively. These mean denitrification rates accounted for $< 6\%$ and $<1\%$ of anoxic DIC production for control and ciprofloxacin treatments, respectively.
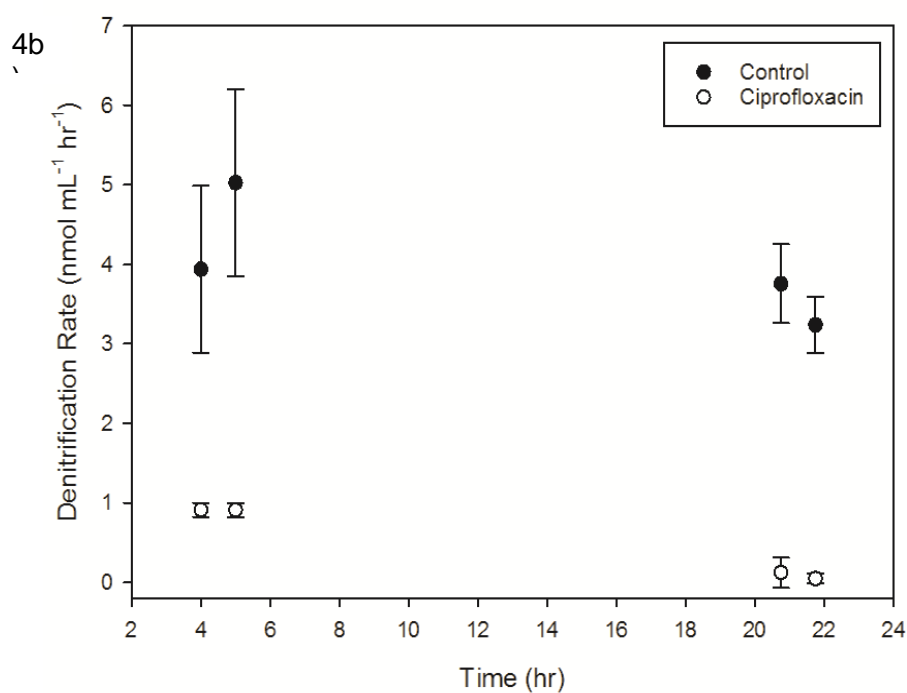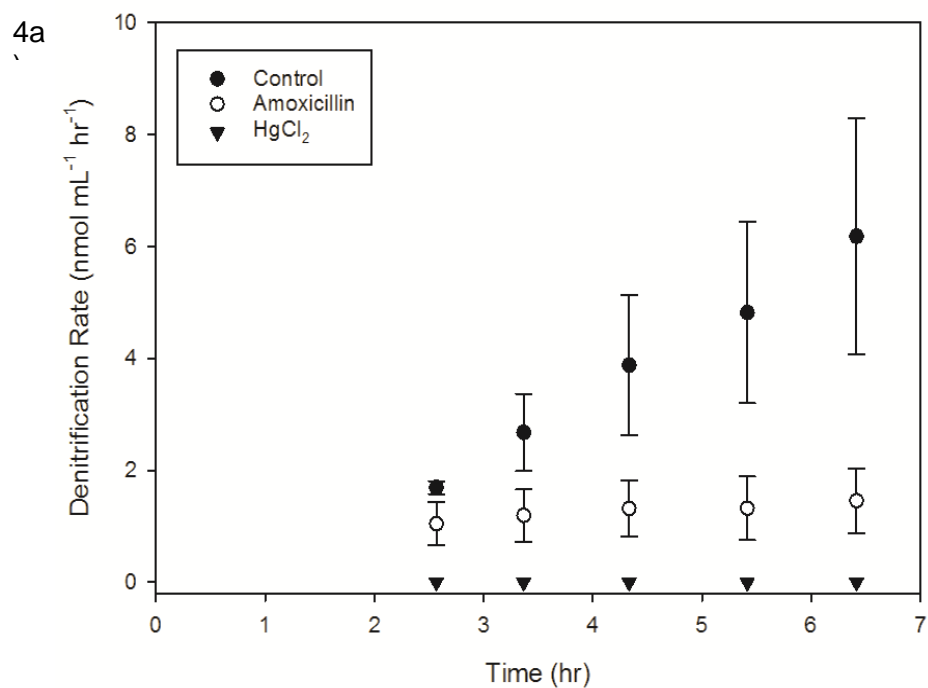
Figure 3.4a and b: Rates of denitrification over time under anoxic conditions in FTR experiments 3 (3.4a) and 4 (3.4b). Concentration of amoxicillin and HgCl₂ in FTR experiment 3 was 130 μmol L⁻¹ and 2.2 mmol L⁻¹, respectively. Concentration of ciprofloxacin in FTR experiment 4 was 150 μmol L⁻¹. Error bars are standard deviation in all instances.

3.5 Discussion

3.5.1 Dissolved inorganic carbon in flow through reactor experiments

In both FTR experiments 1 and 2, there was no statistical difference between oxic DIC production rates and rates of dissolved oxygen consumption ($p<0.05$), indicating aerobic respiration is dominating DIC production under oxic conditions (Table 3.4). Interestingly, rates of oxic and anoxic DIC production in FTR experiments 1 and 2 were also very similar and were shown to have no statistical difference between the datasets ($p>0.05$). This suggests that the community responsible for respiring under oxic conditions (and producing DIC), is likely the same community respiring under anoxic conditions, as there is no change in rate. Despite denitrification being the next most energetically favourable process following aerobic respiration (reactions ii and i, respectively), at no point during FTR experiment 1 did the measured denitrification rate approach the expected denitrification rate (Figure 3.1). In fact, the mean measured denitrification rate made up <5% of mean anoxic DIC production leaving approximately 95% of anoxic DIC production without a known source. These findings are consistent with the research presented in chapter 2 of this thesis, indicating a highly reproducible phenomenon.

3.5.2 Volatile fatty acid analysis by ion chromatography

Acetate was detected in FTR effluent samples taken during anoxic sampling rounds and was in the approximate concentration range of between 0.1 to 0.5 μmol L^{-1}. The maximum detected concentration of 0.5 μmol L^{-1} corresponded to a FTR production rate of 27 nmol mL^{-1} hr^{-1}, accounting for 23.4% of anoxic DIC production in FTR experiment 1. While this is a substantial proportion of the anoxic DIC production, this concentration range fell below the method limit of quantitation (4 μmol L^{-1}) and therefore cannot be considered reliable. The 1 in 50 dilution factor necessitated by the high chloride concentration of seawater samples meant that the effective limit of quantitation for acetate in FTR effluent samples

corresponded to a 200 μmol L^{-1}, highlighting the inadequacy of this analytical methodology. Effluent from FTRs should be analyzed using a method that has a lower limit of quantitation to allow for more robust conclusions to be made.

However, the presence of an acetate peak indicates that the concentration was at least high enough to exceed the detection limit, meaning a conservative estimate for the acetate concentration in FTR effluent during anoxic sampling rounds would be at least 5 μmol L^{-1}, corresponding to a production rate of 5.3 nmol mL^{-1} hr^{-1}. This would mean that acetate-producing fermentation reactions uncoupled to heterotrophic metabolism, were likely contributing at least 4.7% of the total anoxic DIC production in FTR experiment 1.

During analysis, no formate or propionate peaks were found in any samples taken during oxic or anoxic sampling rounds, but due to the high dilution factor, it can only be concluded that the concentration of these analytes did not exceed the effective detection limit concentration of 5 μmol L^{-1}.

3.5.3 Solid phase micro-extraction method optimization

Analyses using the CAR/PDMS SPME fibre consistently had the highest average peak area for all C1-3 alcohols and fatty acids targeted. The DVB/CAR/PDMS fibre bound target analytes least effectively, despite sharing two of the three fibre coatings with the more efficient CAR/PDMS fibre.

Relative to the control analyses, the Control + salt treatment appeared to only marginally improve the adsorption efficiency of the CAR/PDMS fibre. The addition of salt likely decreased the solubility of the alcohols and VFAs and allowed for a greater proportion to be volatilized into the vial headspace, increasing the total quantity of analytes adsorbed to the fibre. The addition of acid to the sample during the SPME pre-treatment had a large improvement of the adsorbing efficiency for the VFA samples. This was likely due to the lowering of the sample pH resulting in the protonation of all VFAs, enabling them to have a

neutral charge, lowering their solubility. This allowed for a greater proportion of the total VFAs to be volatilized into the headspace and adsorb onto the fibre. There was no observed change in the adsorption efficiency of the alcohol analytes compared with the same peaks in the control treatment. This is likely due no chemical change being brought about to the alcohols following the addition of acid and would therefore produce an adsorption efficiency near identical to that observed in the control treatment. At approximately 60 minutes of exposure the quantity that could be bound appeared to plateau. The system had likely reached a point where the adsorption of target analytes onto the fibre had found an equilibrium with adsorbed analytes moving from the fibre to the headspace.

3.5.4 VFA and alcohol analysis of effluent using SPME GC-MS

No peaks for formate, methanol, propionate or 1-propanol were detected in any of the anoxic sampling rounds that were analyzed for FTR experiment 2. However, the sizeable differences in limits of detection for these analytes result in very different conclusions regarding their respective prevalence in FTR effluent (Table 3.5). As the limit of detection for methanol and formate was 150 μmol L^{-1}, it can only be concluded that these analytes were not present in FTR effluent at concentrations exceeding this value. Since various fermentation processes are expected to be utilized in combination with one another, this conclusion is not useful, as methanol and formate producing fermentation reactions uncoupled to heterotrophic metabolism may still be occurring at high rates and contributing to anoxic DIC production. For more robust conclusions, FTR effluent samples should be analyzed using a method with a far lower limit of detection and quantitation.

The detection limits of 1-propanol and propionate were 0.04 and 0.02 μmol L^{-1}, respectively, and as no peak for either analyte was detected, it is highly likely that these compounds were not accumulating in effluent during FTR experiment 2. 1-propanol and propionate producing

fermentation reactions, uncoupled to heterotrophic metabolism therefore do not contribute substantially to the >95% of anoxic DIC unassigned to a known process.

Ethanol and acetate were both detected in effluent samples from anoxic sampling rounds of FTR experiment 2 effluent, however, the peak area of each analyte was below the respective limits of quantitation (Table 3.5) and therefore cannot be reliably quantified. However, as the peak areas corresponded to approximately the respective analyte detection limits, conservative estimates of their concentrations may be made. These peaks corresponded to approximately 1 μmol L^{-1} for both ethanol and acetate, which represented production rates of 1.3 nmol mL^{-1} hr^{-1}. These rates only accounted for 0.7 and 1.4% of anoxic DIC production rates for acetate and ethanol producing fermentation reactions, respectively, leaving the vast majority of anoxic DIC production without a known source.

3.5.5 Antibiotic FTR experiments and the prokaryotic contribution to anoxic DIC production

In FTR experiments 3 and 4, anoxic DIC production not only persisted during antibiotic treatments (Table 3.6), but there was no statistical difference between the control and antibiotic treatments with respect to mean anoxic DIC production rates. This indicates that prokaryotic microorganisms were not contributing substantially to anoxic DIC production, which is highly consistent with the foundational observation of this research, namely that terminal heterotrophic metabolic processes (reactions v-viii), typically performed by prokaryotes, contribute <5% of anoxic DIC production.

The possibility of bacteria being resistant to amoxicillin and ciprofloxacin was investigated by quantifying the rate of denitrification in the presence and absence of these antibiotics (Figure 3.4a and 3.4b). In FTR experiment 3, amoxicillin inhibited denitrification by factors of 2 to 5, compared to the control, over the course of the experiment. Whilst in FTR experiment 4, ciprofloxacin inhibited denitrification to a far greater extent, between factors of

4 to 35, compared to the control treatment. The greater degree of inhibition observed in FTR experiment 4 was likely due to ciprofloxacin being effective towards a broader range of bacteria compared to amoxicillin. These findings indicate that antibiotic resistant bacteria do not explain these observations.

Negligible dissolved oxygen consumption rates, anoxic DIC production rates and denitrification rates observed in the $HgCl_2$ treatment of FTR experiment 3 confirm that this preservative has halted the large majority of metabolism within the FTR. As almost all anoxic DIC production has ceased, this adds further support to a conclusion presented in Chapter 2 of this thesis, namely, that abiotic processes such as calcium carbonate dissolution do not substantially contribute to anoxic DIC production in permeable sediments.

These observations suggest that eukaryotes, not bacteria, are responsible for the vast majority of DIC production in permeable sediments, which represents a considerable departure from the contemporary understanding of microbiological activity in permeable sediments.

3.6 Conclusion

Quantification of C1-3 alcohols and volatile fatty acids in sample effluent from FTR experiments 1 and 2 has determined that between 2.1% and 4.7% of anoxic DIC production can be attributed to fermentation reactions, uncoupled to heterotrophic metabolism. While there remains a large proportion of anoxic DIC production unassigned to a known process (>90%), fermentation remains the most likely explanation of how microbes are continuing to respire and produce DIC under anoxic conditions. The dominant pathway(s) have not been identified in this research. Based on the dominance of eukaryotes revealed in FTR experiments 3 and 4, future research should target typical products of eukaryotic fermentation reactions, such as dissolved hydrogen and intracellularly stored wax esters.

3.7 References

1   Rossello-Mora, R., Thamdrup, B., Schafer, H., Weller, R. & Amann, R. The response of the microbial community of marine sediments to organic carbon input under anaerobic conditions. *Syst. Appl. Microbiol.* 22, 237-248, (1999).

2   Holmer, M. & Kristensen, E. Organic matter mineralization in an organic rich sediment. Experimental stimulation of sulfate reduction by fish food pellets. *FEMS Microbiol. Ecol.* 14, 33-44, (1994).

3   Weiss, M. S. *et al.* Molecular architecture and electrostatic properties of a bacterial porin. *Science* 254, 1627-1630, (1991).

4   Catalanotti, C., Yang, W., Posewitz, M. C. & Grossman, A. R. Fermentation metabolism and its evolution in algae. *Front. Plant. Sci.* 4, 150, (2013).

5   Canfield, D. E., Kristensen, E. & Thamdrup, B. in *Aquatic Geomicrobiology* Vol. 48 *Advances in Marine Biology* Ch. 10, 383-414 (Academic Press Ltd-Elsevier Science Ltd, 2005).

6   Canfield, D. E., Thamdrup, B. & Hansen, J. W. The anaerobic degredation of organic matter in danish coastal sediments- iron reduction, manganese reduction and sulfate reduction. *Geochim. Cosmochim. Acta* 57, 3867-3883, (1993).

7   Fenchel, T. & Finlay, B. Oxygen and the Spatial Structure of Microbial Communities. *Biological Reviews* 83, 553-569, (2008).

8   Fenchel. Thermodynamics and calculation of energy yields of metabolic processes. *Bacterial Biogeochemistry: The Ecophysiology of Mineral Cycling, 2nd Edition*, 284-292, (1998).

9   Kessler, A. J. *et al.* Quantifying denitrification in rippled permeable sands through combined flume experiments and modeling. *Limnol. Oceanogr.* 57, 1217-1232, (2012).

10   Evrard, V., Glud, R. N. & Cook, P. L. M. The kinetics of denitrification in permeable sediments. *Biogeochemistry* 113, 563-572, (2013).

11   Strohm, T. O., Griffin, B., Zumft, W. G. & Schink, B. Growth yields in bacterial denitrification and nitrate ammonification. *Appl. Environ. Microbiol.* 73, 1420-1424, (2007).

12   Revsbech, N. P., Trampe, E., Lichtenberg, M., Ward, D. M. & Kuhl, M. In Situ Hydrogen Dynamics in a Hot Spring Microbial Mat during a Diel Cycle. *Appl. Environ. Microbiol.* 82, 4209-4217, (2016).

13   Hoehler, T. M., Alperin, M. J., Albert, D. B. & Martens, C. S. Thermodynamic control on hydrogen concentrations in anoxic sediments. *Geochim. Cosmochim. Acta* 62, 1745-1756, (1998).

14   Wolfe, A. J. The acetate switch. *Microbiol. Mol. Biol. Rev.* 69, 12-+, (2005).

15   Alam, K. Y. & Clark, D. P. Anaerobic fermentation balance of escherichia coli as observed by invivo nuclear magnetic resonance spectroscopy. *J. Bacteriol.* 171, 6213-6217, (1989).

16   Gottschalk, G. *Bacterial Metabolism*. 2nd Edition edn, (Springer-Verlag, 1985).

17   Dien, B. S., Cotta, M. A. & Jeffries, T. W. Bacteria engineered for fuel ethanol production: current status. *Appl. Microbiol. Biotechnol.* 63, 258-266, (2003).

18   Kamp, A., de Beer, D., Nitsch, J. L., Lavik, G. & Stief, P. Diatoms respire nitrate to survive dark and anoxic conditions. *Proc. Nat. Acad. Sci. USA* 108, 5649-5654, (2011).

19   Kreuzberg, K. Starch fermentation via a formate producing pathway in chlamydomonas reinhardii, chlorogonium elongatum and chlorella fusca. *Physiol. Plant.* 61, 87-94, (1984).

20   Ohta, S., Miyamoto, K. & Miura, Y. Hydrogen evolution as a consumption mode of reducing equivalents in green algal fermentation. *Plant Physiol.* 83, 1022-1026, (1987).

21   Atteia, A., van Lis, R., Tielens, A. G. M. & Martin, W. F. Anaerobic energy metabolism in unicellular photosynthetic eukaryotes. *Biochimica Et Biophysica Acta-Bioenergetics* 1827, 210-223, (2013).

22   Mus, F., Dubini, A., Seibert, M., Posewitz, M. C. & Grossman, A. R. Anaerobic acclimation in Chlamydomonas reinhardtii - Anoxic gene expression, hydrogenase induction, and metabolic pathways. *J. Biol. Chem.* 282, 25475-25486, (2007).

23   Meuser, J. E. *et al.* Phenotypic diversity of hydrogen production in chlorophycean algae reflects distinct anaerobic metabolisms. *J. Biotechnol.* 142, 21-30, (2009).

24   Gaffron, H. & Rubin, J. Fermentative and photochemical production of hydrogen in algae. *The Journal of general physiology* 26, 219-240, (1942).

25   Klein, U. & Betz, A. Fermentative metabolism of hydrogen evolving chlamydomonas moewusii. *Plant Physiol.* 61, 953-956, (1978).

26   Valdemarsen, T. & Kristensen, E. Degradation of dissolved organic monomers and short-chain fatty acids in sandy marine sediment by fermentation and sulfate reduction. *Geochim. Cosmochim. Acta* 74, 1593-1605, (2010).

27   Inui, H., Miyatake, K., Nakano, Y. & Kitaoka, S. Wax ester fermentation in euglena gracilis. *FEBS Lett.* 150, 89-93, (1982).

28   Tucci, S., Vacula, R., Krajcovic, J., Proksch, P. & Martin, W. Variability of Wax Ester Fermentation in Natural and Bleached Euglena gracilis Strains in Response to Oxygen and the Elongase Inhibitor Flufenacet. *J. Eukaryot. Microbiol.* 57, 63-69, (2010).

29   Roychoudhury, A. N., Viollier, E. & Van Cappellen, P. A plug flow-through reactor for studying biogeochemical reactions in undisturbed aquatic sediments. *Appl. Geochem.* 13, 269-280, (1998).

30   Berardigrassias, L., Lepennec, M. P. & Chauviere, P. Invitro activity of penicillin G and amoxicillin against 14 strains of streptococcus milleri. *Pathol. Biol.* 36, 632-634, (1988).

31   Meylan, P. R., Francioli, P. & Glauser, M. P. Discrepancies between MBC and actual killing of viridans group streptococci by cell wall active antibiotics. *Antimicrobial Agents and Chemotherapy* 29, 418-423, (1986).

32   *Materials Safety Data Sheet: Amoxil Paediatric Drops*, 2017).

33   Van Bambeke, F., Michot, J. M., Van Eldere, J. & Tulkens, P. M. Quinolones in 2005: an update. *Clin. Microbiol. Infect.* 11, 256-280, (2005).

34   Drlica, K., Malik, M., Kerns, R. J. & Zhaol, X. L. Quinolone-mediated bacterial death. *Antimicrobial Agents and Chemotherapy* 52, 385-392, (2008).

35   Zhanel, G. G. *et al.* A critical review of the fluoroquinolones - Focus on respiratory tract infections. *Drugs* 62, 13-59, (2002).

36   Davis, R., Markham, A. & Balfour, J. A. Ciprofloxacin - An updated review of its pharmacology, therapeutic efficacy and tolerability. *Drugs* 51, 1019-1074, (1996).

37   Naslund, J., Hedman, J. E. & Agestrand, C. Effects of the antibiotic ciprofloxacin on the bacterial community structure and degradation of pyrene in marine sediment. *Aquat. Toxicol.* 90, 223-227, (2008).

38   Ebert, I. *et al.* Toxicity of the fluoroquinolone antibiotics enrofloxacin and ciprofloxacin to photoautotrophic aquatic organisms. *Environ. Toxicol. Chem.* 30, 2786-2792, (2011).

39   Evrard, V., Glud, R. N. & Cook, P. L. M. The kinetics of denitrification in permeable sediments. *Biogeochemistry* 113, 563-572, (2012).

40   Bourke, M., Kessler, A. & Cook, P. Influence of buried Ulva lactuca on denitrification in permeable sediments. *Mar. Ecol. Prog. Ser.* 498, 85-94, (2014).

41   Robinson, A. A., Belden, J. B. & Lydy, M. J. Toxicity of fluoroquinolone antibiotics to aquatic organisms. *Environ. Toxicol. Chem.* 24, 423-430, (2005).

42   Oshima, M. *et al.* Highly sensitive determination method for total carbonate in water samples by flow injection analysis coupled with gas-diffusion separation. *Analyt. Sci.* 17, 1285-1290, (2001).

43   Nielsen, L. P. Denitrification in sediment determined from nitrogen isotope pairing. *FEMS Microbiol. Ecol.* 86, 357-362, (1992).

Chapter 4: Eukaryotic dark fermentation dominates anoxic permeable sediments

4.1 Abstract

Permeable sediments are common across continental shelves and are critical contributors to marine biogeochemical cycling. Organic matter in permeable sediments is dominated by microalgae, which as eukaryotes, have different anaerobic metabolic pathways to prokaryotes, such as bacteria and archaea. In this research, analyses of flow-through reactor experiments have shown that anaerobic production of dissolved inorganic carbon was consistently accompanied by large dissolved hydrogen production rates, suggesting the presence of fermentation. The production of both dissolved inorganic carbon and hydrogen persisted following administration of broad spectrum bactericidal antibiotics, but ceased following treatment with metronidazole. Metronidazole inhibits the ferredoxin/hydrogenase pathway of fermentative eukaryotic hydrogen production, suggesting that pathway as the source of hydrogen and dissolved inorganic carbon production. Metabolomic analysis showed large increases in lipid production at the onset of anoxia, consistent with documented pathways of anoxic dark fermentation in microalgae. Cell counts revealed a predominance of microalgae in the sediments. These findings indicate that microalgal dark fermentation could be an important energy-conserving pathway in permeable sediments.

4.2 Introduction

In permeable sediments, under anoxic conditions, established energetic favourability yields indicate that denitrification should be the dominant process and therefore be a major source of dissolved inorganic carbon (DIC), should nitrate be present. Research presented in chapter 2 of this thesis has consistently shown that the combined rates of denitrification, iron and sulfate reduction accounted for <5 % of DIC production in anoxic FTR experiments. This large quantity of DIC could not be attributed to either calcium carbonate dissolution or respiration by meiofauna. Furthermore, in FTR experiments presented in chapter 3 of this thesis, large quantities of DIC continued to be produced despite the presence of the broad spectrum antibiotics, amoxicillin and ciprofloxacin, indicating that eukaryotic microalgae are likely responsible for the majority of metabolism in permeable sands, under anoxic conditions.

Microalgae are globally ubiquitous in photic sediments and often have a biomass exceeding phytoplankton in overlying waters[1]. In permeable (sandy) sediments, their biomass may comprise $10 - 40\%$ of the organic carbon pool based on previously reported carbon to chlorophyll *a* ratios [2,3]. In contrast, bacterial biomass has previously been reported to comprise <10% of the organic carbon pool in sandy sediments[4]. This is also consistent with the dominance of microalgae in mediating carbon flows in such sediments[5]. Given their high biomass, it is reasonable to expect that microalgae will undertake a large fraction of the carbon mineralization and energy generation pathways in comparison to bacteria. Despite this, it remains widely assumed that bacterial fermentation and sulfate reduction are the main mechanisms of DIC production in anoxic permeable sediments[6]. Surprisingly, prior to this research, there have been no systematic studies of electron acceptor utilisation in freshly collected sands and, despite their dominance, the role of microalgae in these processes[7].

The dynamic nature of permeable sediments means that microalgae are often observed to be evenly distributed to in excess of 15 cm within sands where dark anoxic conditions will prevail [1,5]. It has been shown that microalgae mixed into the dark sediment can remain viable for long periods of time (half lives of 6-22 days), highlighting their adaptation to this dynamic environment[8]. However, the metabolic basis of how they survive light and oxygen fluctuations is unclear. Nitrate respiration has previously been shown to sustain the survival of axenic cultures of phototrophic eukaryotes in dark anoxic conditions[9]; however, it remains to be determined whether nitrate respiration is a relevant strategy in the environment and it is unlikely that it is sufficient to support microalgal populations in oligotrophic systems with low nitrate concentrations.

One possible source of large quantities of DIC in anoxic sediments could be fermentation. Fermentation is a broad category of microbially-mediated reactions that involves organic carbon simultaneously undergoing oxidation and reduction, serving as both the electron acceptor and the electron donor[10]. It is well understood that fermentation takes place in all sediments but was considered to be strongly coupled to the previously mentioned heterotrophic metabolic pathways, thereby preventing the accumulation of fermentative products.

While some microalgae have been shown to undertake fermentation under dark anoxic conditions, for example chlorophytes[11,12], there have been no studies to date to quantify the importance of this in the environment.

Dark fermentation in microalgae may result in the production of H_2 and CO_2 as well as a wide variety of organic end products, depending on the microalgal species, pathway and environmental conditions[12,13]. For example, *Chlamydomonas* excrete acetate, ethanol, and formate or glycerol at ratios that vary depending on the species[14-16]. Additionally, some algae do not release fermentative products from the cell at all and instead they accumulate them

intracellularly. For instance, Inui et al (1982)[17] have found that *Euglena gracilis* generates large concentrations of wax esters which are stored in the cytosol[18] that are reoxidised to generate ATP upon return to oxic conditions.

There are two well-studied eukaryotic metabolic processes that produce hydrogen: photobiological production and dark fermentative metabolism[10]. In photobiological production, light-excited electrons derived from water (direct biophotolysis) or organic compounds (indirect biophotolysis) are transferred to ferredoxin and then [FeFe]-hydrogenase resulting in H_2 production[19,20]. By contrast, dark fermentative metabolism involves the glycolytic breakdown of organic compounds (e.g. intracellularly stored starch). The resulting pyruvate is then oxidised to acetyl-CoA by pyruvate ferredoxin oxidoreductase (PFR) resulting in carbon dioxide [10,12]. Acetyl-CoA is then converted to stored lipids. The ferredoxin reduced by PFR is in turn reoxidised by [FeFe]-hydrogenase resulting in hydrogen production[21].

This process can be effectively inhibited by low concentrations of metronidazole[22]. Metronidazole is a nitroimidazole compound that has been demonstrated to preferentially oxidize the reduced form of ferredoxin, thereby blocking hydrogen production[23]. The reduced form of metronidazole may then be oxidized by dissolved oxygen and will produce a superoxide radical that may damage the cell.

The primary hypothesis of this research chapter is that eukaryotic microalgae are predominantly using dark fermentation to sustain cell function in permeable sediments under anoxic conditions, which results in large quantities of DIC being produced. This hypothesis will be investigated using a combination of flow through reactor (FTR) experiments and culture experiments, using microalgal cultures grown from sample site sediments.

The key research questions addressed in this chapter will be:

1) Can meaningful concentrations of a key fermentative product, such as dissolved hydrogen, be detected in FTR effluent?

2) Are other key fermentative products, such as fatty acids, accumulating intracellularly during extended anoxic incubation?

3) What pathway is responsible for the production of dissolved hydrogen and does the presence of nitrate affect the rate of production?

4.3 Methods

4.3.1 Flow through reactor experiments

Flow through reactors (FTRs), were packed using approximately the top 15 cm layer of sediment from Port Phillip Bay, Victoria, Australia (site coordinates are 37°51'8.73"S, 144°57'27.07"E). The FTRs used were acrylic cylinders with a diameter of 4.6 cm and a length of 3 cm sediment. PVC caps were placed at either end of the cylinder, and were machined with grooves converging to a central outlet port overlaid with 0.1 mm nylon mesh to allow even plug flow through the FTR. Plug flow within these FTRs has been verified during breakthrough curve experiments performed by Evrard *et al*[24] and Bourke *et al*[25]. Freshly collected sample seawater was pumped through the FTRs using a peristaltic pump located upstream. Seawater was pumped in an upwards direction from the base of the FTR to assist in maintaining plug flow. Reservoirs were maintained in oxic/anoxic states by continuous purging with air or argon respectively.

Sediment was sieved using a 2mm mesh to remove large debris, such as shell grit, rocks and macroalgae, which can interfere with FTR plug flow. The system was confirmed to have a negligible leak rate of oxygen by running deoxygenated water through the system, which was then observed to have a concentration of <1 μmol L^{-1} at the outlet.

For dissolved hydrogen, a loss of 3.6% was observed when a solution containing 50 μmol L^{-1} H_2 was pumped through the FTR set up. Water samples at the FTR outlet were collected by directly connecting glass syringes to the outlet, ensuring no bubbles were introduced. Reaction rates were calculated based on the difference between the relevant solute concentration in the reservoir and the outlet of the FTR, the reactor volume and the flow rate through the reaction.

Four FTR experiments were performed (Table 4.1) with the overarching goal of investigating what process was responsible for the large majority of DIC production in permeable sediments, under anoxic conditions, what compounds are being produced by this process and what factors might be influencing the rates of production.

Table 4.1: Summary of flow through reactor experiment duration, conditions, sampling regime and purpose.

FTR experiment	Date performed	Purpose	Sampling	Experimental summary
1	23.07.15	To examine the influence of elevated concentrations of $^{15}NO_3^-$, the antibiotic ciprofloxacin and the preservative $HgCl_2$ on dissolved hydrogen production.	Dissolved Oxygen (DO), H_2, DIC.	Sampling occurred once per day, over 5 days. Oxic conditions were maintained for the first day, then changed to anoxic for all proceeding days. Inlet reservoir was spiked with 60 µmol L^{-1} $^{15}NO_3^-$ up until 44 hours into the experiment, then the reservoir was changed to regular seawater. At the 142nd hour the reservoir was returned to 60 µmol L^{-1} $^{15}NO_3^-$. At the 156th hour a dose of the broad spectrum antibiotic, ciprofloxacin, was added to the reservoir (150 µmol L^{-1}). At the 165th hour the reservoir was dosed with $HgCl_2$ (2.2 mmol L^{-1}).Flow velocity was maintained at 0.51 mL min^{-1}.
2	5.08.15	To examine whether dissolved hydrogen production is dependent upon the presence of nitrate and whether fermentation products are accumulating intracellularly.	DO, H_2, DIC, N_2, Sulfide, chlorophyll a and metabolome	Sampling occurred once per day, over 9 days. 2 experimental treatments were used in parallel, one with a regular seawater reservoir and the other having a 50 µmol L^{-1} $^{15}NO_3^-$spiked seawater reservoir. The treatments had 5 and 3 FTRs, respectively. All FTR conditions were oxic for the first two days, then anoxic for all proceeding days. FTRs in the regular seawater treatment were removed and frozen throughout the experiment for metabolome analysis. The broad spectrum antibiotic, ciprofloxacin, was added to both reservoirs at the end of the seventh day (150 µmol L^{-1}). Flow velocity was maintained at 0.39 mL min^{-1}.
3	29.10.15	To examine whether dissolved hydrogen is produced via a ferredoxin pathway.	DO, H_2, DIC and chlorophyll a.	Sampling occurred once per day, over 5 days. FTR conditions were oxic for the first day, then anoxic for all proceeding days. All reservoirs were spiked with 60 µmol L^{-1} $^{15}NO_3^-$ two parallel treatments were used, each having 3 FTRs. These included a control seawater reservoir and one where the reservoir was spiked with metronidazole (115 µmol L^{-1}). Flow velocity was maintained at 0.87 mL min^{-1}.
4	11.08.16	To quantify production rates of methane under anoxic conditions.	DO, H_2 and CH_4.	Experiment extended over a 5 day period. DO and H_2 were sensed continuously throughout. Methane sampling occurred once per day. FTR conditions were oxic for the first day and anoxic for the remainder of the experiment. Reservoir was spiked with 50 µmol L^{-1} $^{15}NO_3^-$. Flow velocity was maintained at 1.6 mL min^{-1}.

4.3.2 FTR experiment sample analysis

4.3.2.1 Denitrification rates

Concentrations of ^{15}N-N_2 in FTR effluent were determined using headspace analysis on a Gas Chromatograph (He carrier) coupled to isotope ratio mass spectrometer (Sercon 20-22). The rates of denitrification reported throughout this chapter are total denitrification ($D_{14}+D_{15}$) and were calculated using the isotope pairing technique[26]. Samples from FTR experiments were transferred from glass syringes into 12 mL Exetainers (Labco, High Wycombe) and preserved with 250 μL of 50% w/v $ZnCl_2$.

4.3.2.2 Dissolved inorganic carbon

The concentration of dissolved inorganic carbon was evaluated using flow injection analysis, fitted with a photometric detector. This method involved acidifying FTR sample effluent so that any carbonate species would be converted to carbon dioxide, which, would then diffuse across a microporous membrane (Accurel® PP Q3/2 tubular membrane, ID 0.6 mm)[27]. The resulting change in pH causes the Bromothymol Blue indicator solution to produce a measurable colour change proportional to the quantity of diffused carbon dioxide. Samples for dissolved inorganic carbon were sampled into 3 mL Exetainers and preserved with 100 μL of 6% $HgCl_2$ before analysis using flow injection analysis[27] with a precision <1%.

4.3.2.3 Dissolved oxygen

Dissolved oxygen was continuously recorded during FTR experiments using Pyroscience Firesting flow through dissolved oxygen sensors. These flow through sensors were attached directly to the inlet and outlet ports of the FTRs.

4.3.2.4 Sulfide

A UV-Visible spectrophotometer (GBC) was used to determine sulfide concentrations in FTR effluent following the Fonselius[28] method. Effluent samples were filtered using

MicroAnalytix 0.2 μm cellulose-acetate filters and were preserved using 100 μL of Zn acetate per mL of sample.

4.3.2.5 Methane

FTR effluent samples for methane analysis were preserved using 100 μL 50% w/v $ZnCl_2$ and given a 4 mL He headspace. Methane concentration in samples was determined using a Varian 3700 Gas Chromatograph with a C-18 Poracil column equipped with a flame ionization detector.

4.3.2.6 Chlorophyll a analysis

Chlorophyll *a* content was analysed using a UV-Visible spectrophotometer (GBC), following a methanol extraction step[29].

4.3.2.7 Metabolome analysis

For metabolome analysis, cells were lysed and metabolites were extracted from FTR sediments using a methanol:chloroform mixture (1:2, v:v; -20C°) for 30 min under sonication. The metabolites in the supernatants were analysed by GC-QTOF-MS and LC-QTOF-MS (both Agilent Technologies) following Godzien, et al.[30] and Kind, et al.[31] with slight modifications.

4.3.2.8 Dissolved Hydrogen

Dissolved hydrogen analysis was performed using a calibrated Unisense H_2-100 sensor fitted with a glass flow through cell connected directly to the FTR outlet.

4.4 Results

4.4.1 Flow through reactor experiments

4.4.1.1 FTR experiment 1

There was no significant difference between the DIC production rates under each of the conditions studied (Figure 4.1) (ANOVA, single factor, $p > 0.05$) with the exception of anoxic regular seawater conditions that had been spiked with $HgCl_2$. Under these conditions, DIC production was markedly lower than at any other point during FTR experiment 1, with mean DIC production rates determined to be only 8 ± 11 nmol mL^{-1} hr^{-1}.
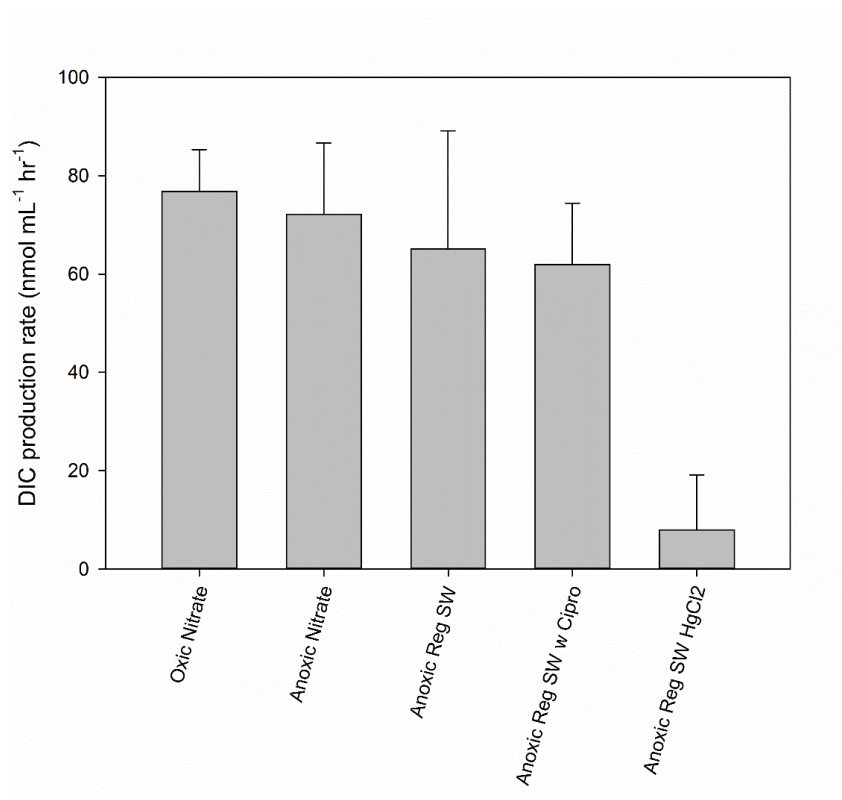
Figure 4.1: Mean rates of DIC production under various conditions from FTR experiment 1. 'Oxic Nitrate' and 'Anoxic Nitrate' conditions involved a reservoir concentration of 60 μmol L^{-1} $^{15}NO_3^-$. Reg SW conditions involved using freshly collected sample seawater with no added nitrate. $HgCl_2$ conditions included a reservoir concentration of 2.2 mmol L^{-1}. Error bars represent standard deviation in all instances.

The mean dissolved oxygen consumption rate was measured during the first 24 hours of the experiment and was 72 ± 6 nmol mL^{-1} hr^{-1}. This value was determined to have no significant difference compared to the DIC production rates observed under the various conditions

studied throughout the experiment (ANOVA, single factor, p>0.05), also with the exception of $HgCl_2$ spiked anoxic regular seawater conditions.

Under oxic, 60 µmol L^{-1} nitrate spiked reservoir conditions, no dissolved hydrogen production was observed (Figure 4.2a). It was only after approximately 48 hours of anoxic conditions that dissolved hydrogen production began, and production rates increased rapidly over a 90 hour period to reach a maximum of 26 nmol mL^{-1} hr^{-1}, which corresponded to an FTR effluent concentration of 34 µmol L^{-1}. Following the change of reservoir conditions from anoxic seawater to anoxic 60 µmol L^{-1} nitrate spiked seawater, dissolved hydrogen production rates declined sharply to only 5 nmol mL^{-1} hr^{-1}. Dissolved hydrogen production rates steadily rose to 13 nmol mL^{-1} hr^{-1} over a 12 hour period, following reservoir conditions being changed back to no added nitrate anoxic seawater (Figure 4.2b). This occurred despite the reservoir being spiked with a high concentration (150 µmol L^{-1}) of the broad spectrum antibiotic ciprofloxacin.

With the addition of $HgCl_2$ to the nitrate free reservoir at a concentration of 2.2 mmol L^{-1}, dissolved hydrogen dropped to zero within two residence times. Dissolved hydrogen production was not observed throughout the remainder of the experiment.

a)

Oxic

Anoxic

60 μM $^{15}NO_3^-$

No Added Nitrate in inlet reservoir

60 μM $^{15}NO_3^-$

y-axis: H$_2$ production rate (nmol mL^{-1} hr^{-1})

x-axis: Time (hrs)
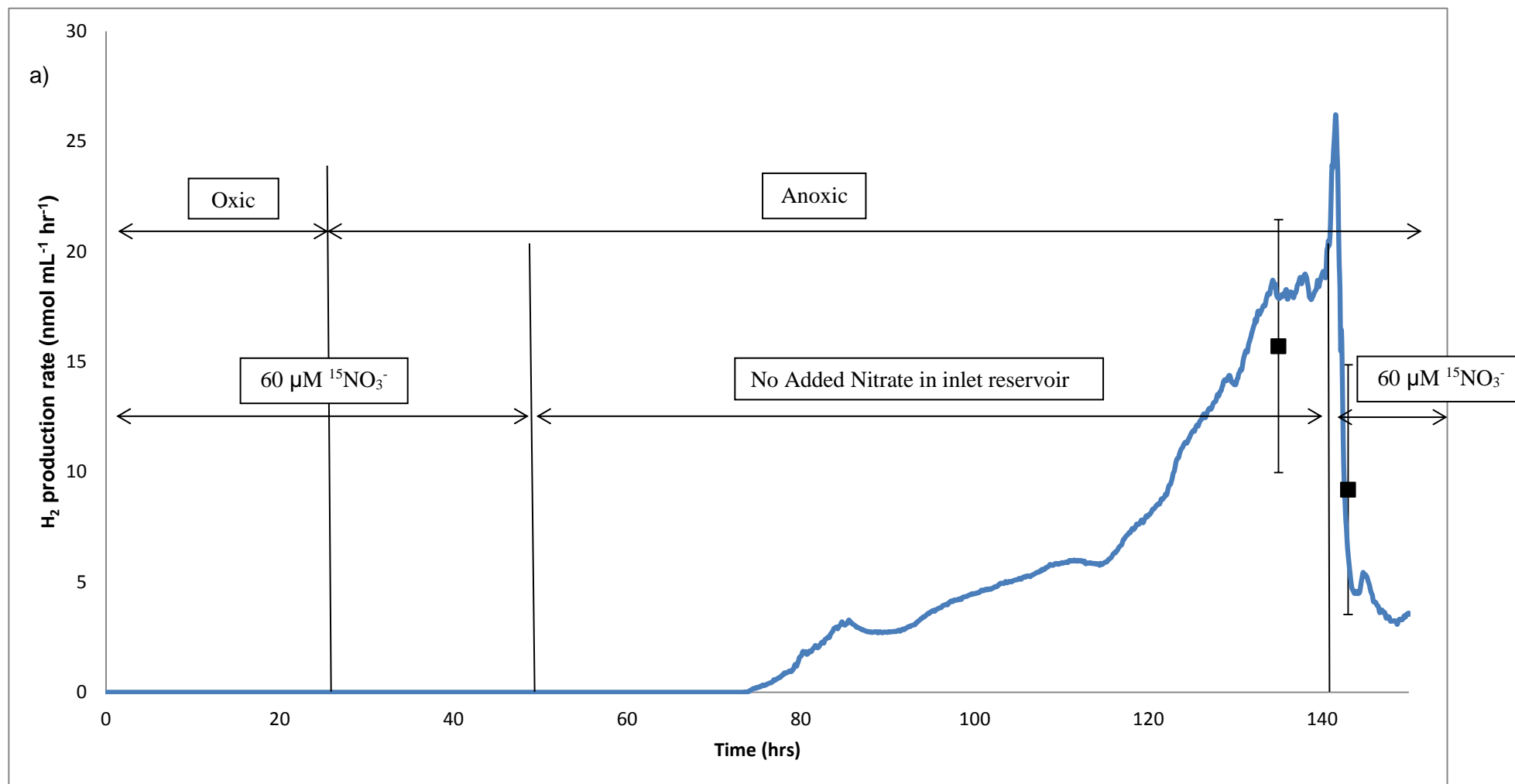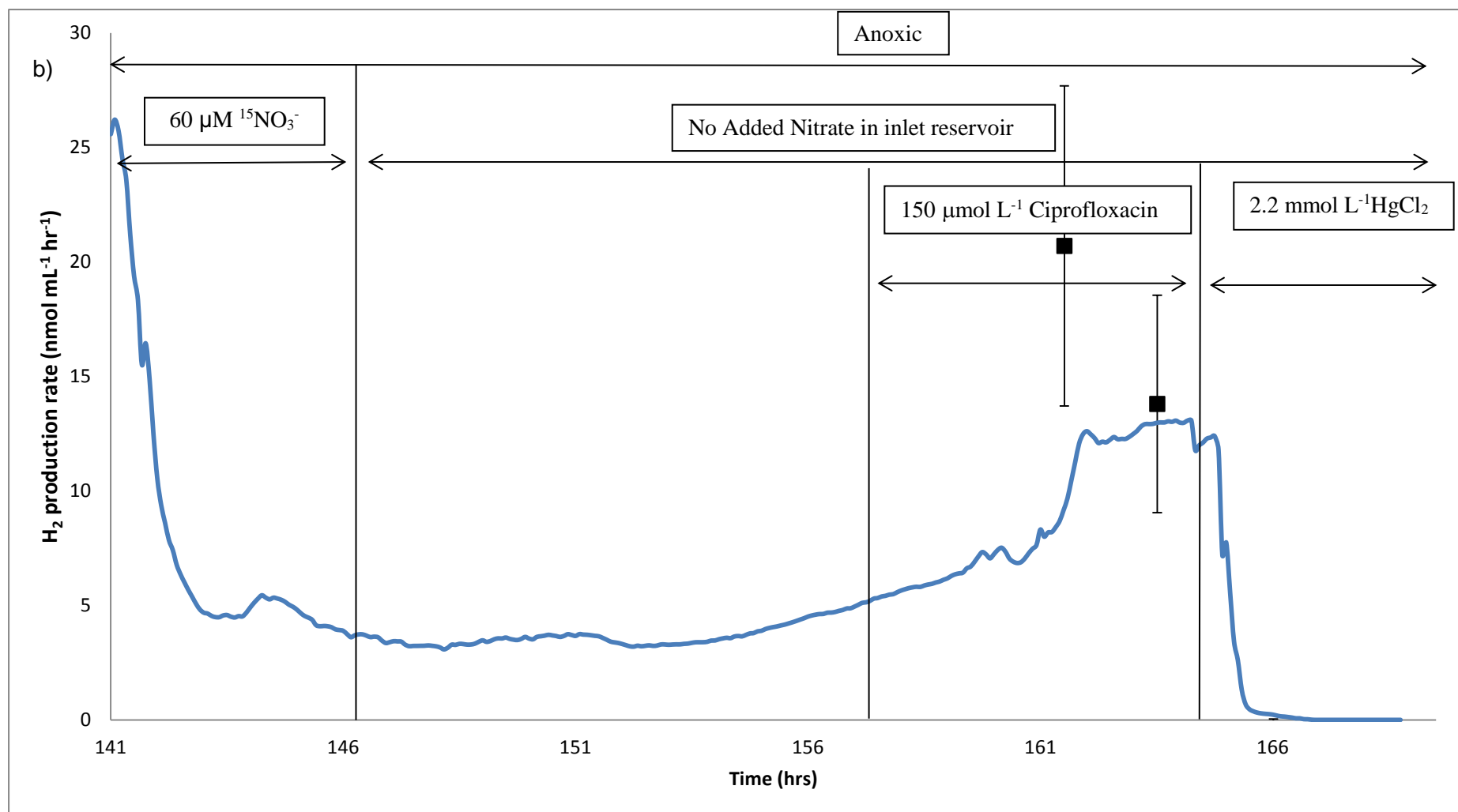
Figure 4.2a and b: Dissolved hydrogen production during FTR experiment 1. Blue line represents continuous measurement of dissolved H₂ from a single FTR. Reservoir conditions are outlined by the text boxes and the extending arrows. Black square data points represent mean dissolved hydrogen production rates across 3 FTRs. All error bars represent standard deviation.

4.4.1.2 FTR experiment 2

There was no significant difference in DIC production between mean oxic and anoxic conditions ($p = 0.76$) and in the presence or absence of nitrate (ANOVA, two factor with replication, $p = 0.44$) (Figure 4.3a). Mean dissolved oxygen consumption rates measured during the first 52 hours of the experiment was determined to be 47 ± 2 nmol mL^{-1} hr^{-1} and 46 ± 1 nmol mL^{-1} hr^{-1}, in control and added nitrate condition, respectively. These values were determined to have no significant difference compared to the oxic DIC production rates observed in their respective treatments (ANOVA, single factor, p>0.05).

Mean denitrification rates under anoxic conditions were determined to be 6 ± 5 nmol mL^{-1} hr^{-1} and 0.8 ± 0.6 nmol mL^{-1} hr^{-1} for added nitrate and control treatments, respectively. Mean sulfide production rates under anoxic conditions were determined to be 0.6 ± 1.2 nmol mL^{-1} hr^{-1} and 6 ± 9 nmol mL^{-1} hr^{-1} for added nitrate and control treatments, respectively. Combined rates of nitrate and sulfate reduction represented 12 and 13% of mean anoxic DIC production for added nitrate and control treatments, respectively.

Dissolved hydrogen production began ~36 hours after the commencement of anoxia (Figure 4.3b). Dissolved hydrogen concentrations in FTR effluent reached 44 ± 10 µmol L^{-1} and 23 ± 4 µmol L^{-1} in the presence and absence of nitrate, respectively. These values correspond to production rates of 26 ± 7 nmol mL^{-1} h^{-1} and 13 ± 2 nmol mL^{-1} h^{-1} whilst DIC production rates in these FTRs were 120 ± 46 nmol mL^{-1} h^{-1} and 80 ± 36 nmol mL^{-1} h^{-1}, respectively. Rates of dissolved hydrogen production in both treatments continued to increase despite the addition of the antibiotic ciprofloxacin at a concentration of 150 µmol L^{-1} (t=166). Rates of dissolved hydrogen production were consistently higher in the added nitrate treatment compared to the control.
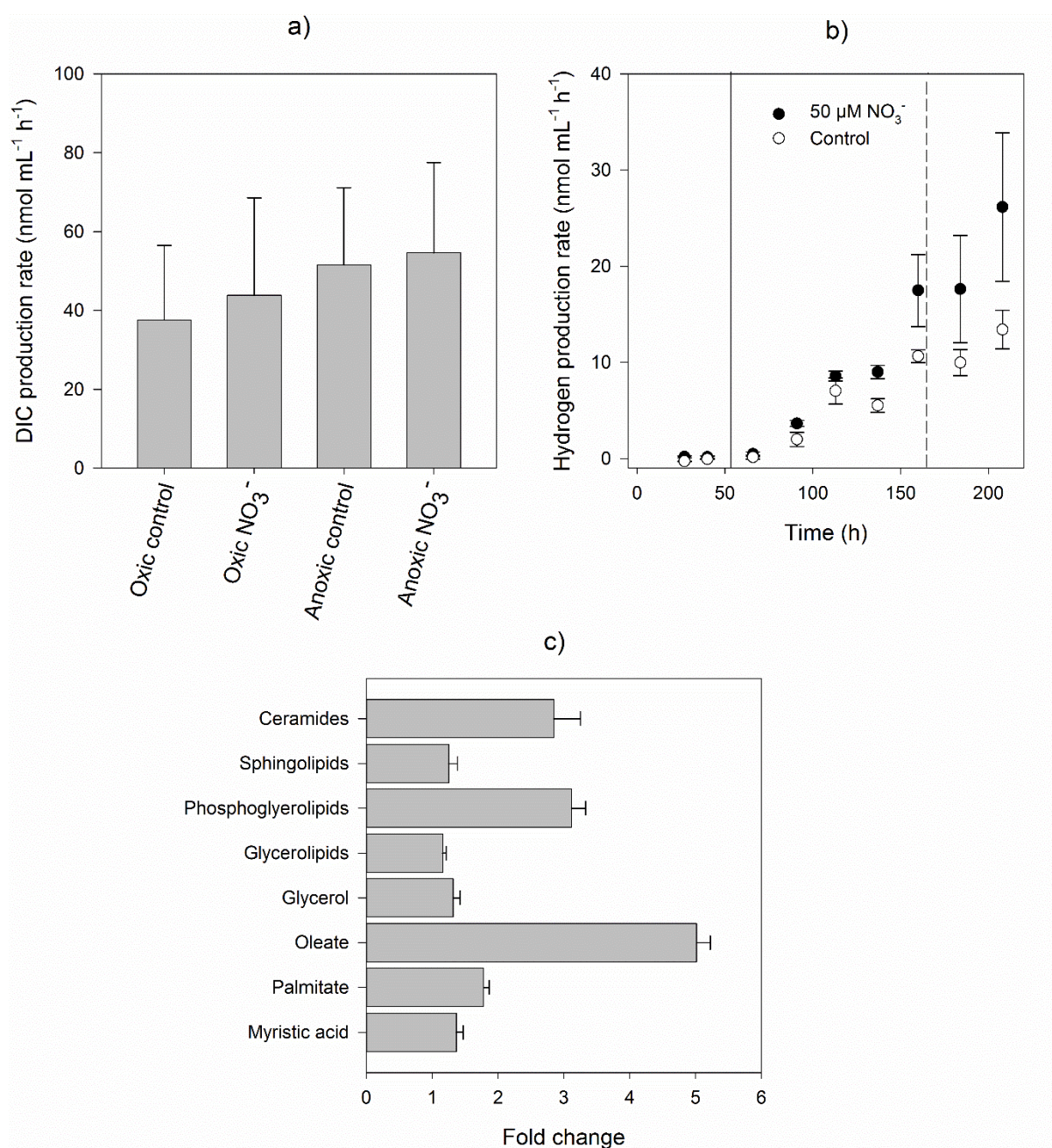
Figure 4.3: DIC, dissolved hydrogen and metabolome results from FTR experiment 2. (a) DIC production rates under oxic and anoxic conditions and in the presence and absence of nitrate. n=3 for each treatment. (b) H₂ production rate over time in the presence and absence of 50 μM NO₃⁻ . The solid line represents a change from oxic to anoxic conditions. The broken line represents addition of 150 μmol L⁻¹ ciprofloxacin. n=3 for both treatments. . (c) The relative concentration of fatty acid metabolites during anoxic hydrogen production compared to oxic conditions (n=3 for each treatment). All error bars are standard deviation.

Metabolomic analysis revealed large increases in the relative concentration of lipids when comparing oxic sediments with hydrogen producing anoxic sediments (Figure 4.3c). A 3 fold increase in phosphoglycerolipids and ceramides and a 5 fold increase in oleate was observed. Sediment from FTR experiments 2 and 3 were analyzed for chlorophyll a content, organic carbon content and organic carbon isotopic enrichment values. Scaling the sediment chlorophyll *a* content to total microalgae using a carbon to chlorophyll *a* ratio of 40^2 gives a sediment MPB carbon content of 850-860 µg/g of dry sediment, which comprises a total organic content of the sediment of 61 and 53% for FTR experiments 2 and 3, respectively (Table 4.2). Isotopic analysis of the organic carbon content present in sediment collected during FTR experiments 2 and 3, revealed $\delta^{13}C$ endpoints of -23.7 and -22.1‰.

Table 4.2: Organic carbon measurements from Port Phillip Bay sediments used in FTR experiments. A carbon to chlorophyll a ratio of 40 was assumed.

Experiment	Chl *a* (µg g^{-1} dry sediment)	Organic carbon estimate (µg g^{-1} dry sediment)	Total organic carbon (µg g^{-1} dry sediment)	Proportion of estimated vs total organic carbon
FTR experiment 2	21	860	1400	61
FTR experiment 3	21	850	1600	53

Cell counting revealed a diverse community of microalgae in sediment collected during FTR experiment 2. Diatoms were particularly abundant, exceeding 10^5 cells per mL, with species from the genus *Amphora*, *Cocconeis*, and *Fragilariopsis* most numerous (Table 4.3).

Table 4.3: Cell count and species identification from Port Phillip Bay sediment collected on 15/05/2015.

Algal taxa	Cell count (Cells mL^{-1})
Diatoms	
Amphora sp.	26000
Attheya decora	5000
Ceratoneis closterium	10000
Cocconeis spp.	19000
Entomoneis sp.	2000
Fragilaria sp.	1000
Fragilariopsis sp.	16000
Grammotophora marina	3000
Naviculoid spp.	9000
Nitzschia spp.	12000
Odontella aurita	2000
Pleurosigma sp.	2000
Dinoflagellates	
Gymnodinioid spp.	4000
Prorocentrum sp.	100
Chrysophytes	
Ochromonas spp.	12000
Chlorophyta	
Pyramimonas spp.	6000
Euglenophyta	
Eutreptiella spp.	100
Unidentified euglenoids	11000
Cyanobacteria	
Cf. Geitlerinema	12000
Cf. Nostoc	2000
Cf. Pseudanabaena	3000

		Relative proportion (%)
Diatoms	107000	68.1
Dinoflagellates	4100	2.6
Other flagellates	29100	18.5
Cyanobacteria	17000	10.8

4.4.1.3 FTR experiment 3

Mean dissolved oxygen consumption rates measured during the first 24 hours of the experiment were determined to be 139 ± 9 nmol mL^{-1} hr^{-1} and 134 ± 8 nmol mL^{-1} hr^{-1}, for control and metronidazole treatments, respectively. Rates of dissolved oxygen consumption approximately matched the rates of oxic DIC production for each treatment (Figure 4.4a), which had mean production rates of 170 ± 20 nmol mL^{-1} hr^{-1} and 140 ± 30 nmol mL^{-1} hr^{-1}, for control and metronidazole treatments, respectively.

For the control treatment, mean DIC production rates under oxic conditions approximately matched those under anoxic DIC conditions to the extent that no statistical difference was found (ANOVA, single factor, $p > 0.05$) (Figure 4.4a). However, the DIC production rate under anoxic conditions for the metronidazole treatment was significantly lower than the mean oxic DIC production in the same treatment (ANOVA, single factor < 0.05), with a difference in mean DIC production of 118 nmol mL^{-1} hr^{-1}.

Under oxic conditions, no dissolved hydrogen production was observed in either treatment. Dissolved hydrogen production began ~24 hours after the commencement of anoxia (Figure 4.4b) for the control treatment and reached a maximum production of 29 ± 2 nmol mL^{-1} h^{-1} (t=141), corresponding to a FTR outlet concentration of 23 ± 2 μmol L^{-1}. Dissolved hydrogen production was not observed at meaningful concentrations in the metronidazole treatment at any point during the experiment, with FTR effluent concentrations being < 0.2 umol L^{-1} for all sampling rounds.
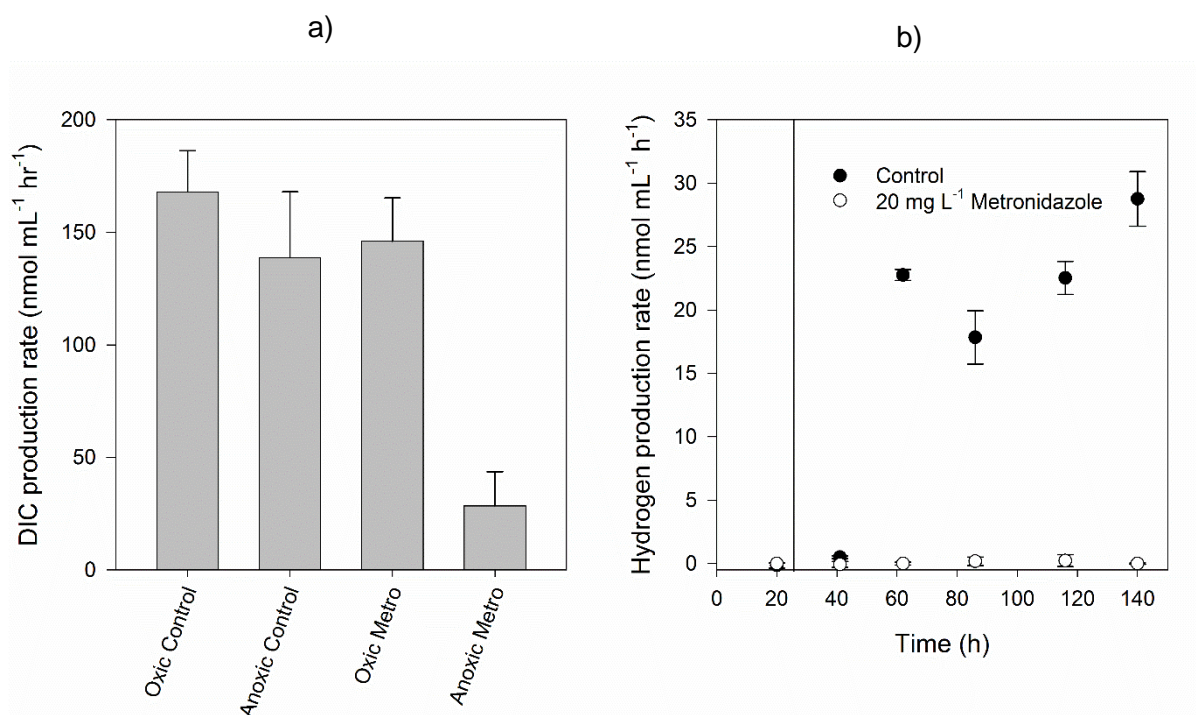
Figure 4.4a and b: DIC (a) and dissolved hydrogen production rates (b) from FTR experiment 3. Treatments included a control sample seawater reservoir treatment and a 115 μmol L^{-1} metronidazole seawater reservoir treatment. (a) DIC production rates under oxic and anoxic conditions and in the presence and absence of metronidazole. (b) H$_2$ production in seawater control and a metronidazole treatment over time. n=3 for both treatments. The solid line represents a change from oxic to anoxic conditions. All error bars are standard deviation.

4.4.1.4 Flow through reactor experiment 4

Mean dissolved oxygen consumption rate measured during the first 24 hours of the experiment was determined to be 112 ± 8 nmol mL^{-1} hr^{-1}. Under oxic conditions, no dissolved hydrogen production was observed. Dissolved hydrogen production began ~24 hours after the commencement of anoxia reaching a maximum of 19.00 ± 0.07 nmol mL^{-1} h^{-1}, corresponding to a FTR outlet concentration of 8.31 ± 0.03 μmol L^{-1} (t=70). No meaningful concentrations of methane were detected in FTR effluent at any stage of this experiment.

4.5 Discussion

4.5.1 FTR experiment 1 and dissolved hydrogen production

FTR experiment 1 revealed that molecular hydrogen (H_2) production began ~36 hours after the commencement of anoxia (Figure 4.2a). Substantial H_2 concentrations were observed in the presence and absence of nitrate, with concentrations almost an order of magnitude higher than previously reported maximum transient concentrations of H_2 by bacterial fermentation of 2 to 6 μmol L^{-1} [32,33]. There appeared to be a sharp decline in hydrogen production following the change from regular anoxic seawater reservoir to a spiked nitrate seawater reservoir (Figure 4.2a). However, this is likely due to the introduction of trace dissolved oxygen, which inhibits the hydrogenase enzyme[34]. The influence of nitrate on hydrogen production was further examined in FTR experiment 2 and will be discussed further later in this discussion.

The addition of the antibiotic ciprofloxacin at a concentration of 150 μmol L^{-1} to the reservoir appeared to have no effect on H_2 production (Figure 4.2b). Single species assays have shown ciprofloxacin to have an EC-50 value of between 15 and 51 nmol L^{-1} for typical gram positive bacteria [35,36], and 241 nmol L^{-1} for the gram negative bacteria of *Pseudomonas putida*[37]. The persistence of hydrogen production despite the presence of ciprofloxacin indicates that eukaryotic microorganisms are responsible for the observed hydrogen production.

Dissolved hydrogen production occurring exclusively under anoxic conditions is consistent with the well-established understanding that fermentation is strictly an anaerobic pathway.

Hydrogen production and DIC production decreased substantially following the introduction of $HgCl_2$ to the reservoir. At the concentrations administered, $HgCl_2$ serves as a chemical preservative and has very likely stopped all metabolism within the sediment, which further confirms hydrogen is being produced via a biologically mediated pathway.

4.5.2 Heterotrophic metabolism and hydrogen production dependence on nitrate

In FTR experiment 2, the rates of electron acceptor utilization indicated that denitrification and sulfate reduction were low when compared to DIC production. They were only able to account for less than 14% of DIC production in both control and added nitrate treatments. No meaningful concentrations of methane were detected in FTR experiment 4 and methanogenesis can be excluded as a potential contributor towards DIC production under anoxic conditions in permeable sediments. This large gap between the rate of DIC production and nitrate reduction is consistent with previous observations by Evrard *et al* 2013[24] and Marchant *et al* 2016[38], suggesting a common, although not ubiquitous[39], phenomenon.

As there was no significant difference in DIC production between oxic and anoxic conditions and in the presence or absence of nitrate (Figure 4.3b), this suggests that the organisms responsible for DIC production under oxic conditions were able to use an energy-conservation pathway to maintain their metabolism under anoxia, and that nitrate or sulfate reduction were not significantly contributing to this.

Consistent with this, cell counts revealed a diverse community of microalgae at the study site (Table 4.3). Diatoms were particularly abundant, exceeding 10^5 cells per mL, with species from the genus *Amphora*, *Cocconeis*, and *Fragilariopsis* most numerous. Scaling the sediment chlorophyll *a* content to total microalgae using a carbon to chlorophyll *a* ratio of 40^5 gives a sediment MPB carbon content of 850-860 µg/g of dry sediment (Table 4.2), which comprises approximately 57% of the total organic content of the sediment, highlighting the likely dominance of these organisms in DIC production.

A comparison of the production rates of hydrogen in this experiment showed that hydrogen was produced in both regular seawater and spiked nitrate seawater treatments. In fact, as Figure 4.3b shows, hydrogen production rates were consistently higher in the nitrate seawater treatment. One possible explanation is that the added nitrate might be stimulating cell growth amongst the eukaryotic microphytes that are most likely responsible for the H_2 production. Although the 9 day

experimental period would be ample time for the eukaryotic microphytes to multiply, this experiment was carried out under dark conditions, which would ordinarily limit cell growth[40]. The fate of the organic end products produced through dark fermentation was also investigated in FTR experiment 2. Metabolomic analyses of sediment collected from dark anoxic FTRs under H_2 production showed a 3 fold increase in phosphoglycerolipids and ceramides and a 5 fold increase in oleate (Figure 4.3c) as compared with oxic conditions. This is consistent with the synthesis of lipids from the fermentation product acetyl-CoA as previously documented for green algae[10]. Sediment isotopic analysis of organic matter revealed that the end member values were -23.7 and -22.1‰ for very FTR experiments 2 and 3, respectively. These are very close to the characteristic value of marine phytoplankton (-21.1‰)[41] and microphytobenthos (-15 to -16‰)[42] values. This indicates that it's highly likely that a high proportion of organic matter present in these sediments is produced by marine phytoplankton.

4.5.3 Eukaryotic dark fermentation pathways for hydrogen production

The most likely pathway to be responsible for the observed H_2 production is dark fermentative metabolism. The transfer of electrons from the reduced form of ferredoxin to hydrogenase, which is required for dark fermentation to proceed, can be effectively inhibited by low concentrations of metronidazole[22]. Consistent with this H_2 production pathway, it was observed that the administration of 115 µmol L^{-1} metronidazole effectively inhibited H_2 production compared to a control treatment (Figure 4.4b). This appears to be strong evidence supporting the notion that dark fermentation is a major metabolic pathway under anoxic conditions in permeable sediments and is likely the dominant process under these conditions (Figure 4.5).

Interestingly, DIC production stays relatively constant in the oxic and anoxic control treatment conditions and the oxic metronidazole treatment, but substantially declines in the anoxic metronidazole treatment (Figure 4.4a). This coincides with a stark difference in hydrogen production, where substantial hydrogen production occurred in the anoxic control treatment, whilst negligible hydrogen production occurred in the anoxic metronidazole treatment. The most likely explanation for this is that metronidazole molecules have successfully been preferentially reduced over hydrogenase enzymes, blocking the production of hydrogen. Furthermore, the superoxide radical produced when the reduced form of metronidazole reduces a diatomic oxygen molecule, has likely had a damaging impact on cell function and stunted microalgal respiration and therefore DIC production.
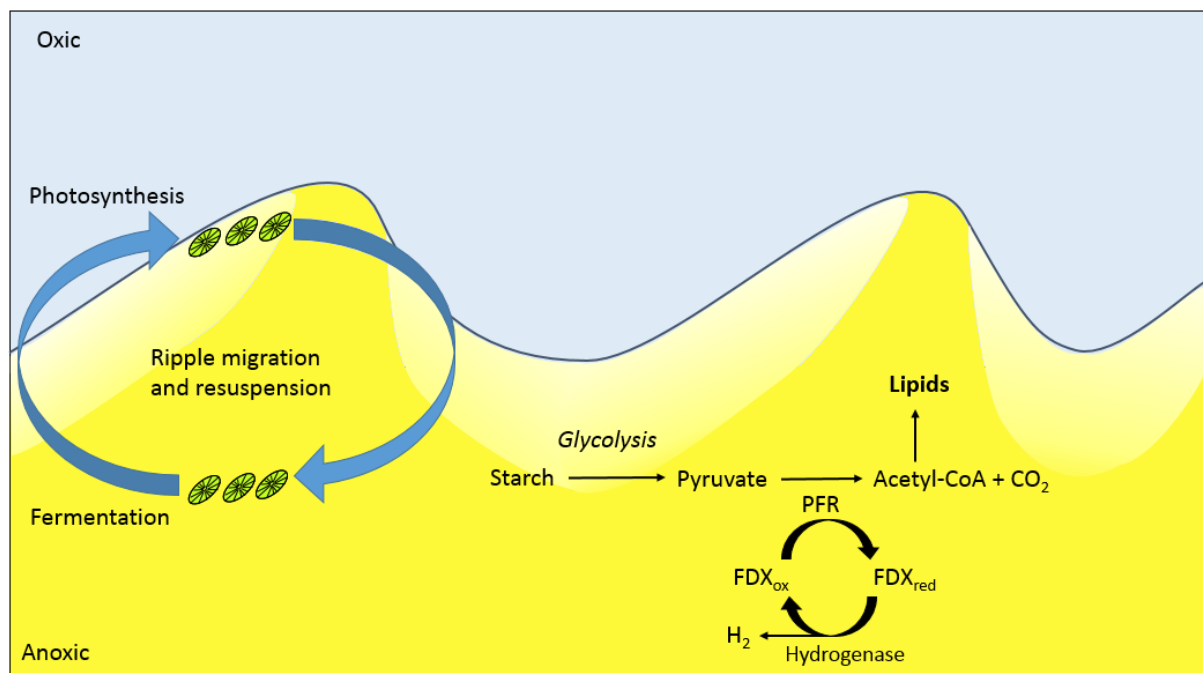
Figure 4.5: Conceptual model of benthic algal metabolism in permeable sediments. In this energetic environment, ripple migration and sediment resuspension regularly move algal cells many centimetres into the sediment where it is dark and anoxic. Under these conditions, microalgae undertake dark fermentation associated with high rates of hydrogen production[10]. Enzyme designations are pyruvate ferredoxin oxidoreductase (PFR) and ferredoxin (FDX). Lightly shaded areas represent declining oxygen concentration within the sediment. Yellow shaded area represents anoxic permeable sediment.

While hydrogen production has been identified as a key feature of dark fermentation, fermentation exists as a broad range of reactions and a variety of stoichiometries are likely being employed

simultaneously. Reactions 1 and 2, indicate possible stoichiometries for the breakdown of glucose to produce oleic acid and other fermentative products and are spontaneous under standard conditions. Under non-standard conditions, both reactions remain spontaneous regardless of high partial pressures of H_2 and CO_2 (0.8 atm), however, reaction 2 becomes most favourable at pCO_2 and $pH_2 < 0.3$ atm (Figure 4.6).

(1) $4.25\ C_6H_{12}O_6 \rightarrow C_{18}H_{34}O_2 + 7.5\ CO_2 + 8.5\ H_2O \quad \Delta G^o = -280\ kJ\ mol^{-1}$

(2) $5\ C_6H_{12}O_6 \rightarrow C_{18}H_{34}O_2 + 12\ CO_2 + 4\ H_2O + 9\ H_2 \quad \Delta G^o = -243\ kJ\ mol^{-1}$
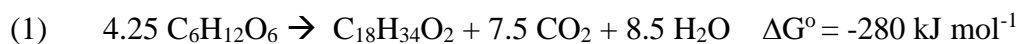
Using a combination of reactions 1 and 2, a wide range of $CO_2:H_2$ production stoichiometries are possible. Our results showed that H_2 was produced between 5-20% of the rate of DIC production, however, we note that the actual hydrogen production rate is most likely higher than this. By analogy with other sediment ecosystems, it is more likely that much of the H_2 produced is immediately recycled by respiratory hydrogenotrophic bacteria inhabiting the sediments[43]. Microbial ecology studies have shown that there is an abundance of both aerobic and anaerobic bacteria in these sediments[32,44,45] with phylotypes similar to known hydrogenotrophs[19,46]. If we assume that denitrification, which was the dominant electron sink, is driven by hydrogenotrophy, with a $2H_2:NO_3^-$ stoichiometry, then the total hydrogen production rates could be double the release measured here. It remains unclear why any release of hydrogen occurs at all given it is rapidly consumed by bacteria. In highly dynamic sand environments, bacterial biomass is likely unable to accumulate and therefore there is a lag time of days to weeks before their growth allows them to utilise hydrogen. In support of this hypothesis, we observe that sands become highly sulfidic ~1 week after collection from the field.
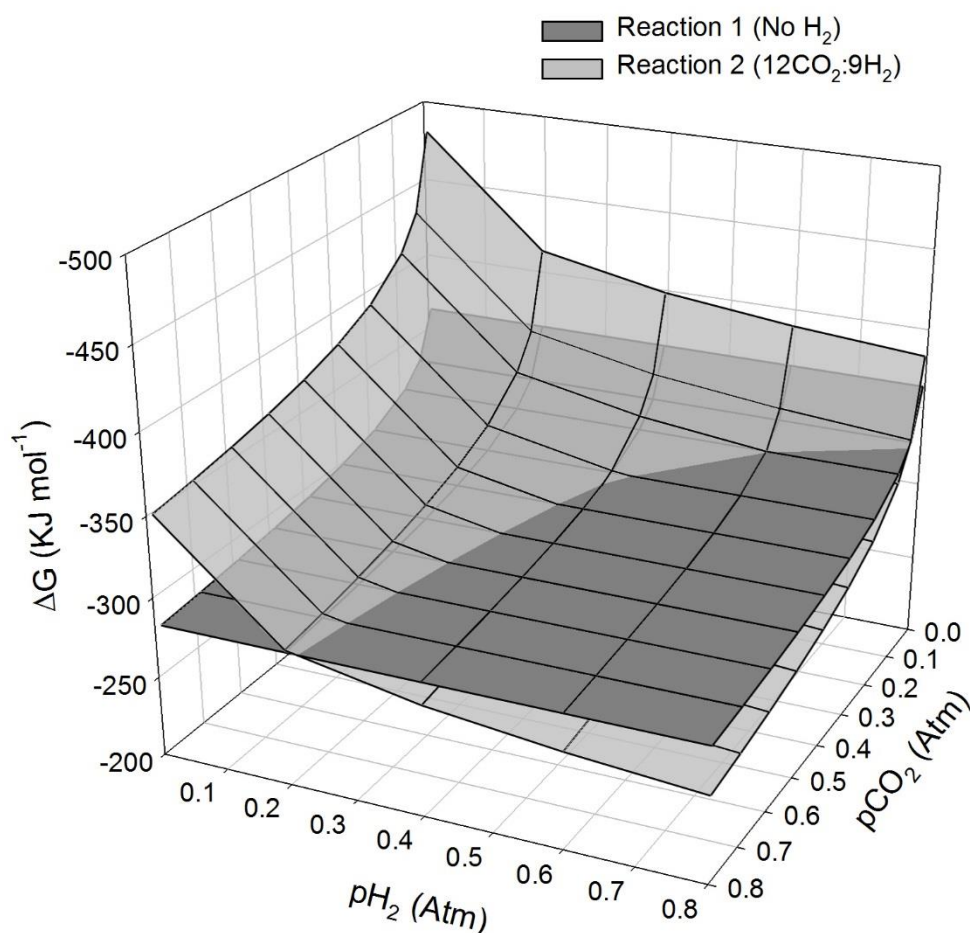
Figure 4.6: Change in Gibbs free energy under non-standard conditions for fermentation of glucose to lipid shown in reactions 1 and 2.

4.5.4 Delay period before observing dissolved hydrogen

Over the course of this investigation the length of time before hydrogen production was observed during anoxic FTR experiments varied from approximately 24 hours to 48 hours. The shortest period coincided with a change in experimental method, which involved swapping inlet FTR tubing to a reservoir that had already been purged with Ar for an extended period (24 hr), rather than purging an existing oxic reservoir to induce anoxic conditions. The key difference between the two approaches would likely result in the removal of trace dissolved oxygen, which as previously mentioned, serves as an inhibitor to the hydrogenase enzyme.

4.6 Conclusion

The results presented here challenge the conventional formulation of anoxic metabolic pathways using the redox cascade in high energy permeable sediments[47,48]. It has been demonstrated that dark fermentation, mediated by microalgae, may be the dominant metabolic pathway, resulting in hydrogen release and DIC production. Given that positive net benthic community production can occur over 33% of the coastal ocean[49], dark fermentation may be a globally important metabolic pathway. It is also plausible that the H_2 produced is recycled by aerobic and anaerobic respiratory bacteria, thereby shaping ecology and biogeochemistry within the temporally and spatially variable ecosystem of the permeable sediment.

4.7 References

1   MacIntyre, H. L., Geider, R. J. & Miller, D. C. Microphytobenthos: The ecological role of the "secret garden" of unvegetated, shallow-water marine habitats .1. Distribution, abundance and primary production. *Estuaries* **19**, 186-201, (1996).

2   Dejonge, V. N. Fluctuatiions in the organic carbon to chlorophyll alpha ratios for the estuarine benthic diatom populations. *Mar. Ecol. Prog. Ser.* **2**, 345-353, (1980).

3   Jahnke, R. A., Nelson, J. R., Marinelli, R. L. & Eckman, J. E. Benthic flux of biogenic elements on the Southeastern US continental shelf: influence of pore water advective transport and benthic microalgae. *Cont. Shelf Res.* **20**, 109-127, (2000).

4   Rusch, A., Forster, S. & Huettel, M. Bacteria, diatoms and detritus in an intertidal sandflat subject to advective transport across the water-sediment interface. *Biogeochemistry* **55**, 1-27, (2001).

5   Evrard, V., Cook, P. L. M., Veuger, B., Huettel, M. & Middelburg, J. J. Tracing carbon and nitrogen incorporation and pathways in the microbial community of a photic subtidal sand. *Aquat. Microb. Ecol.* **53**, 257-269, (2008).

6   Valdemarsen, T. & Kristensen, E. Degradation of dissolved organic monomers and short-chain fatty acids in sandy marine sediment by fermentation and sulfate reduction. *Geochim. Cosmochim. Acta* **74**, 1593-1605, (2010).

7   Boudreau, B. P. *et al.* Permeable marine sediments: Overturning an old paradigm. *EOS, Trans. Am. Geophys. Union* **82**, 133-136, (2001).

8   Veuger, B. & van Oevelen, D. Long-term pigment dynamics and diatom survival in dark sediment. *Limnol. Oceanogr.* **56**, 1065-1074, (2011).

9   Kamp, A., de Beer, D., Nitsch, J. L., Lavik, G. & Stief, P. Diatoms respire nitrate to survive dark and anoxic conditions. *Proc. Nat. Acad. Sci. USA* **108**, 5649-5654, (2011).

10   Catalanotti, C., Yang, W., Posewitz, M. C. & Grossman, A. R. Fermentation metabolism and its evolution in algae. *Front. Plant. Sci.* **4**, 150, (2013).

11   Zhang, L. P., Happe, T. & Melis, A. Biochemical and morphological characterization of sulfur-deprived and H-2-producing Chlamydomonas reinhardtii (green alga). *Planta* **214**, 552-561, (2002).

12   Atteia, A., van Lis, R., Tielens, A. G. M. & Martin, W. F. Anaerobic energy metabolism in unicellular photosynthetic eukaryotes. *Biochimica Et Biophysica Acta-Bioenergetics* **1827**, 210-223, (2013).

13   Ohta, S., Miyamoto, K. & Miura, Y. Hydrogen evolution as a consumption mode of reducing equivalents in green algal fermentation. *Plant Physiol.* **83**, 1022-1026, (1987).

14   Mus, F., Dubini, A., Seibert, M., Posewitz, M. C. & Grossman, A. R. Anaerobic acclimation in Chlamydomonas reinhardtii - Anoxic gene expression, hydrogenase induction, and metabolic pathways. *J. Biol. Chem.* **282**, 25475-25486, (2007).

15   Klein, U. & Betz, A. Fermentative metabolism of hydrogen evolving chlamydomonas moewusii. *Plant Physiol.* **61**, 953-956, (1978).

16   Meuser, J. E. *et al.* Phenotypic diversity of hydrogen production in chlorophycean algae reflects distinct anaerobic metabolisms. *J. Biotechnol.* **142**, 21-30, (2009).

17   Inui, H., Miyatake, K., Nakano, Y. & Kitaoka, S. Wax ester fermentation in euglena gracilis. *FEBS Lett.* **150**, 89-93, (1982).

18   Tucci, S., Vacula, R., Krajcovic, J., Proksch, P. & Martin, W. Variability of Wax Ester Fermentation in Natural and Bleached Euglena gracilis Strains in Response to Oxygen and the Elongase Inhibitor Flufenacet. *J. Eukaryot. Microbiol.* **57**, 63-69, (2010).

19   Greening, C. *et al.* Genomic and metagenomic surveys of hydrogenase distribution indicate H-2 is a widely utilised energy source for microbial growth and survival. *Isme Journal* **10**, 761-777, (2016).

20   Ghirardi, M. L. *et al.* Hydrogenases and hydrogen photoproduction in oxygenic photosynthetic organisms. *Annu. Rev. Plant Biol.* **58**, 71-91, (2007).

21   Dubini, A., Mus, F., Seibert, M., Grossman, A. R. & Posewitz, M. C. Flexibility in anaerobic metabolism as revealed in a mutant of chlamydomonas reinhardtii lacking hydrogenase activity. *J. Biol. Chem.* **284**, 7201-7213, (2009).

22   Lloyd, D. & Kristensen, B. Metronidazole inhibition of hydrogen production invivo in drug sensitive and resistant strains of trichomonas vaginalis. *J. Gen. Microboil.* **131**, 849-853, (1985).

23   Lau, A. H., Lam, N. P., Piscitelli, S. C., Wilkes, L. & Danziger, L. H. Clinical pharmacokinetics of metronidazole and other nitroimidazole antiinfectives. *Clinical Pharmacokinetics* **23**, 328-364, (1992).

24   Evrard, V., Glud, R. N. & Cook, P. L. M. The kinetics of denitrification in permeable sediments. *Biogeochemistry* **113**, 563-572, (2012).

25   Bourke, M. F. *et al.* Metabolism in anoxic permeable sediments is dominated by eukaryotic dark fermentation. *Nature Geoscience* **10**, 30-35, (2017).

26   Nielsen, L. P. Denitrification in sediment determined from nitrogen isotope pairing. *FEMS Microbiol. Ecol.* **86**, 357-362, (1992).

27   Oshima, M. *et al.* Highly sensitive determination method for total carbonate in water samples by flow injection analysis coupled with gas-diffusion separation. *Analyt. Sci.* **17**, 1285-1290, (2001).

28   Fonselius, S. H. in *Methods of seawater analysis* (ed K Grasshoff) 91-100 (Springer-Verlag Chemie, 2007).

29   Jeffrey, S. W. & Humphrey, G. F. New spectrophotometric equations for determining chlorophylls *a, b, c1* and *c2* in higher plants, algae and natural phytoplankton. *Biochem. Physiol. PFL.* **167**, 191-194, (1975).

30   Godzien, J. *et al.* In-vial dual extraction liquid chromatography coupled to mass spectrometry applied to streptozotocin-treated diabetic rats. Tips and pitfalls of the method. *J. Chromatogr.* **1304**, 52-60, (2013).

31   Kind, T. *et al.* FiehnLib: Mass Spectral and Retention Index Libraries for Metabolomics Based on Quadrupole and Time-of-Flight Gas Chromatography/Mass Spectrometry. *Anal. Chem* **81**, 10038-10048, (2009).

32   Hoehler, T. M., Albert, D. B., Alperin, M. J. & Martens, C. S. Acetogenesis from CO_2 in an anoxic marine sediment. *Limnol. Oceanogr.* **44**, 662-667, (1999).

33   Finke, N. & Jorgensen, B. B. Response of fermentation and sulfate reduction to experimental temperature changes in temperate and Arctic marine sediments. *Isme Journal* **2**, 815-829, (2008).

34   Benemann, J. R., Berenson, J. A., Kaplan, N. O. & Kamen, M. D. Hydrogen evolution by a chloroplast ferredoxin hydrogenase system. *Proc. Nat. Acad. Sci. USA* **70**, 2317-2320, (1973).

35   Halling-Sorensen, B., Lutzhoft, H. C. H., Andersen, H. R. & Ingerslev, F. Environmental risk assessment of antibiotics: comparison of mecillinam, trimethoprim and ciprofloxacin. *J. Antimicrob. Chemother.* **46**, 53-58, (2000).

36   Robinson, A. A., Belden, J. B. & Lydy, M. J. Toxicity of fluoroquinolone antibiotics to aquatic organisms. *Environ. Toxicol. Chem.* **24**, 423-430, (2005).

37   Kummerer, K., Al-Ahmad, A. & Mersch-Sundermann, V. Biodegradability of some antibiotics, elimination of the genotoxicity and affection of wastewater bacteria in a simple test. *Chemosphere* **40**, 701-710, (2000).

38   Marchant, H. K. *et al.* Coupled nitrification-denitrification leads to extensive N loss in subtidal permeable sediments. *Limnol. Oceanogr.* **61**, 1033-1048, (2016).

39   Pallud, C., Meile, C., Laverman, A. M., Abell, J. & Van Cappellen, P. The use of flow-through sediment reactors in biogeochemical kinetics: Methodology and examples of applications. *Mar. Chem.* **106**, 256-271, (2007).

40   Fernie, A. R., Obata, T., Allen, A. E., Araujo, W. L. & Bowler, C. Leveraging metabolomics for functional investigations in sequenced marine diatoms. *Trends Plant Sci.* **17**, 395-403, (2012).

41   Currin, C. A., Newell, S. Y. & Paerl, H. W. The role of standing dead spartina alterniflore and benthic microalgae in salt marsh food webs. Considerations based on multiple stable isotope analysis. *Mar. Ecol. Prog. Ser.* **121**, 99-116, (1995).

42   Middelburg, J. J. *et al.* The fate of intertidal microphytobenthos carbon: An in situ C-13-labeling study. *Limnol. Oceanogr.* **45**, 1224-1234, (2000).

43   Schwartz, E., Fritsch, J. & Friedrich, B. in *The Prokaryotes: Prokaryotic Physiology and Biochemistry* (eds Eugene Rosenberg *et al.*) 119-199 (Springer Berlin Heidelberg, 2013).

44   Cosgrove, J. & Borowitzka, M. A. *Chlorophyll Fluorescence Terminology: An Introduction.* Vol. 4 (Springer, 2010).

45   Tomas, C. R. *Identifying marine phytoplankton*. (1997).

46   Hirst, A. D. & Goldberg, D. M. Application of new ultra-micro spectrophotometric determination for serum hydroxybutyrate dehydrogenase activity to diagnosis of myocardial infarction. *Brit. Heart. J.* **32**, 114-&, (1970).

47   Canfield, D. E. *et al.* Pathways of organic carbon oxidation in 3 continental margin sediments. *Mar. Geol.* **113**, 27-40, (1993).

48   Canfield, D. E., Thamdrup, B. & Hansen, J. W. The anaerobic degradation of organic matter in danish coastal sediments- iron reduction, manganese reduction and sulfate reduction. *Geochim. Cosmochim. Acta* **57**, 3867-3883, (1993).

49   Gattuso, J. P. *et al.* Light availability in the coastal ocean: impact on the distribution of benthic photosynthetic organisms and their contribution to primary production. *Biogeosciences* **3**, 489-513, (2006).

Chapter 5: Hydrogen production in dark anoxic microalgal culture incubations

5.1 Abstract

Dissolved hydrogen production in anoxic permeable sediments was previously thought to occur primarily through the fermentation of organic polymers during carbon mineralization. However, recent findings have indicated that far higher rates of hydrogen production may be occurring in dark anoxic permeable sediment via eukaryotic dark fermentation. The capability of marine eukaryotic microalgae was therefore examined during a series of axenic culture incubation experiments. Hydrogen production was observed in all five distinct diatoms cultures (*Fragilariopsis* sp.) and the chlorophyte (*Pyramimonas*) culture, under dark anoxic conditions. The addition of acetate to microalgal cultures appeared to have no effect on dissolved hydrogen production. In microalgal experiments, hydrogen concentration would reach its maximum within 24 hours of incubation then gradually decline, indicating that a hydrogen consumption process may be occurring. These findings indicate that microalgal hydrogen production via dark fermentation could be an important energy conserving pathway in permeable sediments and further supporting the hypothesis outlined in prior research that marine eukaryotic microalgae are capable of hydrogen production.

5.2 Introduction

In marine systems, dissolved hydrogen production may be produced via several biologically mediated pathways, including heterotrophic fermentation during organic carbon mineralization, photobiological synthesis and dark fermentation[1]. Hydrogen production via heterotrophic fermentation is typically performed by a mutualistic consortia of prokaryotic microorganisms during anaerobic organic carbon mineralization[2]. These microorganisms employ hydrolytic and fermentative reactions to gradually break down large particulate organic polymers[3]. Fermentation reactions include a highly diverse group of pathways that each involve organic carbon simultaneously undergoing oxidation and reduction[4] and in addition to dissolved hydrogen, common products include volatile fatty acids, short chain alcohols and CO_2[2,5]. The products of these fermentative reactions are generally considered not to accumulate in sediments, as these reactions are thought to be closely coupled to terminal heterotrophic reactions[2,6-8], such as denitrification or sulfate reduction.

Hydrogen production via photobiological synthesis and dark fermentation are both performed by eukaryotic microalgae, such as green algae and diatoms, but differ greatly in the environmental conditions required for each to occur. In photobiological hydrogen synthesis, light-excited electrons derived from water (in direct biophotolysis) or organic compounds (in indirect biophotolysis) are transferred to ferredoxin and then [FeFe]-hydrogenase resulting in H_2 production[9,10]. As this pathway requires illumination, photosynthesis is likely to occur and the oxygen produced effectively inhibits hydrogenase[11], halting hydrogen synthesis. Interestingly, sustained hydrogen production will occur if rates of oxygen consumption via cellular respiration exceed the rate of photosynthetically derived oxygen generation[12,13].

By contrast, hydrogen production via dark fermentation occurs in dark, anoxic permeable sediment whereby eukaryotic microorganisms are unable to photosynthesize and must instead ferment intracellularly stored starch as a means of sustaining cell function[14]. While there very

likely exists a variety of dark fermentative pathways, generally, the glycolytic breakdown of starch produces pyruvate, which is then oxidised to acetyl-CoA by pyruvate ferredoxin oxidoreductase (PFR), resulting in carbon dioxide generation[1,4]. Electron transport proceeds via PFR to ferredoxin to hydrogenase, which results in hydrogen production[15]. Acetyl-CoA may then be converted to stored lipids[16] and reoxidised upon return to oxic conditions.

During flow through reaction (FTR) experiments presented in chapter 4, anoxic dissolved inorganic carbon (DIC) production was consistently accompanied by high production rates of dissolved hydrogen as well as a substantial accumulation of lipids in the sediment metabolome. Furthermore, broad spectrum antibiotic treatments revealed that hydrogen production persisted, while other bacterially mediated processes were inhibited, indicating that eukaryotic microorganisms were likely responsible for this process. Hydrogen production was successfully inhibited during a FTR experiment treatment employing metronidazole, which effectively inhibits the ferredoxin-hydrogenase hydrogen production pathway. These findings are each highly consistent with dark fermentation, indicating the observed hydrogen production was very likely produced via eukaryotic dark fermentation. However, to further support this hypothesis, the capability of sediment eukaryotic microorganisms to produce hydrogen under dark anoxic conditions must be confirmed. Therefore, the primary hypothesis of this research chapter is that axenic eukaryotic microalgal cultures, such as diatoms and chlorophytes, will produce hydrogen when incubated under dark anoxic conditions.

The key research questions addressed in this chapter will be:

1) Under dark, anoxic incubations, do diatom and green alga cultures produce hydrogen?

2) Does the addition of an added source of organic carbon, in the form of acetate, affect rates of the production of hydrogen?

5.3 Methods

5.3.1 Microalgal culture experiments

A total of six microalgal cultures were isolated from sediment collected from Elwood Beach in Port Phillip Bay, Victoria, Australia (37°53'23.156"S, 144°59'1.869"E) and grown in F/2 medium under continuous illumination at 60 μmol photons m^{-2} s^{-1}. Algal cultures were stored at a constant temperature of 18 °C in a temperature controlled room and continuously resuspended using either a shaker table or magnetic stirring apparatus. These included five diatom species (all *Fragilariopsis* sp.) and a chlorophyte (*Pyramimonas* sp.).

Five microalgal culture experiments were performed (Table 5.1) with the overarching goals of confirming that these cultures were capable of dissolved hydrogen production, identifying what maximum dissolved hydrogen concentrations could be observed and whether the presence of organic carbon in the form of acetate, could augment rates of dissolved hydrogen production.

For microalgal counts, sediment and culture samples were preserved with Lugols iodine solution and identified and quantified at MicroAlgal Services, Ormond, Victoria, Australia. This was achieved using a Zeiss standard compound microscope equipped with phase contrast optics with up to 400x magnification used in a Sedgewick-Rafter counting chamber. The identification of microphytobenthos present in the sediment samples was carried out using reference material from Tomas [17].

Prior to incubation experiments, microalgal cultures were treated with antibiotics so as to ensure no bacterial growth occurred. In culture experiment 1, amoxicillin was used at a concentration of 20 mg L^{-1}, however, in all subsequent culture incubation experiments, this was changed to a dilute antibiotic cocktail containing ampicillin, streptomycin and tetracycline with final concentrations of 40, 20 and 8 mg L^{-1}, respectively. This change was

implemented as the dilute antibiotic cocktail would be effective against a broader range of bacteria.

Culture incubation conditions varied throughout experiments 1-5 (Table 5.1). Such conditions included the use of a shaker table, incubation temperature and the inclusion of a preconcentration step. These changes were implemented in an ongoing effort to improve microalgal culture health, as revealed by quantum yield analysis. During incubation experiments, the storage of cultures was gradually changed from glass exetainers with rubber septums to glass gas tight vials. This was done so as to minimise hydrogen loss via diffusion through the exetainer rubber septum.

Table 5.1: Summary of microalgal culture experiments.

Culture Experiment	Date	Purpose	Incubation and storage conditions	Parameters measured	Experimental Summary
1	23.11.15	To examine whether cultures would produce dissolved hydrogen when incubated anoxically.	Incubated in 6 mL gastight exetainers with rubber septums. Stored in dark, anoxic conditions at room temperature (between 20-25 °C). Broad spectrum antibiotic amoxicillin added at 20 mg L^{-1}	DO, H_2.	Microalgal cultures samples were divided across four exetainers each. One exetainer from each culture was measured for dissolved hydrogen each day, for four days.
2	04.01.16	To examine whether the presence of acetate would affect the production of dissolved hydrogen by microalgal cultures.	Incubated in 3 mL gastight exetainers with rubber septums. Stored in dark, anoxic conditions at room temperature (between 20-25 °C). Dilute antibiotic cocktail added.	DO, H_2, QY.	Microalgal cultures samples were concentrated by a factor of 10 using a centrifuge, separated into two treatments: a control treatment and one spiked to have a 100 μmol L^{-1} acetate concentration. Anoxic cultures were divided across seven exetainers each and one exetainer from each culture was measured for dissolved hydrogen each day, for seven days. Culture QY measured once after 3 days of incubation.
3	15.01.16	A validation experiment to examine whether dark conditions or the dilute antibiotic cocktail were responsible for poor culture health.	Cultures stored in 50 mL transparent plastic containers. Stored in 18 degree refrigerated room on shaker table. Light and dark conditions depending on treatment.	QY.	Anoxic cultures were divided into four treatments: light conditions with and without the dilute antibiotic cocktail and dark conditions with and without the dilute antibiotic cocktail. QY measured over a 7 day period.
4	07.02.16	To examine whether the presence of acetate would affect the production of dissolved hydrogen by microalgal cultures.	Cultures incubated in 8 mL gastight glass vials. Stored in dark, anoxic conditions, at room temperature (between 20-25 °C).	DO, H_2, QY.	Anoxic microalgal cultures samples were separated into two treatments: a control treatment and one spiked to have a 100 μmol L^{-1} acetate concentration. Cultures were divided across seven glass vials per culture with one vial being sensed for dissolved hydrogen each day, for only two days. Separate anoxic culture samples were also incubated under dark conditions and measured for QY daily.
5	01.06.16	To examine whether hydrogen production would persist throughout experiment.	Cultures incubated in 8 mL gastight glass vials. Stored in dark, anoxic conditions in 18 degree refrigerated room on shaker table. Cultures continuously agitated using glass beads and shaker table.	DO, H_2 and QY	Anoxic microalgal cultures samples were divided across seven glass vials, with one vial being sensed for dissolved hydrogen each day, for seven days. Separate anoxic culture samples were also incubated under dark conditions and measured for QY daily.

5.3.1.1 Dissolved oxygen

The rate of dissolved oxygen consumption by the microalgal cultures were determined using Pyroscience Firesting retractable oxygen microsensors. Cultures were enclosed in 3 mL glass exetainers with rubber septums at 100% dissolved oxygen saturation and declining oxygen concentration was measured over time. Consumption rates were determined by taking the gradient of the linear regression plot of dissolved oxygen vs time.

5.3.1.2 Dissolved hydrogen

Dissolved H_2 analyses were performed using a calibrated Unisense H_2-100 sensor fitted with a glass flow through cell. Incubated cultures were drawn slowly through this flow through cell using a glass syringe.

5.3.1.3 Quantum yield

Cultures were analyzed for the quantum yield (QY) of photosystem II, which is a relative measure of electron transport rates through that photosystem and is widely considered to be a key metric of microalgal health or degree of stress[18]. Quantum yield was measured by storing the cultures in dark conditions for approximately 15 minutes and measuring QY using a Walz PhytoPAM fluorometer. Quantum yield values of between 0.5-0.6 are indicative of acceptable algal health for diatoms and chlorophytes[19-21].

5.4 Results

5.4.1 Culture experiments

5.4.1.1 Culture experiment 1

Dissolved hydrogen was detected in all five diatom cultures and also in the single chlorophyte culture. Hydrogen was produced resulting in a mean maximum concentration of 0.8 ± 0.5 μmol L^{-1} after 118 hours of anoxic incubation (Figure 5.1). Dissolved oxygen consumption rate was determined to be approximately 2.1 μmol hr^{-1}.
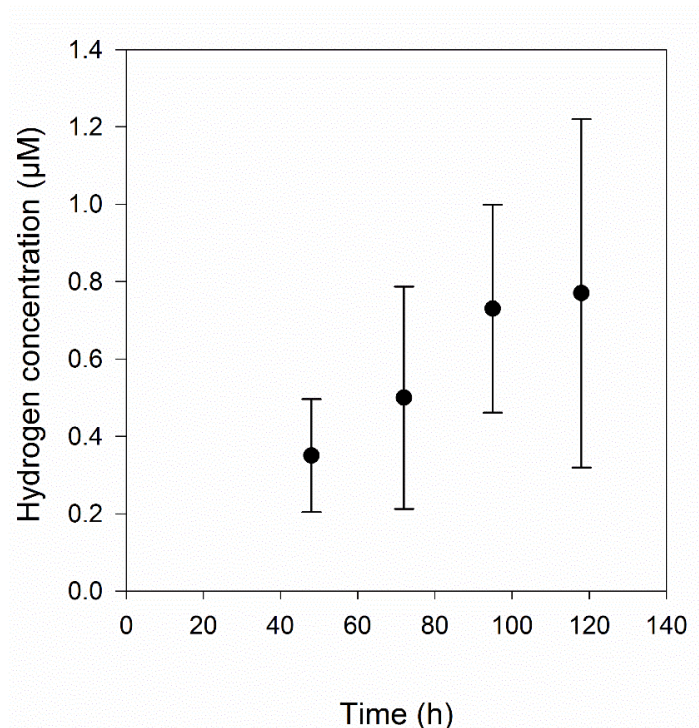
Figure 5.1: Dissolved hydrogen concentrations over time in culture experiment 1. Storage and incubation conditions outlined in table 5.1 (n=6). All error bars represent standard deviation.

5.4.1.2 Culture experiment 2

Dissolved hydrogen was detected in all microalgal cultures throughout this experiment, in both treatments. Dissolved hydrogen reached the maximum observed concentrations, for both treatments, only 18 hours into anoxic incubation at the first sampling round, which corresponded to 0.9 ± 0.3 and 0.8 ± 0.2 μmol L^{-1} for control and added acetate treatments, respectively (Figure 5.2). Dissolved hydrogen concentrations declined sharply in the 19 hours between the first and second

sampling rounds, and continued to decline throughout the experiment. Minimum dissolved

hydrogen concentrations for both treatments were observed in the final sampling round of the

experiment (t=129 hr), with concentrations falling below the 0.1 umol L^{-1} detection limit of the

dissolved hydrogen sensor, with concentrations of 0.05 ± 0.02 and 0.03 ± 0.03 µmol L^{-1}, for control

and added acetate treatments, respectively. Dissolved hydrogen concentrations were not

consistently higher in either control or added acetate treatments. Dissolved oxygen consumption

rate were determined to be approximately 6.19 µmol hr^{-1} and 6.02 µmol hr^{-1}, for control and added

acetate treatments, respectively. Quantum yield analysis revealed values of $0.09 \pm .06$ and $0.04 \pm$

0.05, for control and added acetate cultures, respectively.
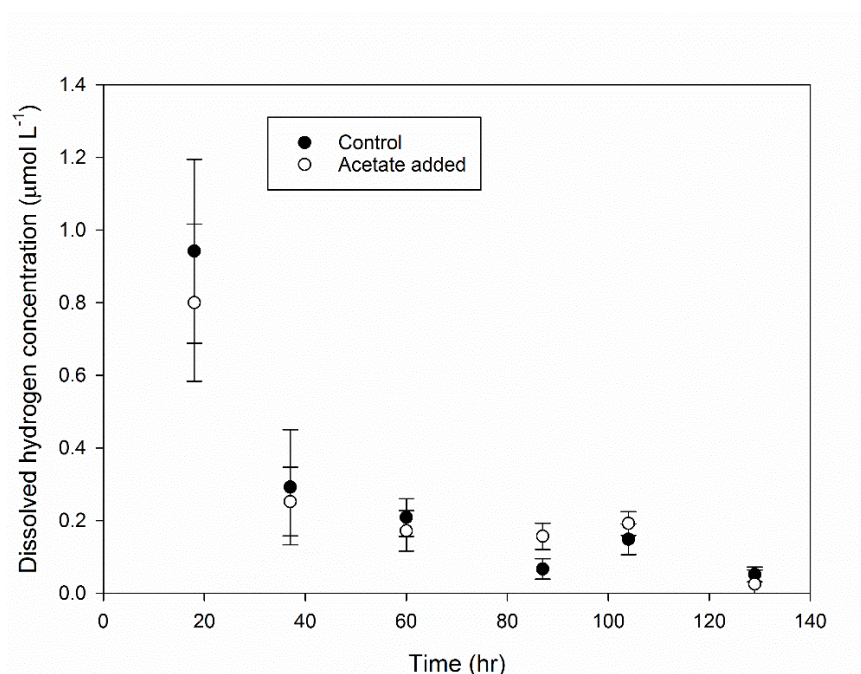
Figure 5.2: Dissolved hydrogen concentrations over time in culture experiment 2 for a control treatment and an added acetate treatment (100 µmol L^{-1}). Storage and incubation conditions outlined in table 5.1. All error bars represent standard deviation.

5.4.1.3 Culture experiment 3

Mean quantum yield values throughout each of the four treatments fell between 0.34- 0.39 at the

commencement of this experiment (Figure 5.3). These values remained relatively stable over the

145 hour incubation, with mean QY values dropping to between 0.3-0.38. No substantial

differences in mean QY values were observed between any of the treatments.
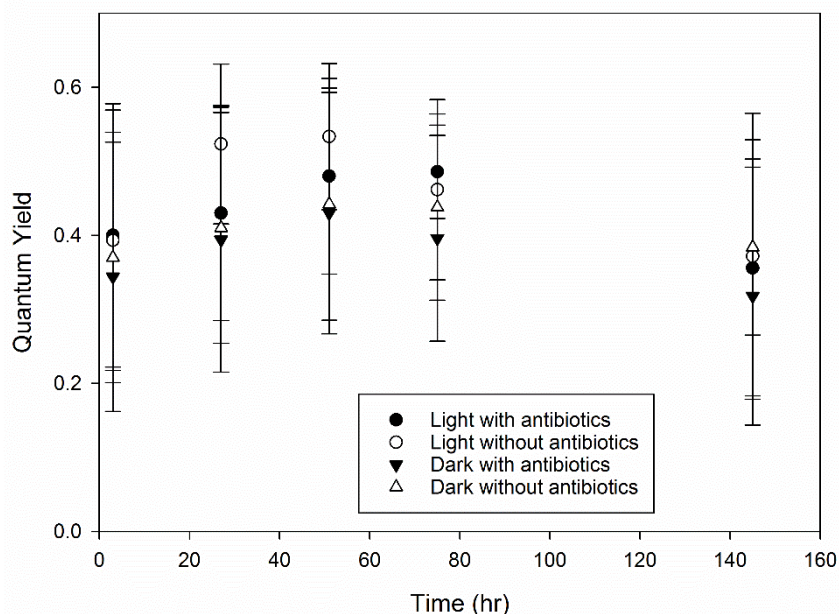
Figure 5.3: Quantum yield results over time in culture experiment 3. Four treatments were incubated under light and dark conditions and with and without a dilute antibiotic cocktail added. Storage and incubation conditions outlined in table 5.1. All error bars represent standard deviation.

5.4.1.4 Culture experiment 4

Dissolved hydrogen was detected in all microalgal cultures throughout this experiment, in both

control and added acetate treatments. Dissolved hydrogen reached the maximum observed

concentrations, for both treatments, only 6 hours into anoxic incubation at the first sampling round,

which corresponded to 0.6 ± 0.2 and 0.4 ± 0.1 μmol L^{-1} for control and added acetate treatments,

respectively (Figure 5.4a). Dissolved hydrogen concentrations declined sharply in the following 22

hours. Minimum dissolved hydrogen concentrations for both treatments were observed in the

second and final sampling round of the experiment (t=28 hr), with concentrations of 0.2 ± 0.1 and

0.2 ± 0.1 μmol L^{-1}, for control and added acetate treatments, respectively. Dissolved hydrogen

concentrations were not consistently higher in either control or added acetate treatments. Dissolved

oxygen consumption rate was determined to be approximately 17.7 μmol hr^{-1} and 16.5 μmol hr^{-1} for

control and added acetate treatments, respectively. Quantum yield analysis revealed values

remained largely unchanged throughout the experiment (Figure 5.4b).
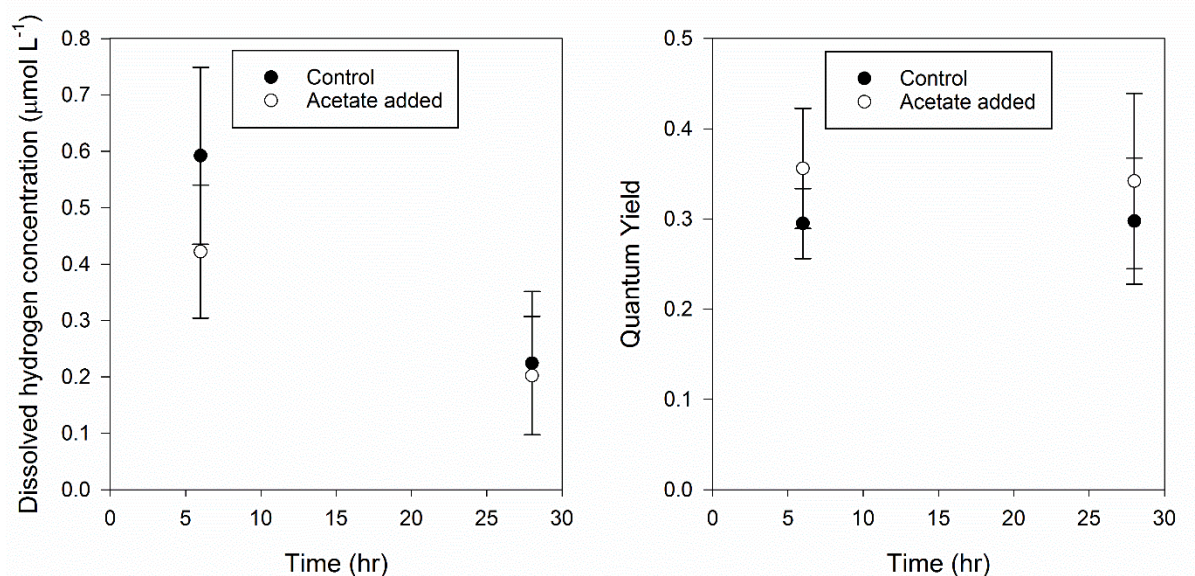
Figure 5.4a and b: Dissolved hydrogen (a) and quantum yield (b) results over time in culture experiment 4 in control and added acetate treatments (100 μmol L^{-1}). Storage and incubation conditions outlined in table x. All error bars represent standard deviation

5.4.1.5 Culture experiment 5

Dissolved hydrogen was detected in all microalgal cultures throughout this experiment. Dissolved

hydrogen reached the maximum observed concentrations, only 10 hours into anoxic incubation at

the first sampling round, which corresponded to 1.4 ± 0.6 μmol L^{-1} (Figure 5.5a). Dissolved

hydrogen concentrations declined gradually throughout the remainder of the experiment. Minimum

mean dissolved hydrogen concentration was observed in the final sampling round of the experiment

(t=144 hr), with a mean concentration of 0.7 ± 0.6 μmol L^{-1}. Dissolved oxygen consumption rate

was determined to be approximately 6.4 μmol hr^{-1}. Quantum yield analysis revealed quotients

remained largely unchanged throughout the experiment. Mean QY of cultures dropped from $0.4 \pm$

0.1 to 0.4 ± 0.1 from the first and last sampling rounds, respectively (Figure 5.5b).
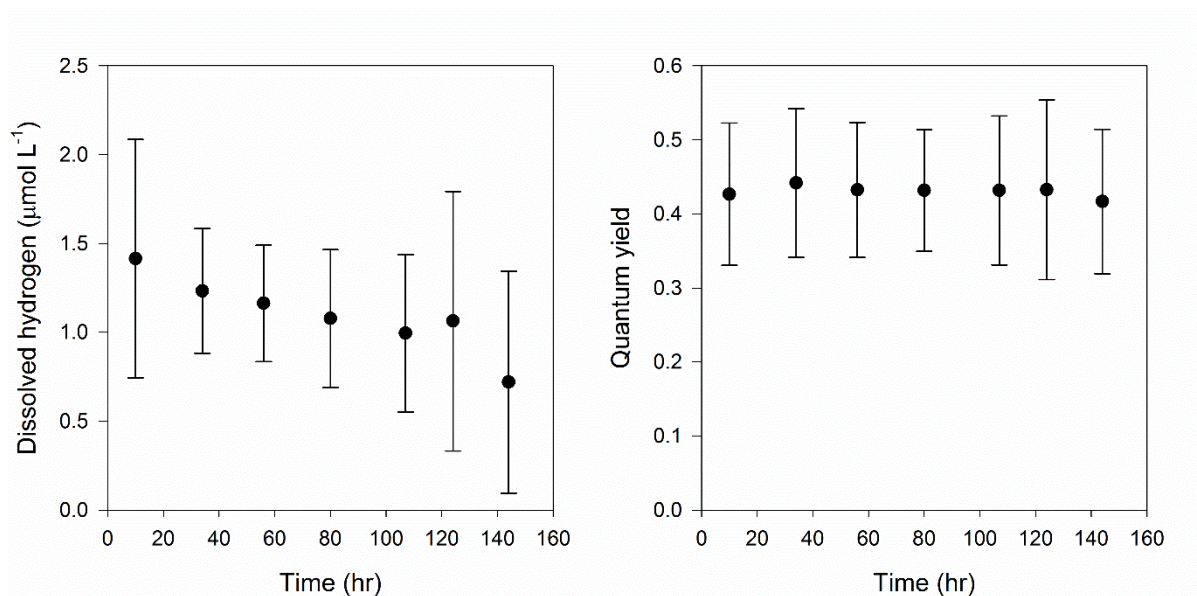
Figure 5.5a and b: Dissolved hydrogen (a) and quantum yield (b) results over time in culture experiment 5. Storage and incubation conditions outlined in table 5.1. All error bars represent standard deviation

5.5 Discussion

5.5.1 Hydrogen production in microalgal culture experiments

Dark anoxic incubations performed in culture experiments 1-5 confirmed that all six cultures rapidly produced H_2. Dissolved hydrogen concentrations generally peaked during the first 24 hours of incubation, then gradually declined. This is inconsistent with observations made during flow through reactor (FTR) experiments where hydrogen production would continue for in excess of 200 hours of anoxic incubation (chapter 6).

While it is well-established that green algae can fermentatively evolve H_2[22], this seems to be the first observation of H_2 production by diatoms. It has previously been observed that such organisms harbor the genes required to fermentatively produce hydrogen[1], i.e. PFR and [FeFe]-hydrogenase, supporting our observations.

It has long been recognized that diatoms can survive for many weeks in darkness[23] and that they may do this through dissimilatory nitrate reduction in dark anoxic conditions[24]. Whilst this mechanism is viable in relatively eutrophic habitats, such as the Wadden Sea, which have high nitrate concentrations over the winter months, this mechanism is unlikely to be viable in relatively oligotrophic habits such as Port Phillip Bay, where nitrate concentrations are very low in the water column (typically < 1 μM) and there is intense competition for the little nitrate that exists. It therefore seems likely that H_2 fermentation is the principle mechanism that these dominant organisms use to persist during anoxia.

5.5.2 Investigation of reduced hydrogen production rates and dissolved hydrogen loss

In culture experiments 2, 4 and 5 the concentration of hydrogen reached the experimental maximum during the first sampling round and sharply declined in all subsequent sampling rounds (Figures 5.2,5.4a and 5.5a). This was particularly surprising as FTR experiments indicated that hydrogen production could occur over extended periods (>200 hours) of anoxic incubation (chapter 6). Furthermore, a decrease in the concentration of dissolved hydrogen not only suggested that production had stopped, but that existing dissolved hydrogen was either lost or consumed. These

two phenomena are separate issues and microalgal culture experiments were designed so that they could each be investigated.

Declining hydrogen production observed in culture experiments 2, 4 and 5 was likely either changing metabolic fermentative pathways to one that did not include the production of hydrogen or poor culture health/stress halting metabolism. Marine diatoms are capable of producing a wide variety of fermentative products in various stoichiometries. If the switching between metabolic pathways was responsible for the observed drop in hydrogen production, further investigation is required to determine what new pathways are being utilized and what factors may influence which pathway is favoured.

The other possible explanation for declining hydrogen production is poor algal health, which can result in the decline of all metabolic activity, including hydrogen production via dark fermentation. Quantum yield analyses performed towards the end of culture experiment 2 revealed very low values of $0.09 \pm .06$ and 0.04 ± 0.05, for control and added acetate cultures, respectively, indicating poor algal health. This was likely in response to one of several methodological incubation factors such as: dark anoxic incubation conditions, the 10:1 algal preconcentration step, or the presence of the antibiotic cocktail. The investigation of these factors and their relation to microalgal culture health will be discussed in greater detail throughout this discussion. However, poor microalgal culture health appears to be an unlikely explanation for declining dissolved hydrogen production rates, since in culture experiments 4 and 5, quantum yield values remained within a healthy range for duration of the incubation (Figures 5.4b and 5.5b, respectively). These healthy quantum yield values persisted despite declining hydrogen production being observed.

Possible explanations for the loss of existing dissolved hydrogen included bacterial consumption, re-uptake by the microalgal culture or ineffectively sealed storage vials. Bacterial consumption is highly unlikely, as a broad spectrum antibiotic cocktail was added to all cultures, which would not only inhibit growth, but also eradicate any potential bacterial contamination.

Hydrogen loss from ineffectively sealed storage vials would likely be a factor in culture experiment 2 (Figure 5.2) as this experiment was performed using gastight exetainers, capped with rubber septums. These septums would likely have allowed dissolved hydrogen to diffuse through and be lost to the atmosphere. However, culture experiments 4 and 5 were performed in gastight glass vials as a means to prevent dissolved hydrogen loss, but despite this, a sharp decline in dissolved hydrogen concentration was observed in these experiments (Figure 5.4a and 5.5a). Hydrogen loss, therefore, cannot explain this decrease in hydrogen concentration in culture experiments 4 and 5. Mechanisms for hydrogen re-uptake, such as uptake hydrogenase and bidirectional hydrogenase, would serve to recycle dissolved H_2 into H^+ ions[25]. However, the extent to which they are expressed in marine diatom and chlorophytes is not clear. Further investigation is required to determine the mechanism by which hydrogen is being consumed.

5.5.3 Examination of the influence of methodological variables on microalgal culture health.

Culture experiment 3 was designed to test whether dark anoxic conditions or the presence of the dilute antibiotic cocktail was responsible for the poor algal health observed in culture experiment 2. Mean quantum yield values for each culture treatment stayed relatively constant throughout the experiment, indicating that neither the presence of the antibiotic cocktail, nor the dark conditions were responsible for the poor quantum yield values observed in culture experiment 2.

One key difference between the incubation conditions across culture experiments 2 and 3 was the use of a preconcentration step to increase cell density in cultures during experiment 2. Given the substantial difference between the health of the cultures from these experiments, as indicated by the quantum yield values, the preconcentration step was very likely a major contributor to poor algal health/stress.

Finally, the higher quantum yield values observed in culture experiment 5 (Figure 5.5b) relative to those found in culture experiment 4 (Figure 5.4b) indicate that performing the culture incubation on a shaker table in an $18°C$ refrigerated room resulted in improved culture health. The microalgal

cultures used in these experiments were grown under such conditions, and their observed decline in health following a deviation from storage conditions indicates these cultures are highly sensitive.

5.5.4 Influence of acetate on hydrogen production

In culture experiments 2 and 4, the influence of adding acetate to cultures on hydrogen production was tested. No difference in the hydrogen concentration, dissolved oxygen consumption or quantum yield values were observed, strongly indicating that the addition of 100 μmol L^{-1} acetate did not affect rates of culture metabolism. This may be due to high organic carbon content of culture medium following the algal growth period. All cultures were grown under abundant light conditions, and would have likely exuded considerable quantities of organic carbon, possibly making the added concentration of 100 μmol L^{-1}, relatively minor by comparison and unlikely to influence metabolic processes. A culture incubation experiment, including dissolved organic carbon (DOC) analysis of F/2 medium, would need to be performed to determine whether the 100 μmol L^{-1} acetate addition represented a substantial increase in DOC content or not.

5.6 Conclusion

For all axenic diatom and chlorophyte cultures, hydrogen production was observed when incubated under dark anoxic conditions, suggesting fermentation was occurring. These results are consistent with the high rates of eukaryotic dark fermentation observed in Port Phillip Bay sediments, from which, these cultures were grown. Through gradual refinement of incubation methodology, it was determined that microalgal cultures were relatively sensitive. Cultures required incubation conditions near identical to those in which they were grown in order to remain healthy. It has also been demonstrated that an added source of organic carbon, such as acetate, does not increase production of dissolved hydrogen or dissolved oxygen consumption.

5.7 References

1   Atteia, A., van Lis, R., Tielens, A. G. M. & Martin, W. F. Anaerobic energy metabolism in unicellular photosynthetic eukaryotes. *Biochimica Et Biophysica Acta-Bioenergetics* **1827**, 210-223, (2013).

2   Canfield, D. E., Kristensen, E. & Thamdrup, B. in *Aquatic Geomicrobiology* Vol. 48 *Advances in Marine Biology* Ch. 10, 383-414 (Academic Press Ltd-Elsevier Science Ltd, 2005).

3   Holmer, M. & Kristensen, E. Organic matter mineralization in an organic rich sediment. Experimental stimulation of sulfate reduction by fish food pellets. *FEMS Microbiol. Ecol.* **14**, 33-44, (1994).

4   Catalanotti, C., Yang, W., Posewitz, M. C. & Grossman, A. R. Fermentation metabolism and its evolution in algae. *Front. Plant. Sci.* **4**, 150, (2013).

5   Rossello-Mora, R., Thamdrup, B., Schafer, H., Weller, R. & Amann, R. The response of the microbial community of marine sediments to organic carbon input under anaerobic conditions. *Syst. Appl. Microbiol.* **22**, 237-248, (1999).

6   Valdemarsen, T. & Kristensen, E. Degradation of dissolved organic monomers and short-chain fatty acids in sandy marine sediment by fermentation and sulfate reduction. *Geochim. Cosmochim. Acta* **74**, 1593-1605, (2010).

7   Finke, N. & Jorgensen, B. B. Response of fermentation and sulfate reduction to experimental temperature changes in temperate and Arctic marine sediments. *Isme Journal* **2**, 815-829, (2008).

8   Kreuzberg, K. Starch fermentation via a formate producing pathway in chlamydomonas reinhardii, chlorogonium elongatum and chlorella fusca. *Physiol. Plant.* **61**, 87-94, (1984).

9   Greening, C. *et al.* Genomic and metagenomic surveys of hydrogenase distribution indicate H-2 is a widely utilised energy source for microbial growth and survival. *Isme Journal* **10**, 761-777, (2016).

10   Ghirardi, M. L. *et al.* Hydrogenases and hydrogen photoproduction in oxygenic photosynthetic organisms. *Annu. Rev. Plant Biol.* **58**, 71-91, (2007).

11   Benemann, J. R., Berenson, J. A., Kaplan, N. O. & Kamen, M. D. Hydrogen evolution by a chloroplast ferredoxin hydrogenase system. *Proc. Nat. Acad. Sci. USA* **70**, 2317-2320, (1973).

12   Melis, A. & Happe, T. Hydrogen production. Green algae as a source of energy. *Plant Physiol.* **127**, 740-748, (2001).

13   Hemschemeier, A., Melis, A. & Happe, T. Analytical approaches to photobiological hydrogen production in unicellular green algae. *Photosynthesis Res.* **102**, 523-540, (2009).

14   Mus, F., Dubini, A., Seibert, M., Posewitz, M. C. & Grossman, A. R. Anaerobic acclimation in Chlamydomonas reinhardtii - Anoxic gene expression, hydrogenase induction, and metabolic pathways. *J. Biol. Chem.* **282**, 25475-25486, (2007).

15   Dubini, A., Mus, F., Seibert, M., Grossman, A. R. & Posewitz, M. C. Flexibility in anaerobic metabolism as revealed in a mutant of chlamydomonas reinhardtii lacking hydrogenase activity. *J. Biol. Chem.* **284**, 7201-7213, (2009).

16   Tucci, S., Vacula, R., Krajcovic, J., Proksch, P. & Martin, W. Variability of Wax Ester Fermentation in Natural and Bleached Euglena gracilis Strains in Response to Oxygen and the Elongase Inhibitor Flufenacet. *J. Eukaryot. Microbiol.* **57**, 63-69, (2010).

17   Tomas, C. R. *Identifying Marine Phytoplankton*. (Academic Press, 1997).

18   Cosgrove, J. & Borowitzka, M. A. *Chlorophyll Fluorescence Terminology: An Introduction*. Vol. 4 (Springer, 2010).

19   Mock, T. & Hoch, N. Long-term temperature acclimation of photosynthesis in steady-state cultures of the polar diatom Fragilariopsis cylindrus. *Photosynthesis Res.* **85**, 307-317, (2005).

20   Domingues, N., Matos, A. R., da Silva, J. M. & Cartaxana, P. Response of the Diatom Phaeodactylum tricornutum to Photooxidative Stress Resulting from High Light Exposure. *Plos One* **7**, (2012).

21   Garrido, M., Cecchi, P., Vaquer, A. & Pasqualini, V. Effects of sample conservation on assessments of the photosynthetic efficiency of phytoplankton using PAM fluorometry. *Deep-Sea Research Part I-Oceanographic Research Papers* **71**, 38-48, (2013).

22   Melis, A. Photosynthetic H2 metabolism in Chlamydomonas reinhardtii (unicellular green algae). *Planta* **226**, 1075-1086, (2007).

23   Dupreez, D. R. & Bate, G. C. Dark survial of the surf diatom anaulus australis drebes et schulz. *Bot. Mar.* **35**, 315-319, (1992).

24   Heisterkamp, I. M., Kamp, A., Schramm, A. T., de Beer, D. & Stief, P. Indirect control of the intracellular nitrate pool of intertidal sediment by the polychaete Hediste diversicolor. *Mar. Ecol. Prog. Ser.* **445**, 181-192, (2012).

25   Tamagnini, P. *et al.* Hydrogenases and hydrogen metabolism of cyanobacteria. *Microbiol. Mol. Biol. Rev.* **66**, 1-+, (2002).

Chapter 6: Fermentation in dark anoxic permeable carbonate sediments

6.1 Abstract

A flow-through reactor experiment using permeable carbonate sediment from Heron Island, has shown that the combined mean rate of denitrification and sulfate reduction accounted for <12% of mean anaerobic dissolved inorganic carbon (DIC) production, leaving the large majority without a known source. Metabolomic analyses revealed very large increases in the relative quantity of C18-23 lipids, including wax monoesters and unsaturated fatty acids, after short term (<24 hrs) exposure to anoxic conditions. Following further anoxic incubation, high rates of dissolved hydrogen production were observed and accompanied by further accumulation of these lipid compounds. These observations indicate that fermentation is likely a major process in anoxic carbonate sediments. A cell count analysis revealed a highly diverse microalgal community with relative proportions of 28.4% of dinoflagellates, 28.4% other flagellates, 10.1% diatoms and 33.1% cyanobacteria, suggesting that anoxic survival via fermentation may be a widely held adaption amongst these microorganisms.

6.2 Introduction

Permeable carbonate sediments have arisen from the breakdown of $CaCO_3$ structures over millennia following their construction by calcifying organisms, such as foraminifera, calcareous algae and molluscs[1,2]. These sediments are comprised of a mix of several carbonate mineral phases, such as low magnesium calcites, high magnesium calcites and aragonite. The higher the magnesium content of the carbonate sediments, the more readily that mineral will be dissolved[3]. Carbonate sediments cover approximately 40% of the global ocean shelf[4] and typically occur in tropical and subtropical conditions.

Similar to silica sediments, advection into permeable carbonate sediments has been shown to transport solutes to far greater depths[5] relative to cohesive sediments. During advective transport, particulate organic matter is filtered from porewater and broken down via high organic carbon mineralization rates[6] allowing for nutrients to be recycled to the oligotrophic environment[7]. Wave action results in continuous sediment resuspension that evenly distributes microorganisms to depths >15 cm, where dark anoxic conditions prevail [8,9]. Under nitrate-rich anoxic conditions, established energetic favourability yields indicate that nitrate reduction to dinitrogen (denitrification) should be the dominant heterotrophic metabolic process and therefore should be a major source of dissolved inorganic carbon. However, recent investigations using flow through reactor experiments by Bourke, et al. [10] Kessler, et al. [11] and Evrard, et al. [12] have revealed that under such conditions, denitrification contributed <5% of DIC production, leaving the vast majority of DIC production without a known source.

It has recently been shown that metabolism in anoxic silica permeable sediments collected from Port Phillip Bay, Victoria, Australia, is dominated by dark fermentation, performed by eukaryotic microalgae[10]. Combined rates of denitrification and sulfate reduction accounted for <13% of DIC production in anoxic FTR experiments (Chapter 4), while high rates of

dissolved hydrogen production and several fold increases of fatty acids were observed, indicating that dark fermentation was dominating.

Fermentation includes a diverse range of microbially-mediated anaerobic reactions that all involve organic carbon simultaneously participating in oxidation and reduction, serving as both the electron acceptor and the electron donor[13]. Fermentation has long been known to occur in both permeable and cohesive sediments, largely utilized to facilitate the breakdown of particulate organic matter[14]. However, these processes were considered to be strongly coupled to terminal heterotrophic metabolic pathways, such as iron (III) and sulfate reduction, preventing the accumulation of fermentative products[15].

Dark fermentative metabolism is a process that involves the glycolytic breakdown of organic compounds, such as intracellularly stored starch, by eukaryotic microorganisms. Dark fermentation has been observed to produce hydrogen and carbon dioxide, as well as a wide variety of organic end products, depending on the microalgal species, pathway and environmental conditions[16,17]. For example, *Chlamydomonas* excrete acetate, ethanol, and formate or glycerol at ratios that vary depending on the species[18,19,20]. While, some microalgae do not release fermentative products from the cell at all, and instead accumulate them intracellularly. For example, *Euglena gracilis* generates large concentrations of wax esters[21] which are stored in the cytosol and are reoxidized to generate ATP upon the return to oxic conditions[22].

Lipid synthesis and accumulation is not a capability exclusive to eukaryotic microalgae. Synthesis of lipids by marine bacteria such as *Marinobacer*[23] and *Alcanivorax*[24] has been frequently reported. Similar to eukaryotic microalgae, these pathways are utilized during nutrient and oxygen limited conditions and while a wide variety of pathways exist, common storage lipids synthesised by prokaryotic microorganisms include triacylglycerols (TAGs), wax esters (WEs) and polyhydroxyalkanoates (PHAs)[25].

The primary hypotheses of this research chapter are twofold: firstly, in anoxic permeable carbonate sediments, metabolism by terminal heterotrophic processes will account for only a small proportion of total DIC production, leaving the large majority without a known source. Secondly, fermentation is a major process under anoxic sediment conditions and is likely resulting in high rates of production of dissolved hydrogen and extensive lipid accumulation, as previously observed in silica permeable sediments (Chapter 4). These hypothesis will be investigated using flow through reactor (FTR) experiments.

The key research questions addressed in this chapter are:

1) In anoxic permeable carbonate sediments, are there large quantities of dissolved inorganic carbon being produced that cannot be attributed to carbonate dissolution or terminal heterotrophic metabolic processes, such as denitrification or sulfate reduction?

2) Can meaningful concentrations of a key fermentative products, such as dissolved hydrogen, be detected in FTR effluent?

3) Are other key fermentative products, such as lipid compounds, accumulating intracellularly during extended anoxic incubation?

6.3 Methods

6.3.1 Site description

Flow through reactors (FTRs) were packed using approximately the top 15 cm layer of sediment from the research station beach site at Heron Island, Queensland, Australia (site coordinates are 23°26'37"S, 151°54'46"E). The depth at low tide was approximately 0.5 m.

6.3.2 Flow through reactors

The FTRs used were acrylic cylinders with a diameter of 4.6 cm and a length of 3 cm sediment. PVC caps were placed at either end of the cylinder, and were machined with grooves converging to a central outlet port overlaid with 0.1 mm nylon mesh to allow even plug flow through the FTR. Freshly collected sample seawater was pumped through the FTRs using a peristaltic pump located upstream. Seawater was pumped in an upwards direction from the base of the FTR to assist in maintaining plug flow. Reservoirs were maintained in oxic or anoxic states by continuous purging with air or argon, respectively. Sample sediment was sieved using a 2mm mesh to remove large debris, such as shell grit, rocks and macroalgae, which can interfere with FTR plug flow.

Plug flow within these FTRs has been verified during breakthrough curve experiments performed by Evrard, et al. [12] and Bourke, et al. [26]. In chapter 2 of this thesis, the degree of gas leakage was found to be negligible, as deoxygenated water was pumped through the system and effluent oxygen saturation changed by <1%. Dissolved hydrogen loss was also found to be minimal, with only 3.6% lost when a solution containing 50 μmol L^{-1} H$_2$ was passed through the system[10].

Water samples were collected at the FTR outlet by directly connecting glass syringes, ensuring no bubbles were introduced. Rates of production and consumption were calculated using FTR volume, flow velocity and the change in concentration of the relevant solute at the reservoir and outlet.

6.3.3 FTR experiment

The FTR experiment was performed over a 140 hour period with oxic conditions maintained for the first 17 hours, then conditions were changed to anoxic for the remainder of the experiment. The inlet reservoir was maintained to have a concentration of 50 µmol L^{-1} $^{15}NO_3^-$. Four FTRs were used and the flow velocity was held at 1.6 mL min^{-1}. During each sampling round, effluent samples were collected so that dissolved inorganic carbon (DIC), denitrification and sulfide production rates could be determined. Sampling for alkalinity production began at t= 58 hr and was included in the sampling regime for the remainder of the experiment. Dissolved oxygen and hydrogen concentrations were measured using flow through sensors. The reservoir was refilled at t=80 hr with sample seawater that had been purged with argon for 120 minutes. Sediment from oxic conditions, anoxic conditions where no hydrogen production was observed and anoxic conditions with hydrogen production observed were frozen for metabolomic analysis.

6.3.4 Sampling and analysis

6.3.4.1 Denitrification rates

Concentrations of ^{15}N-N_2 in FTR effluent were determined using headspace analysis on a Gas Chromatograph (He carrier) coupled to isotope ratio mass spectrometer (Sercon 20-22). The rates of denitrification reported throughout this chapter are total denitrification ($D_{14}+D_{15}$) and were calculated using the isotope pairing technique[27]. Samples from FTR experiments were transferred from glass syringes into 12 mL Exetainers (Labco, High Wycombe) and preserved with 250 µL of 50% w/v $ZnCl_2$.

6.3.4.2 Dissolved inorganic carbon

The concentration of dissolved inorganic carbon (DIC) was evaluated using flow injection analysis, fitted with a photometric detector. This method involved acidifying FTR sample

effluent so that any carbonate species would be converted to carbon dioxide, which, would then diffuse across a microporous membrane (Accurel® PP Q3/2 tubular membrane, ID 0.6 mm)[28]. The resulting change in pH causes the Bromothymol Blue indicator solution to produce a measurable colour change proportional to the quantity of diffused carbon dioxide. Samples for dissolved inorganic carbon were sampled using 3 mL exetainers and preserved with 100 μL of 6% $HgCl_2$ before analysis.

6.3.4.3 Dissolved oxygen

Dissolved oxygen was continuously recorded during FTR experiments using Pyroscience Firesting flow through dissolved oxygen sensors. These flow through sensors were attached directly to the inlet and outlet ports to allow for a highly representative determination of the dissolved oxygen concentration entering and exiting the FTR.

6.3.4.4 Dissolved hydrogen

Dissolved hydrogen analysis was performed using a calibrated Unisense H_2-100 sensor fitted with a glass flow through cell connected directly to the FTR outlet.

6.3.4.5 Sulfide

A UV-Visible spectrophotometer (GBC) was used to determine sulfide concentrations in FTR effluent following the Fonselius[29] method. Effluent samples were filtered using MicroAnalytix 0.2 μm cellulose-acetate filters and were preserved using 100 μL of Zn acetate per mL of sample.

6.3.4.6 Metabolome analysis

For metabolome analysis, cells were lysed and metabolites were extracted from FTR sediments using a methanol:chloroform mixture (1:2, v:v; -20C°) for 30 min under sonication. The metabolites in the supernatants were analysed by GC-QTOF-MS and LC-QTOF-MS (both Agilent Technologies) following Godzien, et al. [30] and Kind, et al. [31] with slight modifications.

6.4 Results

The sediment was found to have a median grain size of 0.9 mm and a permeability of 27 $x10^{12}$ m^2. The porosity of the sediment was determined to have a value of 0.55. Under anoxic conditions, the reservoir pH was found to be 8.528 at t= 79 hrs. The mean dissolved oxygen consumption rate, was determined to be 489 ± 18 nmol mL^{-1} hr^{-1} at t=15. There was no significant difference between this value and the oxic DIC production rate recorded during the same sampling round, which was 686 ± 174 nmol mL^{-1} hr^{-1} (ANOVA, single factor, p>0.05) (Figure 6.1). Mean DIC production under anoxic conditions was determined to be 382 ± 142 nmol mL^{-1} hr^{-1}.and was also found to have no statistical difference to the oxic DIC production rate (ANOVA, single factor, p>0.05).

Figure 6.1: Dissolved inorganic production rates over time. Dashed line represents the change from oxic to anoxic conditions. All error bars represent standard deviation.

Under oxic reservoir conditions, no dissolved hydrogen production was observed (Figure 6.2). After approximately 41 hours of anoxic conditions (t=55 hr), dissolved hydrogen production began and production rates increased rapidly over a 24 hour period to reach a maximum of 46 ± 1 nmol mL^{-1} hr^{-1} at t=79 hr, which corresponded to a FTR effluent concentration of 23.3 ± 0.3 μmol L^{-1}. Dissolved hydrogen production rates dropped sharply

after the experimental maximum was reached and gradually declined until hydrogen production increased during the final sampling round to 23 ± 3 nmol mL^{-1} hr^{-1}.
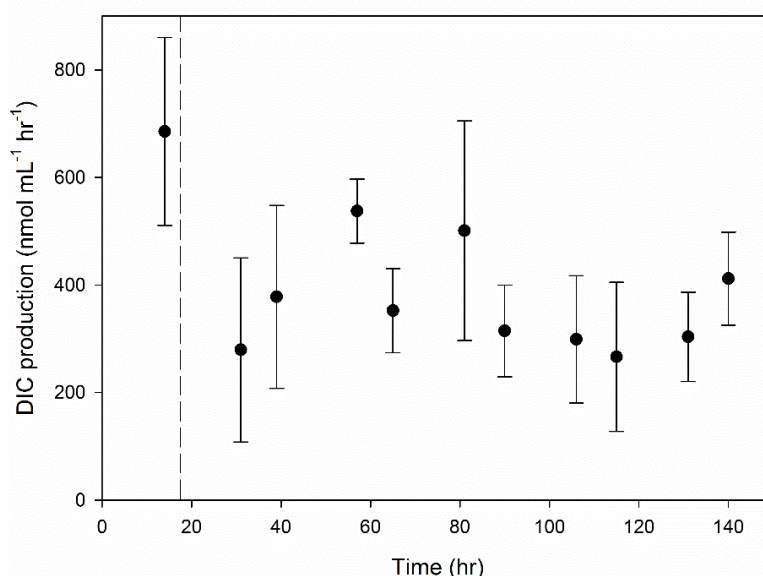

Figure 6.2: Dissolved hydrogen production rates over time. Dashed line represents the change from oxic to anoxic conditions. All error bars represent standard deviation.

Mean denitrification rates under anoxic conditions were determined to be 3 ± 2 nmol mL^{-1} hr^{-1} (Figure 6.3a). Rates of total denitrification gradually increased over time, however, the maximum denitrification rate of 6 ± 1 nmol mL^{-1} hr^{-1} was observed during the first anoxic sampling round at t=31 hrs. The mean sulfide production rate under anoxic conditions was determined to be 40 ± 50 nmol mL^{-1} hr^{-1} (Figure 6.3b). Sulfide production began approximately 43 hours after the commencement of anoxic conditions (t=57 hrs) and gradually increased to the maximum observed rate of 170 ± 40 nmol mL^{-1} hr^{-1} during the final sampling round (t=140 hrs). The stoichiometric ratios of denitrification and sulfide production (listed in section 2.1 of this thesis) were used to calculate the relative contribution of these processes towards the total DIC production rate. Combined rates of total denitrification and sulfate reduction represented <12% of mean anoxic DIC production.

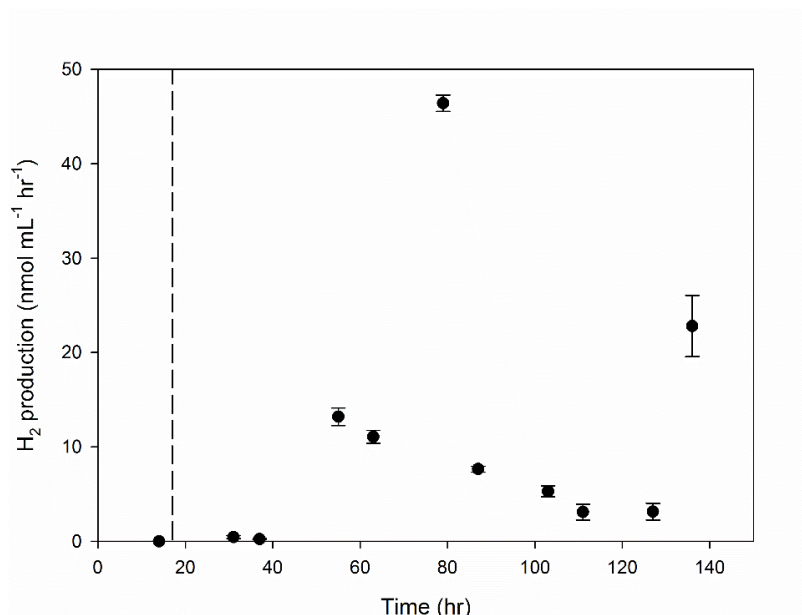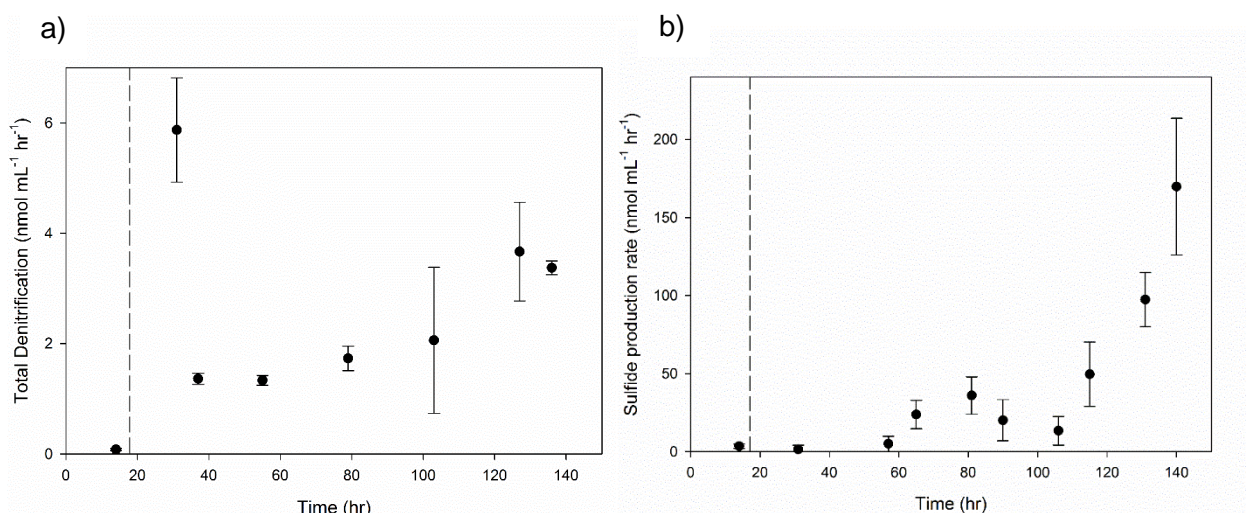**Figure 6.3a and 6.3b: Denitrification (a) and sulfide production (b) rates over time. Dashed lines represents the change from oxic to anoxic conditions. All error bars represent standard deviation.**

As alkalinity samples were only taken from t=57 hrs onwards, oxic alkalinity production could not be determined. Mean anoxic alkalinity production was -20 ± 70 nmol mL^{-1} hr^{-1} (Figure 6.4).
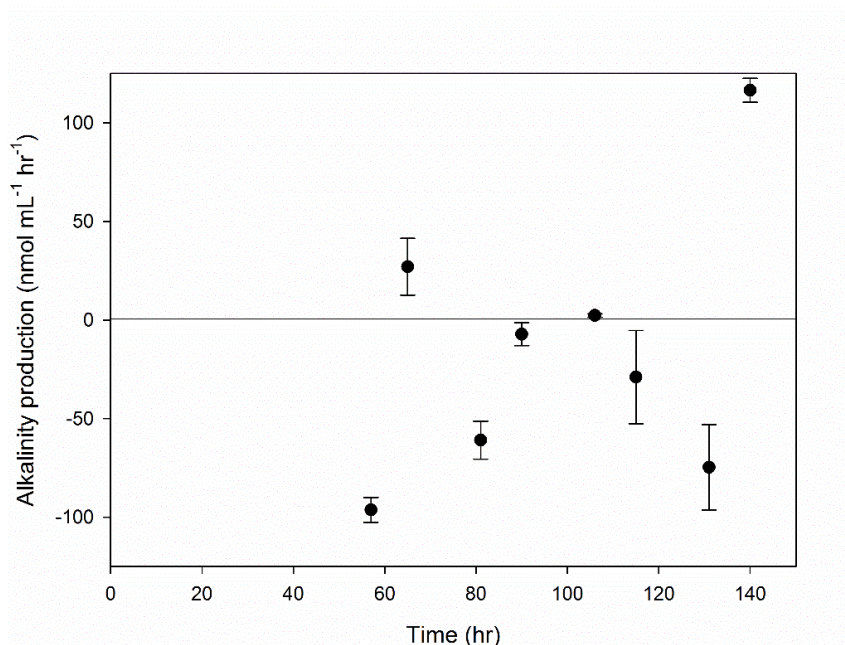
Figure 6.4: Anoxic alkalinity production rates over time. All error bars represent standard deviation.

The metabolome present in sediment samples from oxic conditions, anoxic conditions where no hydrogen was observed and anoxic sediments where hydrogen was observed, were analyzed and 5860 individual compounds were identified and quantified in terms of relative abundance. The relative abundances of the 5860 detected compounds across each of the three sediment conditions are summarized in a heat map (Figure 6.5a). The variation amongst these metabolomes is summarized in a principal component plot (Figure 6.5b) and shows relatively close grouping of metabolome data points within the three sediment conditions.

a)

b)
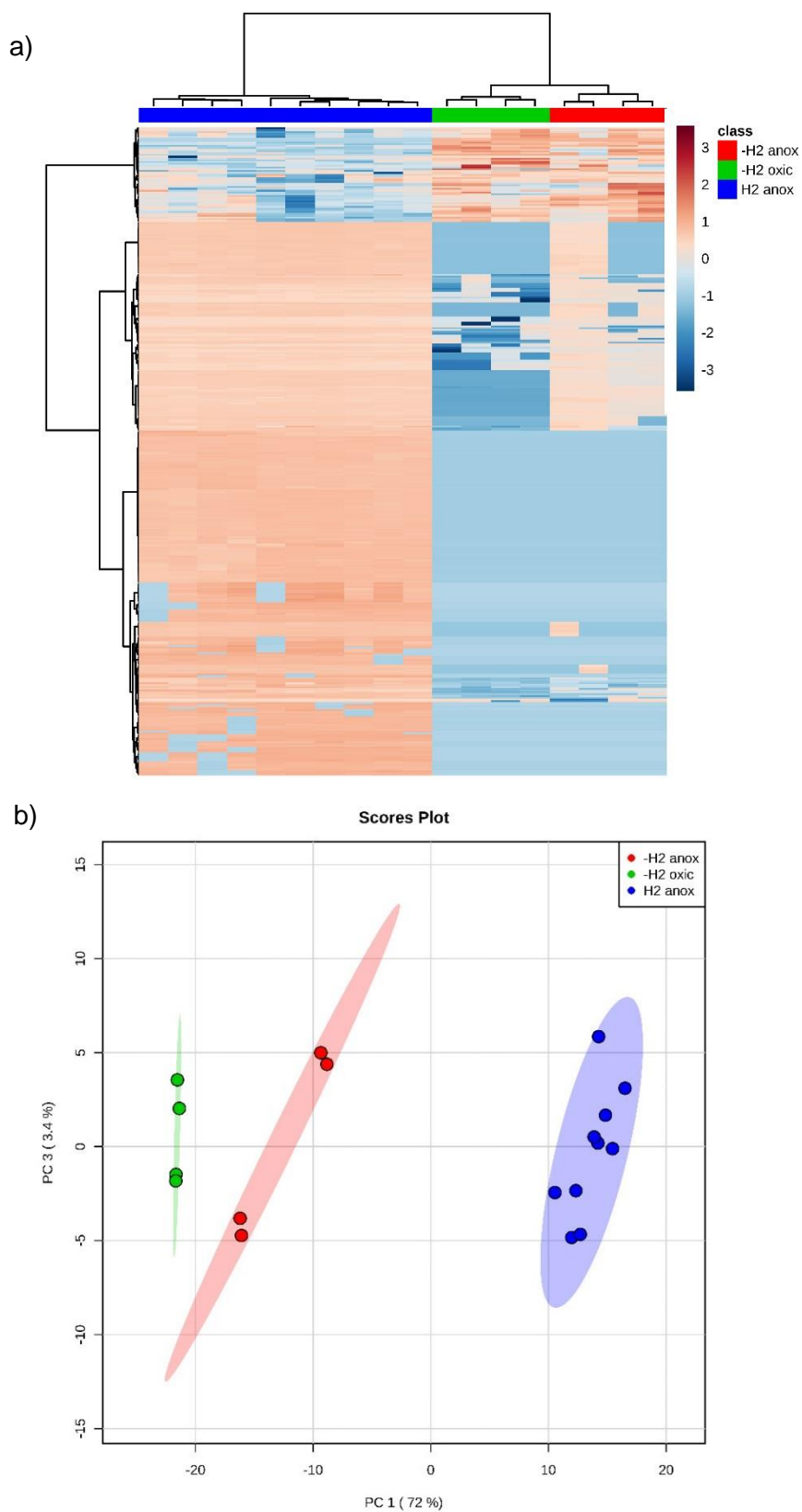
Figure 6.5a and 6.5b: a) a heatmap and b) principal component plot showing the differences in the metabolome of sediments taken from three sediment conditions. Oxic conditions without hydrogen observed (green), anoxic conditions without hydrogen observed (red) and anoxic conditions with hydrogen production observed (blue).

The metabolic components with the five highest overall relative abundances were identified and their relative abundances across the three sediment conditions were quantified (Figure 6.6). All five compounds were C18-23 lipids and included wax monoesters and unsaturated fatty acids. The most abundant metabolic component was octadecanoic acid, which increased by a factor of 59.6 following a change from oxic to anoxic conditions where no hydrogen was observed. The relative abundance of octadecanoic acid increased by a factor of 102.2 when comparing oxic conditions to anoxic conditions where hydrogen was observed. Of these five most abundant metabolites, the metabolic component that exhibited the greatest proportional change was ethyl-5, 8, 11, 14, 17-pentanoate. Relative to oxic conditions, this compound increased by a factor of 148.5 in anoxic conditions without hydrogen observed and by a factor of 1037.0 in anoxic conditions with hydrogen observed.
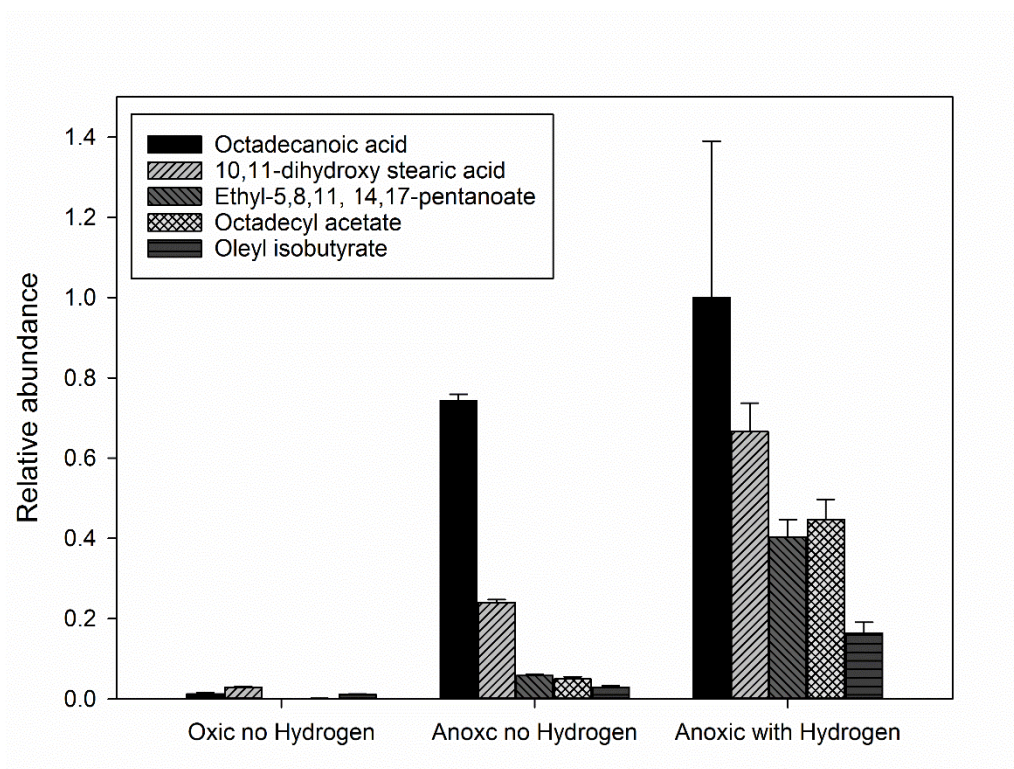
Figure 6.6: Sediment metabolome analysis: relative abundances of the five most significant analytes in sediment samples taken from oxic no hydrogen, key fatty acid metabolites between oxic conditions and anoxic with hydrogen production observed. All error bars represent standard deviation.

The cell count performed on Heron island sediment indicated a diverse community of microalgae. Dinoflagellates and other flagellates were particularly abundant, exceeding $2x10^5$ cells per mL, with species from the genus *Prorocentrum cf. maculosa.*, and *Goniomonas amphinema* most numerous (Table 6.1).

Table 6.1: Cell count and species identification from Heron island sediment.

Algal taxa	Cell count (Cells mL$^{-1)}$	Relative proportion (%)
Diatoms		
Amphora sp.	15000	
Ceratoneis closterium	25000	
Fragilaria sp.	5000	
Naviculoid spp.	10000	
Nitzschia spp.	25000	
Pleurosigma sp.	5000	
Dinoflagellates		
Gymnodinioid spp.	40000	
Prorocentrum cf. maculosa.	200000	
Chrysophytes		
Ochromonas spp.	70000	
Cryptophytes		
Goniomonas amphinema	90000	
Hemiselmis sp.	5000	
Chlorophyta		
Pyramimonas spp.	45000	
Euglenophyta		
Unidentified euglenoids	30000	
Cyanophytaa		
cf. Geitlerinema	40000	
Cf. Pseudanabaena	240000	
Cf. Trichodesmium	50	
Diatoms	85000	10.1
Dinoflagellates	240000	28.4
Other flagellates	240000	28.4
Cyanophyta	280050	33.1

6.5 Discussion

As oxic DIC production was not significantly different from rates of dissolved oxygen consumption, aerobic respiration is likely responsible for the vast majority of DIC production under oxic conditions. There was also no significant difference between mean oxic and anoxic DIC production rates (Figure 6.1), suggesting that the community responsible for the majority of oxic respiration, is likely the same community respiring under anoxic conditions.

According to the established understanding of heterotrophic energetic favourability in sediments, denitrification should be dominating under anoxic conditions when nitrate is present. It would therefore be reasonable to expect the denitrification rate to be approximately 80% of the anoxic DIC production rate (based on the reaction stoichiometry, 4 NO_3^- consumed for 5 CO_2 produced[32]). However, total rates of denitrification were found to be negligible compared to anoxic DIC production (Figure 6.3a), strongly indicating that another anoxic process is dominating and producing large quantities of DIC. Even when comparing mean anoxic DIC production with the mean combined rates of total denitrification and sulfide production (Figure 6.3b), these processes only accounted for <12% of mean anoxic DIC production.

This large gap between the rate of anoxic DIC production and heterotrophic metabolism is consistent with previous observations by Bourke, et al. [10], Evrard et al 2013[33] and Marchant *et al* 2016 [34], suggesting a common phenomenon.

The anoxic alkalinity production rates are highly variable (Figure 6.4). The mean alkalinity production of -20 nmol mL^{-1} hr^{-1} indicated that the process dominating anaerobic respiration in permeable carbonate sediments likely consumed alkalinity as it progressed. Alkalinity production rates began to increase following the replacement of the anoxic reservoir at t=80. Despite extensive purging, this reservoir possibly contained trace dissolved oxygen, which if present, would have enabled low rates of sulfide oxidation. This process would have produced alkalinity and may have been responsible for the observed increase in alkalinity production that coincided with the reservoir change.

Ordinarily, the high rates of anoxic DIC production (Figure 6.1) would be expected to result in a decrease in porewater pH due to the formation of carbonic acid. The lower pH would augment rates of calcium carbonate dissolution and make biotic DIC production difficult to distinguish from abiotic mineral dissolution. However, the pH of the porewater was determined to be slightly alkaline, with a pH value of 8.528 at t=79 hr. This has likely arisen due to the continuous reservoir purging using Ar, preventing the accumulation of DIC and carbonic acid. As a consequence, the contribution of calcium carbonate dissolution is likely negligible. The observed negative mean alkalinity production rate further supports this notion, as meaningful rates of calcium carbonate dissolution would result in high alkalinity production rates.

Substantial dissolved hydrogen production rates were observed throughout the FTR experiment (Figure 6.2) with concentrations almost an order of magnitude higher than previously reported maximum transient concentrations of hydrogen by bacterial fermentation of 2 to 6 μM[15,35]. Dissolved hydrogen is a common product of fermentation and high production rates under dark anoxic conditions indicate that eukaryotic dark fermentation may be dominating anoxic carbonate sediments. The sharp decline in hydrogen production at t=87 hr can be explained by the introduction of trace dissolved oxygen when the reservoir was refilled at t=80 hr. This would have inhibited hydrogenase enzymes[36], causing the observed decrease in hydrogen production.

Analysis of the sediment metabolome, under the three conditions listed, indicated that there was a substantial change in the relative abundances of the 5860 identified metabolites. The shading depicted in the heat map (Figure 6.5a) shows that the majority of the metabolites increased in relative abundance, following the change from oxic conditions to anoxic conditions where dissolved hydrogen was observed. This observation is consistent with the accumulation of lipids observed during eukaryotic dark fermentation that was found to dominate anoxic permeable silica sediments[10] (chapter 4).

The principal component plot (Figure 6.5b) groups data points based on the similarity of the metabolome. The high degree of clustering indicates that sediment metabolome subsamples were

relatively consistent within sediment condition groups. The substantial separation between data point clusters highlights the differences between sediment group metabolomes and has likely arisen due to the sustained increase in relative abundance of metabolites as anoxic conditions progressed, as seen in the heat map (Figure 6.5a). These observations reflect extensive metabolic reprogramming during anoxic conditions within carbonate sediments.

Of the five most abundant metabolites present in the sediment metabolome, all were identified as C18-23 lipids, and were all either wax monoesters or unsaturated fatty acids (Figure 6.6). Each of these five lipid compounds consistently increased in relative abundance as anoxic conditions persisted. Lipid accumulation, under dark anoxic conditions has previously been observed in axenic eukaryotic microalgal cultures of *euglena gracillis*[21,22] and coupled with the observed high dissolved hydrogen production rates, this indicates that eukaryotic dark fermentation could be a major process in anoxic carbonate sediments.

However, as marine bacteria have also been found to accumulate lipids, it is unclear what proportion of the lipids accumulated in the sediment metabolome were synthesized by the prokaryotic and eukaryotic communities. In future work, broad spectrum antibiotic treatments could be used to determine the respective contribution of these groups of microorganisms.

While only a relative quantitation of metabolites was undertaken, the fact that these lipid compounds were the most abundant out of all sediment metabolites identified, suggests that fermentation resulting in lipid synthesis may be a major process in anoxic permeable carbonate sediments.

As extensive lipid accumulation was measured under anoxic conditions where no hydrogen production was observed, fermentation is likely occurring under short term (<24hr) anoxia. The lack of hydrogen production observed during this period may be due to select fermentation reactions and stoichiometries being utilized over others. In Chapter 4, reactions 1 and 2 demonstrated how oleate and DIC producing dark fermentation reactions that do and do not produce hydrogen were both favourable. In support of this hypothesis, the diverse range of lipids being

accumulated in the sediment metabolome indicate that a range of fermentation reactions are likely being employed. Alternatively, dissolved hydrogen may in fact be being produced during short term anoxia, however, rapid consumption by hydrogenotrophic bacteria prevents accumulation within the porewater.

While C18 lipids have been studied extensively in eukaryotic microalgal cultures[37,38], the majority of research has been within the context of stimulating lipid production through limiting nutrients or exposure to excess light[37]. This highlights a promising avenue for future research that merits further investigation. This future work could include a direct quantification of the metabolome, targeting key metabolites, rather than the relative quantification presented in chapters 5 and 6 of this thesis. This would mean precise quantities of metabolites could be determined, allowing for the calculation of fermentation production rates, clarifying the dominance of these processes in anoxic permeable sediments.

Sediment cell count analysis (Table 6.1) revealed a well-established and diverse community of microalgae, with cyanobacteria, dinoflagellates and other flagellates being abundant, exceeding $2x10^5$ cells per mL. Given the high degree of microalgal biodiversity and the fact that the most abundant compounds present in the sediment metabolome were various C18-23 lipids, the capability of anaerobic fermentation resulting in lipid accumulation may be more widespread than previously thought.

6.6 Conclusion

The large discrepancy between rates of anoxic dissolved inorganic carbon production and combined rates of denitrification and sulfate reduction can likely be attributed to high rates of fermentation. This is supported by the observed high production rates of dissolved hydrogen as well as the substantial accumulation of lipids in the sediment metabolome. Both factors suggest that fermentation is a major process in anoxic carbonate sediments. These observations are consistent with the high rates of eukaryotic dark fermentation found to occur in silica Port Phillip Bay sediments, though the high degree of microalgal biodiversity observed in this research, suggests that anoxic survival via fermentation may be a widely held adaptation for survival in anoxic carbonate sediments.

6.7 References.

1   Gattuso, J. P., Frankignoulle, M. & Wollast, R. Carbon and carbonate metabolism in coastal aquatic ecosystems. *Annu. Rev. Ecol. Syst.* **29**, 405-434, (1998).

2   Tucker, M. E. & Wright, V. P. in *Carbonate Sedimentology*   70-100 (Blackwell Publishing Ltd., 2009).

3   Morse, J. W., Andersson, A. J. & Mackenzie, F. T. Initial responses of carbonate-rich shelf sediments to rising atmospheric pCO(2) and "ocean acidification": Role of high Mg-calcites. *Geochim. Cosmochim. Acta* **70**, 5814-5830, (2006).

4   Milliman, J. D. & Droxler, A. W. Neritic and pelagic carbonate sedimentation in the marine environment: Ignorance is not bliss. *Geologische Rundschau* **85**, 496-504, (1996).

5   Oberdorfer, J. A. & Buddemeier, R. W. Coral reef hydrology. Field studies of water movement within a barrier reef. *Coral Reefs* **5**, 7-12, (1986).

6   Rocha, C. Sandy sediments as active biogeochemical reactors: compound cycling in the fast lane. *Aquat. Microb. Ecol.* **53**, 119-127, (2008).

7   Rasheed, M., Badran, M. I. & Huettel, M. Influence of sediment permeability and mineral composition on organic matter degradation in three sediments from the Gulf of Aqaba, Red Sea. *Estuarine Coastal and Shelf Science* **57**, 369-384, (2003).

8   MacIntyre, H. L., Geider, R. J. & Miller, D. C. Microphytobenthos: The ecological role of the "secret garden" of unvegetated, shallow-water marine habitats 1. Distribution, abundance and primary production. *Estuaries* **19**, 186-201, (1996).

9   Evrard, V., Cook, P. L. M., Veuger, B., Huettel, M. & Middelburg, J. J. Tracing incorporation and pathways of carbon and nitrogen in microbial communities of photic subtidal sands. *Aquat. Microb. Ecol.* **53**, 257-269, (2008).

10   Bourke, M. F. *et al.* Metabolism in anoxic permeable sediments is dominated by eukaryotic dark fermentation. *Nature Geoscience* **10**, 30-35, (2017).

11   Kessler, A. J. *et al.* Quantifying denitrification in rippled permeable sands through combined flume experiments and modeling. *Limnol. Oceanogr.* **57**, 1217-1232, (2012).

12   Evrard, V., Glud, R. N. & Cook, P. L. M. The kinetics of denitrification in permeable sediments. *Biogeochemistry* **113**, 563-572, (2012).

13   Catalanotti, C., Yang, W., Posewitz, M. C. & Grossman, A. R. Fermentation metabolism and its evolution in algae. *Front. Plant. Sci.* **4**, 150, (2013).

14   Canfield, D. E., Thamdrup, B. & Hansen, J. W. The anaerobic degradation of organic matter in danish coastal sediments- iron reduction, manganese reduction and sulfate reduction. *Geochim. Cosmochim. Acta* **57**, 3867-3883, (1993).

15   Finke, N. & Jorgensen, B. B. Response of fermentation and sulfate reduction to experimental temperature changes in temperate and Arctic marine sediments. *ISME J* **2**, 815-829, (2008).

16   Ohta, S., Miyamoto, K. & Miura, Y. Hydrogen evolution as a consumption mode of reducing equivalents in green algal fermentation. *Plant Physiol.* **83**, 1022-1026, (1987).

17   Atteia, A., van Lis, R., Tielens, A. G. M. & Martin, W. F. Anaerobic energy metabolism in unicellular photosynthetic eukaryotes. *Biochimica Et Biophysica Acta-Bioenergetics* **1827**, 210-223, (2013).

18   Mus, F., Dubini, A., Seibert, M., Posewitz, M. C. & Grossman, A. R. Anaerobic acclimation in Chlamydomonas reinhardtii - Anoxic gene expression, hydrogenase induction, and metabolic pathways. *J. Biol. Chem.* **282**, 25475-25486, (2007).

19   Klein, U. & Betz, A. Fermentative metabolism of hydrogen evolving chlamydomonas moewusii. *Plant Physiol.* **61**, 953-956, (1978).

20   Meuser, J. E. *et al.* Phenotypic diversity of hydrogen production in chlorophycean algae reflects distinct anaerobic metabolisms. *Journal of Biotechnology* **142**, 21-30, (2009).

21   Inui, H., Miyatake, K., Nakano, Y. & Kitaoka, S. Wax ester fermentation in euglena gracilis. *FEBS Lett.* **150**, 89-93, (1982).

22   Tucci, S., Vacula, R., Krajcovic, J., Proksch, P. & Martin, W. Variability of Wax Ester Fermentation in Natural and Bleached Euglena gracilis Strains in Response to Oxygen and the Elongase Inhibitor Flufenacet. *J. Eukaryot. Microbiol.* **57**, 63-69, (2010).

23   Holtzapple, E. & Schmidt-Dannert, C. Biosynthesis of isoprenoid wax ester in Marinobacter hydrocarbonoclasticus DSM 8798: Identification and characterization of isoprenoid coenzyme A synthetase and wax ester synthases. *J. Bacteriol.* **189**, 3804-3812, (2007).

24   Kalscheuer, R. *et al.* Analysis of Storage Lipid Accumulation in Alcanivorax borkumensis: Evidence for Alternative Triacylglycerol Biosynthesis Routes in Bacteria. *J. Bacteriol.* **189**, 918-928, (2007).

25   Manilla-Perez, E., Lange, A. B., Hetzler, S. & Steinbuchel, A. Occurrence, production, and export of lipophilic compounds by hydrocarbonoclastic marine bacteria and their potential use to produce bulk chemicals from hydrocarbons. *Appl. Microbiol. Biotechnol.* **86**, 1693-1706, (2010).

26   Bourke, M., Kessler, A. & Cook, P. Influence of buried Ulva lactuca on denitrification in permeable sediments. *Mar. Ecol. Prog. Ser.* **498**, 85-94, (2014).

27   Nielsen, L. P. Denitrification in sediment determined from nitrogen isotope pairing. *FEMS Microbiol. Ecol.* **86**, 357-362, (1992).

28   Oshima, M. *et al.* Highly sensitive determination method for total carbonate in water samples by flow injection analysis coupled with gas-diffusion separation. *Analyt. Sci.* **17**, 1285-1290, (2001).

29   Fonselius, S. H. in *Methods of seawater analysis* (ed K Grasshoff) 91-100 (Springer-Verlag Chemie, 2007).

30   Godzien, J. *et al.* In-vial dual extraction liquid chromatography coupled to mass spectrometry applied to streptozotocin-treated diabetic rats. Tips and pitfalls of the method. *J. Chromatogr.* **1304**, 52-60, (2013).

31   Kind, T. *et al.* FiehnLib: Mass Spectral and Retention Index Libraries for Metabolomics Based on Quadrupole and Time-of-Flight Gas Chromatography/Mass Spectrometry. *Anal. Chem* **81**, 10038-10048, (2009).

32   Canfield, D. E., Kristensen, E. & Thamdrup, B. in *Aquatic Geomicrobiology* Vol. 48 *Advances in Marine Biology* Ch. 10, 383-414 (Academic Press Ltd-Elsevier Science Ltd, 2005).

33   Evrard, V., Glud, R. N. & Cook, P. L. M. The kinetics of denitrification in permeable sediments. *Biogeochemistry* **113**, 563-572, (2013).

34   Marchant, H. K. *et al.* Coupled nitrification-denitrification leads to extensive N loss in subtidal permeable sediments. *Limnol. Oceanogr.* **61**, 1033-1048, (2016).

35   Hoehler, T. M., Albert, D. B., Alperin, M. J. & Martens, C. S. Acetogenesis from CO2 in an anoxic marine sediment. *Limnol. Oceanogr.* **44**, 662-667, (1999).

36   Ghirardi, M. L. *et al.* Hydrogenases and hydrogen photoproduction in oxygenic photosynthetic organisms. *Annu. Rev. Plant Biol.* **58**, 71-91, (2007).

37   Yu, W. L. *et al.* Modifications of the metabolic pathways of lipid and triacylglycerol production in microalgae. *Microbial Cell Factories* **10**, (2011).

38   Lee, J.-Y., Yoo, C., Jun, S.-Y., Ahn, C.-Y. & Oh, H.-M. Comparison of several methods for effective lipid extraction from microalgae. *Bioresour. Technol.* **101**, S75-S77, (2010).

7 Discussion

7.1 Research chapter summaries

This thesis has investigated dissolved anoxic metabolism in anoxic permeable sediments. The specific findings from each chapter are summarised briefly below, and discussed together in the following section.

7.1.1 Chapter 2: Investigation of dissolved inorganic carbon production in anoxic permeable sediments.

In this research chapter, flow through reactor experiments revealed that heterotrophic metabolic processes only accounted for <7% of total anoxic dissolved inorganic carbon (DIC) production in permeable sediments. This phenomenon was observed in all four FTR experiments performed, indicating a highly reproducible phenomenon, and the contribution of three possible sources of anoxic DIC production was evaluated. These sources were dissimilatory nitrate reduction to ammonium (DNRA) via pools of intracellularly stored nitrate, calcium carbonate dissolution and meiofaunal respiration.

DNRA via pools of intracellularly stored nitrate was discounted as a possible major source of anoxic DIC production after the quantity of nitrate present in intracellular pools was found to be negligible compared to rates of anoxic DIC production. Calcium carbonate dissolution was also discounted after no net increase in the ratio of dissolved Ca^{2+} to Na^+ ions was observed and alkalinity production rates were found to be negative under anoxic conditions.

The contribution of meiofaunal respiration to anoxic DIC production was also estimated to be negligible as the expected decline in anoxic DIC production typical of meiofaunal anoxic survival was not observed in a FTR experiment featuring extended periods of anoxia. Isotopic analysis of DIC from FTR effluent gave a $^{13}C/^{12}C$ enrichment endpoint revealing the breakdown of organic material, produced by phytoplankton and microphytobenthos, as the source of anoxic DIC production (as opposed to carbonate dissolution). The process generating the majority of DIC under anoxic conditions is therefore highly likely to be a biotic process.

7.1.2 Chapter 3: Investigation of fermentation as a possible source of dissolved inorganic carbon production in anoxic permeable sediments

It was hypothesized that fermentation, uncoupled to heterotrophic metabolism, could be a major source of DIC production in anoxic permeable sediments. However, due to broad range of possible fermentation pathways, quantifying total rates of fermentation posed a substantial challenge. During this research, FTR effluent was analyzed for typical fermentation products to determine whether fermentation uncoupled to heterotrophic metabolism was occurring at substantial rates, and whether it could be responsible for the large proportion of anoxic DIC production, without a known source. The typical fermentative products targeted were C1-3 alcohols and fatty acids and were quantified using solid phase micro extraction gas chromatography-mass spectrometry. Ethanol and acetate were detected, however, based on established fermentation stoichiometries, these concentrations accounted for only between 2.1 and 4.7% of anoxic DIC production. The pathways producing these compounds, at least, were not occurring at high enough rates to be responsible for the large quantities of anoxic DIC observed in permeable anoxic sediments.

FTR experiments employing the broad spectrum antibiotics, amoxicillin and ciprofloxacin, revealed that anoxic DIC production remained constant, while bacterial processes, such as denitrification, were inhibited. Eukaryotic microorganisms are therefore most likely responsible for the majority of anoxic DIC production in permeable sediments, however, further research must be undertaken so that the dominant pathway being utilized may be identified.

7.1.3 Chapter 4: Eukaryotic dark fermentation dominates anoxic permeable sediments.

In chapter 3, it was found that eukaryotic microorganisms were likely responsible for the large quantities of DIC produced in anoxic permeable sediments. As C1-3 alcohol and fatty acid-producing fermentation reactions had been shown to account for <5% of anoxic DIC production, targeted analysis of typical fermentative products was shifted to dissolved hydrogen, a common product of eukaryotic fermentation pathways.

During FTR experiments, anoxic DIC production was consistently accompanied by large dissolved hydrogen production rates, suggesting the presence of fermentation. The production of both DIC and hydrogen persisted following administration of broad spectrum bactericidal antibiotics, but ceased following treatment with metronidazole. Metronidazole inhibits the ferredoxin/hydrogenase pathway of fermentative eukaryotic hydrogen production, suggesting that pathway as the source of hydrogen and DIC production. Metabolomic analysis showed large increases in lipid production at the onset of anoxia, consistent with documented pathways of anoxic dark fermentation in microalgae. Cell counts revealed a predominance of microalgae in the sediments. These findings indicate that microalgal dark fermentation could be an important energy-conserving pathway in anoxic permeable sediments.

7.1.4 Chapter 5: Hydrogen production in anoxic microalgae culture incubations

In previous research, FTR experiments employing antibiotic treatments suggested eukaryotic fermentation as the likely source of DIC and dissolved hydrogen production in anoxic permeable sediments. To further support these conclusions, the ability of eukaryotic microalgal cultures to produce hydrogen, when subjected to dark anoxic conditions, had to be demonstrated.

To this end, five diatom (*Fragilariopsis* sp.) cultures and one chlorophyte (*Pyramimonas*) cultures were subjected to several dark anoxic incubation experiments. Hydrogen production was observed across all cultures and the addition of acetate appeared to have no effect on dissolved hydrogen production. Quantum yield analyses indicated that theses cultures were highly sensitive, as it was necessary to maintain temperature and stirring conditions used during their growth to maintain culture health. Dissolved hydrogen production in all cultures would generally reach the experimental maximum within 24 hours of dark anoxic incubation, then the hydrogen concentration would decrease sharply, indicating a possible mechanism of consumption. These findings indicate that microalgal hydrogen production via dark fermentation could be an important energy conserving

pathway in permeable sediments and further supporting the hypothesis outlined in prior research that marine eukaryotic microalgae are capable of hydrogen production.

7.1.5 Chapter 6: Fermentation in dark anoxic permeable carbonate sediments.

Prior to chapter 6, all research presented in this thesis has been within the context of anoxic permeable silica sediments and has consistently found that heterotrophic metabolism accounted for only a small proportion of total anoxic DIC production. FTR experiments were repeated using permeable carbonate sediments from Heron Island in order to determine whether this phenomenon could be observed under these conditions. Metabolomic analyses revealed very large increases in the relative quantity of C18-23 lipids, including wax monoesters and unsaturated fatty acids, after short term (<24 hrs) exposure to anoxic conditions. Following further anoxic incubation, high rates of dissolved hydrogen production were observed and accompanied by further accumulation of these lipid compounds. These observations indicate that fermentation is likely a major process in anoxic carbonate sediments. A cell count analysis revealed a highly diverse microalgal community with relative proportions of 28.4% of dinoflagellates, 28.4% other flagellates, 10.1% diatoms and 33.1% cyanobacteria, suggesting that anoxic survival via fermentation may be a widely held adaption amongst these microorganisms

7.2 Anoxic metabolism in permeable sediments

The five research chapters presented in this thesis provides some insight into understanding metabolism in anoxic permeable sediments and has highlighted areas that merit further investigation.

Throughout this research, it was consistently observed that rates of heterotrophic metabolic processes, including denitrification, iron and sulfate reduction, accounted for only a small proportion of total DIC production, ranging between 1-12% across the various FTR experiments performed. There appeared to be a large majority of DIC production in anoxic permeable sediments

that could not be attributed to any known process. This phenomenon conflicted with the widely held assumption that heterotrophic metabolic processes dominated anoxic permeable sediments and investigating this became the chief focus of this research.

The evidence presented in this thesis indicated that dark fermentation may be the dominant metabolic pathway in anoxic permeable sediments, resulting in hydrogen release, lipid accumulation and DIC production. The high rate of dissolved hydrogen production, observed throughout this research, suggests that hydrogen production is likely occurring in situ and may be being recycled by aerobic and anaerobic respiratory bacteria, potentially shaping ecology and biogeochemistry within the temporally and spatially variable ecosystem of the permeable sediment. Given that positive net benthic community production can occur over 33% of the coastal ocean, dark fermentation may be a globally important metabolic pathway.

Given that microalgae were found to be responsible for large quantities of anoxically produced DIC and dissolved hydrogen via dark fermentation, these results are likely to be generalizable to any system dominated by microalgae that regularly exposes them to dark anoxic conditions. As this phenomenon was observed in both carbonate and silica sands, and over a range of different permeabilities and porosities, it's unlikely that these factors would limit dark fermentation by microalgae. These results are therefore highly generalizable to global permeable sediments.

7.3 Recommendations for future research

The work presented in this thesis represents a significant step towards understanding metabolism in anoxic permeable sediments, however, there remains a great deal still to be investigated.

For instance, the dissolved hydrogen production observed during FTR experiments should not be considered to be the total rate of hydrogen produced. Hydrogen-consuming bacteria, or hydrogenotrophic bacteria, reside in sediments and are very likely metabolising a portion of the total dissolved hydrogen produced. High concentrations of dissolved hydrogen were observed in FTR effluent because rates of consumption were lower than rates of production. However, in order

to produce a comprehensive electron budget for metabolism in anoxic permeable sediments, the total hydrogen production rate must be known. This could be determined using a FTR experiment that employed two parallel treatments, a control reservoir and a reservoir spiked with broad spectrum antibiotic, such as ciprofloxacin. The difference between the respective rates of hydrogen production would represent the rate of consumption by the hydrogenotrophic bacteria. Throughout this research, dissolved hydrogen concentrations have been determined using a calibrated Unisense H_2-100 sensor, fitted with a glass flow through cell. This sensor has a small (5%) sensitivity to hydrogen sulfide, necessitating the quantification of sulfide production rates so that the magnitude of this error may be estimated. Quantifying hydrogen production via a secondary method that is unaffected by the presence of other solutes, would further support the conclusions of this research. One such method could include analysis of FTR effluent via gas chromatography-with a reduced gas detector.

Another area worthy of investigation would be to determine whether hydrogen production can be observed in in situ anoxic permeable sediments and how the rates of production compare to those observed in FTR experiments. Prior to this research, it was widely accepted that in permeable sediments, dissolved hydrogen would be rapidly consumed by hydrogenotrophic prokaryotes, preventing accumulation. Porewater in anoxic in situ conditions will be subjected to far longer residence times compared to those used in this research, and it would be very interesting to see how this affects hydrogen concentrations.

Hydrogen production during dark anoxic incubations of diatom and chlorophyte cultures also merits further investigation. In chapter 5, the maximum hydrogen concentration for each culture incubation experiment was observed within the first 24 hours of incubation. This is in stark contrast to hydrogen production observed in FTR experiments, which continued to increase over extended periods of anoxia. The factor(s) responsible for this phenomenon are unclear and could be explored using culture incubation experiments that feature sampling for dissolved hydrogen and metabolomics at a relatively high frequency. This could shed light on what fermentation pathways

are being utilized and whether different pathways are favoured at different periods of the incubation.

Lastly, a more comprehensive electron budget for anoxic metabolism in permeable sediments should be completed. In this research, the large accumulation of wax monoesters and unsaturated fatty acids could not be translated into a given portion of the electron budget as the method of quantification only accounted for a relative fold increase. In future research, this could be improved upon by incorporating a direct quantification of the metabolome, targeting key metabolites. This would mean precise quantities of metabolites could be determined, allowing for the calculation of fermentation production rates, clarifying the dominance of this process in anoxic permeable sediments.